Persulfate Oxidation Coupled with Microbial Sulfate Reduction as a Combined Remedy

by

Mahsa Shayan

A thesis
presented to the University of Waterloo
in fulfillment of the
thesis requirement for the degree of
Doctor of Philosophy
in
Civil Engineering

Waterloo, Ontario, Canada, 2015

AUTHOR'S DECLARATION

I hereby declare that I am the sole author of this thesis. This is a true copy of the thesis, including any required final revisions, as accepted by my examiners.

I understand that my thesis may be made electronically available to the public.

Abstract

Groundwater contamination by petroleum hydrocarbon (PHC) compounds including the high impact and persistent aromatic compounds such as benzene, toluene, ethyl benzene and xylene (BTEX) poses serious risk to human health and the environment. The coupling or sequential use of different remediation technologies, also referred to as a "treatment train", has become an emerging strategy for the treatment of PHC-contaminated sites. Minimizing clean-up cost and time as well as maximizing the overall treatment efficiency are the primary goals of combined remedies. Coupling *in situ* chemical oxidation (ISCO) and enhanced bioremediation (EBR) is an example of a plausible treatment train. The general concept behind an integrated ISCO/EBR system is the use of chemical oxidation to target the bulk of the contaminant mass near the source, followed by the enhancement of biological processes to "polish" the remaining mass in the source and the downgradient plume.

Persulfate ($S_2O_8^{2-}$) is a persistent but yet aggressive oxidant which can rapidly destroy a wide variety of PHC compounds. Persulfate degrades complex organic compounds into simpler and more bioavailable organic substrates and produces sulfate, an electron acceptor. The anaerobic environment that is created is ideal for sulfate reduction to be enhanced. Therefore, enhanced bioremediation under sulfate reducing conditions is expected to dominate the mass removal processes following the consumption of persulfate.

To assess the viability and performance of a persulfate/EBR treatment train, the role of the intertwined mass removal processes (e.g., persulfate oxidation vs sulfate reduction) and the impact of persulfate on indigenous microbial processes need to be quantified. Hence, a pilot-scale trial was conducted in a 24 m long experimental gate at the University of Waterloo Groundwater Research Facility at CFB Borden over a period of 13 months. After a quasi steady-state plume of dissolved benzene, toluene and xylene (BTX) was established in the gate, two persulfate injection episodes were conducted to create a chemical oxidation zone. As this chemical oxidation zone migrated downgradient it was extensively monitored as it transitioned into an enhanced bioremediation zone. Mass loss estimates and geochemical indicators were used to identify the distinct transition between the chemical oxidation and enhanced biological reactive zones. Compound specific isotope analysis (CSIA) was used to delineate the dominant mass removal process, and to track the fate of the sulfate. Molecular biology tools, including specific metabolite detection and quantitative polymerase chain

reaction analysis were used to understand the effect of persulfate on the population and activity of the indigenous microorganisms with a focus on the SRB community.

A modelling tool was developed to simulate the coupled processes involved in a persulfate/EBR treatment train, and to quantify the impact of various parameters on the performance of this treatment system. The existing BIONAPL/3D model was enhanced (BIONAPL/PS) with the capabilities of simulating the majority of processes involved in a persulfate/EBR treatment train including: density-dependent advective-dispersive transport, persulfate decomposition, sulfate production, chemical oxidation, and biodegradation of PHC compounds under various redox conditions. The BIONAPL/PS model formulation was validated against observations from a series of column experiments designed to mimic various phases of a persulfate/EBR treatment train, and then was used to capture the observations from the pilot-scale trial. This latter effort was aimed to evaluate the model capability to simulate a complex system with multiple components within a dynamic flow system. The modelling tool was also used to evaluate options for performance optimization.

Multiple lines of evidence from the pilot-scale trial confirmed that the BTX plume was degraded with this persulfate/EBR treatment train (>70% BTX mass removed). Chemical oxidation was the dominant mass removal process in the vicinity of the persulfate injections (i.e., ChemOx zone), whereas enhanced bioremediation (including enhanced microbial sulfate reduction and methanogenesis) dominated BTX degradation in the downgradient portions of the experimental gate (i.e., the EBR zone). The transformation of the ChemOx zone into the EBR zone was also observed following depletion of persulfate from the system. The population and activity of SRB communities which were temporarily inhibited in the ChemOx zone immediately after persulfate injection, rebounded and increased by three (3) orders of magnitude after persulfate depletion. This significant enhancement in the microbial population was linked to increased sulfate concentrations, and the breakdown of complex substrates into simpler, more bioavailable compounds. The data also demonstrated that once flow in the experimental gate was stopped, the activity and population of the SRB community decreased as a result of the lack of sulfate, and methanogenic activity increased. In general, the data collected confirmed that the activity of both SRB and methanogens was enhanced under the geochemical conditions created following persulfate injection.

BIONAPL/PS provided a suitable platform in which the complex processes involved in a persulfate/EBR treatment train could be captured including the degradation of PHC compounds following persulfate injection, formation of ChemOx and EBR zones, depletion of persulfate, and the

generation and consumption of sulfate. Benchmarking of BIONAPL/PS against data from the pilot-scale trial highlighted the impact of persulfate on the subsequent sulfate reduction process. It was shown that aerobic degradation and sulfate reduction acted sequentially as the dominant mass removal process during the plume generation phase; however, immediately after persulfate injection, sulfate reduction was inhibited in the ChemOx zone and persulfate oxidation dominated the removal of BTX mass. Upon the depletion of persulfate, microbial sulfate reduction was re-established and became the dominant mass removal process at this location. Persulfate oxidation was responsible for the majority (78%) of the mass loss that occurred in the vicinity of the persulfate injections, followed by sulfate reduction (21%) and aerobic biodegradation (1%). Alternatively, it was observed that microbial sulfate reduction was responsible for most of the mass removal at a downgradient location with an increased rate that corresponded to the arrival of high sulfate concentrations. Reaction kinetics, transport parameters and design options (i.e., persulfate concentration, and injection period/interval and rate) were identified as the key factors which influence the overall system performance. It was also found that a less aggressive persulfate treatment step (i.e., lower dosage, duration and extent) improves the overall treatment efficiency by minimizing the inhibitory effect of persulfate on the subsequent microbial processes.

Results from this research effort indicated that persulfate oxidation coupled with enhanced bioremediation appears to be a viable approach to treat dissolved PHC compounds *in situ*. The inhibitory impact of persulfate on the population and activity of indigenous microbial communities (including SRB) was shown to be short term. Stable isotope analysis of BTX and sulfate, and monitoring of process-specific functional genes and intermediate metabolites proved useful to evaluate system performance and to identify temporal changes in the dominant degradation pathway. For an effective persulfate/EBR treatment train, a carefully balanced design which takes into account the interactions among the physical, chemical and biological processes is required. The combination of experimental and modelling efforts provided key insights into an effective design of a combined persulfate/EBR remedy, and lessons learned will be useful for remediation engineers and scientists.

Acknowledgements

I would like to express my utmost gratitude to my supervisor Prof. Neil Thomson for his continuous support and insightful guidance throughout my doctoral studies; for giving me the opportunity to join his research team and for letting me enjoy the best academic experience one could have ever asked for. I am truly grateful to him for his patience, inspiration and valuable advice during the writing of this dissertation. I am also deeply indebted to my co-supervisor Prof. Jim Barker, whose vision, broad knowledge and encouragement have been of great value to me. I am sincerely thankful to both my super supervisors for putting me in contact with a world-class team of experts during my PhD research project and for supporting me to attend many conferences and workshops where I was able to challenge myself and stay on the cutting edge of my research field.

Thanks to Dr. John Molson for his continuous help and technical support during the development and application of the BIONAPL/PS model which constitutes an important contribution to this research. I am also truly grateful for his kindness and hospitality during the time I spent at Laval University in Quebec City to work on the model development. I am thankful to Dr. Ramon Aravena for his helpful feedback and guidance regarding the application of isotope analysis, and also for reviewing my thesis chapters. I also would like to thank Prof. Eugene Madsen for his insight and guidance regarding the application of molecular biology tools in my research.

This research was performed as part of a strategic research project initiated by Chevron Energy Technology Company, executed jointly by University of Neuchatel, University of Waterloo and Cornell University with the goal to develop and apply "New Tools for Remediation Performance Assessment of Petroleum Hydrocarbon Contaminated Sites". I would like to sincerely thank Tim Buscheck, Ravi Kolhatkar, Eric Daniels, Thomas Hoelen and Katharine North of Chevron Energy Technology Company for many helpful discussions and suggestions during our meetings and conference calls. Special thanks to Dr. Daniel Hunkeler and Dr. Daniel Bouchard who provided insight into the application of isotopic data as a novel site characterization tool, and also for facilitating the carbon and hydrogen isotope analyses in their laboratory at University of Neuchatel, Switzerland. I would also like to thank Dr. Chris DeRito for performing extensive molecular biology analyses, and developing tools and methods customized to measure biomarkers for this research in Prof. Madsen's research laboratory at Cornell University. I also would like to acknowledge Dr. Robin Slawson of Wilfrid Laurier University and her master student Christopher Bartlett who helped me

with the design and execution of the laboratory column experiments, which contributed significantly to the verification of the BIONAPL/PS model, and also for performing complementary microbiology analyses on samples from the Borden site. I am grateful to the members of my advisory committee Prof. Wayne Parker and Dr. James Craig for their time, support and great input on my work.

Financial support for this research was provided jointly by Chevron Energy Technology Company, the American Petroleum Institute (API), and a Natural Sciences and Engineering Research Council (NSERC) of Canada Collaborative Research and Development Grant (N.R. Thomson) for which I am very grateful. I would also like to thank the Southern Ontario Watershed Consortium (SOWC) for their infrastructure support at the University of Waterloo Groundwater Research Facility at Canadian Forces Base Borden.

I would also like to express my special thanks to an amazing group of super experienced field and lab technicians without whom this work would have not been possible: Bob Ingleton, Paul Johnson, Shirley Chatten, Wayne Noble, Phyllis Diebolt, Justin Harbin, Rachel Karimi, and Marianne VanderGriendt. Also, I am so indebted to my colleagues and friends in the departments of Civil and Environmental Engineering and Earth and Environmental Sciences at the University of Waterloo for their kind help and support during my field and laboratory work. In particular I would like to thank Dr. Massimo Marchesi who helped me greatly during the extensive field work and in realizing the site's geochemistry. I would like to express my gratitude to my fellow grad students, Felipe Solano, Wei Yunxiao, Jessica Van Der Rest, Geoff Kovacik, Gu Xiaogang, Paulo Casado, Ana Maciel, Bruno Pirilo Conicelli, Lucas Andreata, Saeid Shafieiyoun, Dario Barletta and co-op students Ian Mercer, Christian Larsen, Wayne Park and Kelli Dobbin who assisted me during my field work activity even in the hardest working conditions. I would like to also thank my friends Elahe, Amin, Parinaz, Rana, Vahid, Fatima, Reza, Negar, Mohamad, Nadia, Maziar, Nazgol, Iman, Sara, Siavash, Laleh, Bahador, Mozhgan and Omid for their companionship and friendship during my stay in Waterloo.

I would like to express my most sincere thanks to my parents, Mahnaz and Hassan, who taught me to be strong and to never give up, who supported and encouraged me in pursuing my dreams throughout my studies in Iran and in Canada, for boosting my self-confidence all these years and for keeping me updated with occurrences back home. Special thanks to my dear brothers, Reza and Ramin, who despite being one ocean and two continents away from me, have always made me laugh loads and feel proud. I also would like to thank my parents- and sisters-in-law for their heartwarming love and support.

Foremost, I would like to thank my dearest Bijan for his unconditional love, support and care throughout the last four years of my life, for making and sharing wonderful times with me, and for always being there during the hard and stressful moments, even at times I was not at my best mood (just sometimes!). I appreciate all the hours he spent on highway 401 commuting between Toronto and Waterloo for me, and all the spoiling Sunday brunches. Special thanks to him for critically proof-reading my thesis, for having faith in me and for keeping me motivated and confident to achieve my goals. Bijan, you are my cornerstone. Thank you for helping me to stay on track and accomplish the biggest milestone of my life (okay, I know that) so far.

Dedication

I want to dedicate my thesis to my grandparents:- Mahin and Hassan whom I cannot wait to see and hug again, and to Tahereh and Rahim whom I kept missing since their eternal journey.

Table of Contents

List of Figures

List of Tables

Chapter 1
Introduction

1.1 GENERAL BACKGROUND

Groundwater contamination by a wide variety of PHC compounds, including the high impact, toxic and persistent aromatic hydrocarbons (e.g., benzene, toluene, ethyl benzene and xylene (BTEX)), poses serious risk to human health and the environment. This risk may persist until the PHC source zone and the associated plume are completely removed or treated (Cozzarelli & Baehr 2003; Alleman & Leeson 1999). Innovative remediation strategies are required to mitigate these issues in an efficientand cost effective manner.

The coupling or sequential use of different remediation technologies, also referred to as a "treatment train" or "combined remedy", has become an emerging strategy over the last several years that aims to combine the strengths of each individual treatment technique to improve the overall system efficiency (Tsitonaki 2008; Sutton et al. 2010; Sahl & Munakata-Marr 2006; Devlin et al. 2004; Morkin et al. 2000). This technology integration can be temporal, where technologies are connected in a logical sequence, or in a spatial manner, where different technologies are applied at different locations across a site depending on the contaminant type and distribution.

Exploiting synergies of *in situ* chemical oxidation (ISCO) and enhanced bioremediation (EBR) is an example of a plausible treatment train for the application at PHC-contaminated sites (Munakata-Marr et al. 2011; Sahl et al. 2007; Sutton et al. 2010; Krembs et al. 2010; Richardson et al. 2011; Tsitonaki et al. 2008). The focus of this study was to assess the feasibility of coupling persulfate oxidation and enhanced bioremediation (EBR) as a combined remedy. Persulfate ($S_2O_8^{2-}$) is a persistent but yet aggressive oxidant that has been successfully applied for the treatment of PHC-contaminated sites (Huling & Pivetz 2006; Tsitonaki et al. 2010). The reaction of persulfate with organic compounds leads to the production of sulfate which can enhance the biodegradation activity of a group of microorganisms known as sulfate reducing bacteria (SRB). Once the persulfate has been consumed, enhanced bioremediation under sulfate reducing conditions is hypothesized to dominate the removal of the remaining contaminant mass. The general concept behind an integrated persulfate/EBR treatment train is the use persulfate to target the contaminant mass in the high concentration zones, followed by EBR (e.g., enhanced sulfate reduction) to "polish" the remaining mass in the source zone and downgradient plume.

To assess the viability and performance of a persulfate/EBR treatment train, the role of the various mass removal processes (e.g., persulfate oxidation vs sulfate reduction) and the impact of persulfate on indigenous microbial processes need to be understood. Moreover, for an effective persulfate/EBR treatment train, it is important to investigate the interaction between the coupled physical, chemical and biological processes involved, and to quantify the impact of design parameters on the performance of the treatment system.

Only two peer-reviewed studies have investigated the impact of persulfate on the population and activity of indigenous microorganisms in laboratory experiments (Tsitonaki 2008; Richardson 2010). The impact of persulfate exclusively on the population and diversity of SRB communities has only been documented in a few laboratory experiments that have been discussed in the grey literature (Bou-Nasr, 2006; Gallagher and Crimi, 2007; Cassidy 2008). These studies concluded that the SRB population initially decreased after exposure to persulfate with a magnitude proportional to the oxidant dose used. The microbial population, however, rebounded over time, and the final population in some systems was greater than that in the control reactors. Unfortunately none of these studies are representative of an engineered persulfate/EBR treatment train and at best provide some information on the temporal (but not the spatial) separation of chemical and biological treatment zones. Moreover, they do not provide detailed characterization of the processes involved in a persulfate/EBR treatment train, and no previous effort has investigated the impact of persulfate on the subsequent BTEX-degrading microbial processes.

1.2 RESEARCH OBJECTIVES

To improve our understanding of an integrated treatment system using persulfate coupled with microbial sulfate biodegradation, the following research objectives were developed:

1. Assess the feasibility of treating a BTX plume using a persulfate/EBR treatment train,
2. Investigate the impact of persulfate on indigenous microbial processes,
3. Quantify the role of various mass removal processes,
4. Identify the impact of key design considerations on the treatment performance of the combined system, and
5. Provide guidance for future applications.

1.3 THESIS SCOPE

The thesis is organized into four chapters. Chapters 2 and 3 are the core chapters that address the research objectives. Chapter 1 provides the framework, and Chapter 4 summarizes the major conclusions and contribution, provides guidance for future applications, and discusses areas of future work.

To assess the viability and performance of a combined persulfate/EBR remedy for the treatment of a dissolved BTX plume, a controlled pilot-scale experiment was designed and executed at the University of Waterloo Groundwater Research Facility at CFB Borden over a period of 13 months. Mass loss estimates and geochemical indicators were used to identify the distinct transition between the chemical oxidation and enhanced biological reactive zones. Compound specific isotope analysis (CSIA) was used to identify the dominant mass removal process, and to demonstrate the occurrence of microbial sulfate reduction. Molecular biology tools, including specific metabolite detection and quantitative polymerase chain reaction analysis were used to understand the effect of persulfate on the population and activity of the indigenous microorganisms with a focus on the SRB community. Chapter 2 is devoted to a discussion of this pilot-scale experiment. The isotope analyses were partly performed by D. Bouchard at University of Neuchatel, and the University of Waterloo Environmental Isotope Laboratory. The molecular biology analyses were performed by C. DeRito at Cornell University.

To quantify the role of the intertwined mass removal processes, and to identify the impact of various parameters on the performance of a persulfate/EBR treatment train, a modelling tool was developed. Chapter 3 focuses on the development and application of the BIONAPL/PS model. BIONAPL/3D was enhanced (BIONAPL/PS) with the capabilities to simulate most of the coupled processes involved in a persulfate/EBR treatment train including: density-dependent advective-dispersive transport, persulfate decomposition, sulfate production, chemical oxidation, and biodegradation of PHC compounds under various redox conditions. The validity of the BIONAPL/PS model formulation was evaluated through simulating a series of column experiments designed to mimic various phases of a persulfate/EBR treatment train. The column experiment was conducted by C. Bartlett of Wilfrid Laurier University. BIONAPL/PS was then used to capture the observations from the pilot-scale trial. The latter effort was aimed to evaluate the model capability to simulate a complex system with multiple components within a dynamic flow system. The modelling tool was also used to evaluate options for performance optimization.

Chapters 2 and 3 are heavily edited by N. Thomson and intended for publication in suitable high quality journals and hence are written as stand-alone chapters and some repetition is unavoidable. These chapters have been prepared with the intent to submit them to *Journal of Contaminant Hydrology*.

Chapter 2

Integrated Plume Treatment using Persulfate Oxidation Coupled with Microbial Sulfate Reduction

Abstract

The integration or sequential use of different remediation technologies, also referred to as a "treatment train" or "combined remedy", has become an emerging strategy for the treatment of PHC-contaminated sites. Minimizing clean-up cost and time as well as maximizing the overall treatment efficiency are the primary goals of combined remedies. Coupling *in situ* chemical oxidation (ISCO) with persulfate ($S_2O_8^{2-}$) and enhanced bioremediation (EBR) under sulfate reducing condition is an example of a plausible treatment train. To assess the viability and performance of a combined persulfate/EBR remedy, a pilot-scale field experiment was conducted at the University of Waterloo Groundwater Research Facility at the Canadian Forces Base (CFB) Borden, ON, Canada. The main objectives of this pilot-scale trial were to characterize the role of the intertwined mass removal processes (e.g., persulfate oxidation vs sulfate reduction) and to quantify the impact of persulfate on indigenous microbial processes. A dissolved benzene, toluene and o-xylene (BTX) plume was allowed to develop over 170 days in a 24 m long experimental gate, with a maximum concentration of approximately 25 mg/L. After a quasi steady-state BTX plume was established, two persulfate injection episodes (10 g/L-unactivated) were conducted on Day 170 and Day 180 to create a chemical oxidation zone. As this chemical oxidation zone migrated downgradient it was extensively monitored as it transitioned into an enhanced bioremediation zone.

Mass loss estimates and geochemical indicators were used to identify the distinct transition between the chemical oxidation and enhanced biological reactive zones. Compound specific isotope analysis (CSIA) was used to distinguish the dominant mass removal process, and to investigate the occurrence of microbial sulfate reduction. Molecular biology tools, including specific metabolite detection and quantitative polymerase chain reaction analysis were also applied to characterize the impact of persulfate on the population and activity of the indigenous microorganisms with a focus on the SRB community. The multiple lines of evidence from this study demonstrated the successful treatment of the BTX plume with a persulfate/EBR treatment train (>70% BTX mass removal). The inhibitory impact of persulfate on the population and activity of indigenous microbial communities

(including SRB) was found to be short term, followed by a substantial increase (three (3) orders of magnitude) in microbial activity beyond the initial level. While chemical oxidation was the dominant mass removal process in the vicinity of the injection zone, the enhanced biodegradation associated with microbial sulfate reduction and methanogenesis was demonstrated to be responsible for destroying the remaining contaminant mass in the downgradient plume. Thus, in situ persulfate oxidation coupled with enhanced bioremediation based on the generation of sulfate appears to be a viable approach to treat dissolved BTX in groundwater.

Keywords: Treatment train; *In situ* chemical oxidation, Enhanced bioremediation, Persulfate, Microbial sulfate reduction, BTEX

2.1 INTRODUCTION

Petroleum hydrocarbons (PHCs) including gasoline, diesel, and jet fuel are among the most common soil and groundwater contaminants (WHO 2005). The worldwide spillage of PHC compounds into the environment is reported to be in the range of 80-1200 million liters per year (Kleikemper 2003). In Canada, about 60% of the contaminated sites involve PHCs (Environment Canada 2010). PHCs are complex mixtures of hundreds of various organic compounds classified based on their chemical structure (Millner et al. 1992; Pawlak et al. 2008). Among all PHC compounds, the monoaromatic hydrocarbons (especially BTEX: benzene, toluene, ethylbenzene, and xylenes) are of the greatest environmental concern due to their toxicity and high water solubility. Benzene, for example, has been classified as a potential carcinogen which may persist in the subsurface for a long period of time due to its low natural attenuation rate (EPA 2004; Rifai & Newell 1998). Effective remediation strategies are required to mitigate the environmental and human-health impacts of BTEX-contaminated groundwater.

Various remediation technologies have been applied to treat PHC-contaminated soil and groundwater including pump-and-treat, permeable reactive barriers, multi-phase extraction (MPE), air-sparging, bioremediation and *in situ* chemical oxidation/reduction. Compared to conventional treatment approaches (e.g., pump-and-treat and MPE), *in situ* remediation technologies are less expensive and more efficient alternatives for the remediation of groundwater contamination (NRC 1994). These technologies are either engineered (e.g., air/bio-sparging and chemical oxidation/reduction) or based on natural processes (e.g., natural attenuation and enhanced

bioremediation). *In situ* technologies are ideal to address the high residual mass of the contaminants in a dissolved plume or non-aqueous phase liquid (NAPL) source zone, without requiring extensive above-ground infrastructure and associated long-term maintenance costs (Siegrist et al. 2011).

In situ chemical oxidation (ISCO) and enhanced bioremediation (EBR) are two technologies that have been extensively applied at sites contaminated with a variety of compounds including PHCs (Sutton et al. 2010). ISCO involves the delivery of a strong oxidizing reagent into the subsurface to transform an organic contaminant into a less harmful intermediate or end-product such as CO_2 (Huling & Pivetz 2006; Watts & Teel 2006). EBR involves the stimulation of indigenous hydrocarbon-utilizing microorganisms by delivering electron acceptors, electron donors (substrates) and/or environmental nutrients to the subsurface (Reinhard et al. 1997; Weiner et al. 1998; Bolliger et al. 1999; Mackay et al. 2000; Cunningham et al. 2001; Hoelen et al. 2006). Low costs, high efficiency, minimal impact on surface infrastructure, and adaptability to a variety of subsurface conditions and contaminant types are the key advantages of these two technologies.

Despite its advantages, ISCO is inefficient in some situations due to geological heterogeneities, insufficient mixing, low oxidant persistence, and formation of impeding by-products (e.g., MnO_2) (Schnarr et al. 1998; Lee & Kim 2002; Xu & Thomson 2008; Sra 2010). For example, oxidant delivery limitations have been shown to be responsible for a portion of the contaminant mass to persist following ISCO treatment and the continuous slow mass transfer from this remaining residual mass leads to contaminant rebound and persistence of dilute plumes downgradient of the source zone (Huling & Pivetz 2006; Thomson et al. 2008; Richardson et al. 2011; Sra et al. 2013b). In addition, ISCO is generally not cost-effective to use to treat contaminants present at low concentrations. EBR is a less expensive technology for treating low concentrations of contaminants; however, it often struggles to degrade complex organic mixtures. Factors such as the availability of substrates, electron acceptors and nutrients as well as the site-specific nature of the active microbial communities often limit the effectiveness of EBR (ITRC 2005). As a result of such limitations, at many sites neither of these two technologies can be applied individually to achieve remediation objectives in a cost- and time-effective fashion (Devlin et al. 2004; Sutton et al. 2010; Sahl & Munakata-Marr 2006; Munakata-Marr et al. 2011).

Recent investigations have shown that the synergistic coupling or sequential use of ISCO and EBR could potentially combine the strengths of each individual technology and minimize their limitations

(ITRC 2005). This technology integration approach (also referred to as a "treatment train" or "combined remedy") has gained increased attention in recent years (Yang et al. 2005; Sahl et al. 2007; Tsitonaki 2008; Krembs et al. 2010; Sutton et al. 2010; Munakata-Marr et al. 2011). The general concept behind an integrated ISCO/EBR treatment train is to use chemical oxidation to target the bulk of the contaminant mass in the zones with high concentrations, followed by the use of EBR to "polish" the remaining mass in the source zone and downgradient plume.

There are a variety of chemical oxidants that may be used in ISCO applications, including hydrogen peroxide, ozone, permanganate and persulfate. Among these, persulfate ($S_2O_8^{2-}$) has been used extensively for soil and groundwater treatment due to its capability to non-selectively destroy a wide range of environmentally relevant contaminants including PHC compounds (Huang et al. 2005; Liang et al. 2008; Sra et al. 2013a; Sra et al. 2013b). Unlike permanganate, persulfate is able to oxidize aromatic hydrocarbons and other fuel-related compounds (Huling & Pivetz 2006; Sra et al. 2013a). Compared to peroxide and ozone, persulfate is more stable and can persist in the subsurface for weeks to months due to its low natural oxidant interaction (NOI) (Sra et al. 2010; Petri et al. 2011). These characteristics make persulfate an attractive choice for a chemical oxidant to treat PHC impacted soils and groundwater. Persulfate chemistry, activation methods, interaction with soil materials, and impact on subsurface geochemistry have been extensively reviewed by Tsitonaki et al. (2010) and Petri et al. (2011).

An inherent advantage of using persulfate in a coupled persulfate/EBR treatment system is the production of an excess amount of sulfate which results from persulfate decomposition (reaction with organic compounds and aquifer materials). This excess sulfate can serve as a terminal electron acceptor and enhance the subsequent microbial sulfate reduction process (Cunningham et al. 2000; Cunningham et al. 2001; Kleikemper et al. 2002b). Therefore, a persulfate/EBR treatment train is expected to combine the aggressive nature of persulfate oxidation with the long-term efficiency of enhanced microbial sulfate reduction (Figure 2.1). Table 2.1 summarizes the general advantages and limitations of persulfate and EBR technologies as individual treatments, and the benefits of applying them as integral parts of an ISCO/EBR treatment train.

Microbial sulfate reduction is an energy-yielding metabolic process during which sulfate is reduced to sulfide, and organic compounds are oxidized to CO_2 and H_2O. This process is mediated by a diverse group of microorganisms known as dissimilatory sulfate reducing bacteria (SRB) which are

abundant in anoxic environments, such as PHC-contaminated aquifers. Substrates for SRB range from hydrogen gas to monoaromatic compounds such as BTEX (Anderson & Lovley, 2000; Davis et al., 1999; Edwards et al. 1992; Fukui et al., 1999). SRB communities capable of complete oxidation of toluene and xylene have been previously identified (Harms et al. 1999; Rabus et al. 1998; Beller et al. 1996; Kleikemper et al. 2002(a)).

SRB capture the energy they required for growth and cell maintenance by coupling the sulfate reduction reaction to the synthesis of ATP (Adenosine triphosphate) in their cytoplasm (Jin & Bethke 2009). Details of energy production during dissimilatory sulfate reduction as well as a thorough overview of the diversity, physiology and distribution of SRB have been provided by Barton and Hamilton (2007); Muyzer and Stams (2008) and Zhou et al. (2011). In general, the rate of microbial sulfate reduction is a function of the SRB specific growth rate, which in turn is controlled by the availability of sulfate and the organic substrate used by the microorganism during energy production. The SRB need to conserve a certain amount of the energy liberated during the reaction for their maintenance and growth, and the lack of cellular energy conservation can halt the sulfate reduction process even before the complete consumption of electron donors and/or sulfate (Roychoudhury & McCormick 2006; Jin & Bethke 2009). It has been demonstrated that when a sufficient supply of sulfate and electron donor is provided, and the cellular energy conservation requirement is satisfied, sulfate reduction is a dominate pathway for the anaerobic biodegradation of organic compounds (Kleikemper et al. 2002(b); Zwolinski et al. 2000; Oude Elferink 1998; Franzmann et al. 2002; Hao et al. 1996; Shen & Buick 2004; Roychoudhury & Merrett 2006). The degradation rate of BTEX compounds has been reported to be highest under sulfate reduction compared to other anaerobic biodegradation pathways such as nitrate- or iron-reduction (Lawrence 2006; Roychoudhury & McCormick 2006; McCormick 2005). The microbial sulfate reduction rate is expected to increase following the application of persulfate, due to:

1. the breakdown of complex PHC compounds into simpler organic substrates that are more bioavailable (i.e., easily assimilated within a SRB cell) and more reactive (i.e., easily broken down inside the cell), and
2. the production of additional sulfate which serves as the source of electron acceptor which is required for microbial maintenance and growth (Sutton et al. 2010; Tsai et al. 2009; Cassidy 2008) .

To design an effective integrated persulfate/EBR treatment train, it is necessary to understand the interactions between persulfate and the indigenous microbial communities. The impact of chemical oxidants on biological processes has been previously reviewed and summarized by others (e.g., Scott & Ollis 1995; Waddell & Mayer 2003; Luhrs et al. 2006; Sahl & Munakata-Marr 2006; Munakata-Marr et al. 2011). These studies have predominantly focused on the impact of conventional oxidants (i.e., hydrogen peroxide, ozone, and permanganate) on the aerobic microorganisms indigenous to aquifers contaminated with polyaromatic hydrocarbons or chlorinated solvents using batch or column experiments. The general observations from these studies have been an increase in the microbial population and stimulation of biodegradation activities following the application of an oxidant which led to the overall increase in contaminant mass removal. In some cases, an initial inhibition of the microbial activity was observed in the presence of higher oxidant concentrations; however, a rebound of the microbial population and activity was reported within a few days to months following oxidant application. It is speculated that the following factors contribute to the rebound and enhancement of the microbial processes after the application of an oxidant:

(1) breakdown of complex organic compounds into simpler/more bioavailable substrates;

(2) decreased concentration of contaminants to levels non-toxic to microorganisms;

(3) generation of by-products that can serve as terminal electron acceptors enhancing a specific biodegradation activity;

(4) decreased microbial diversity where the domination of a few microbial species (due to the prevalence of a specific geochemical condition) reduces the competition for substrates and thus can enhance the effectiveness;

(5) persistence and growth of indigenous microbes in the dead-end pores where they can survive and thrive under non-ideal conditions, and

(6) capability of some microbial communities to develop defense mechanisms against the toxic effects of oxidants (Chapelle et al. 2005; Kulik et al. 2006; Nam et al. 2001; Sutton et al. 2010; Miller et al. 1996; Kastner et al. 2000; Azadpour-Keeley et al. 2004; Sahl & Munakata-Marr 2006; Cassidy 2008; Cassidy et al. 2009; Pardieck et al. 1992).

There are only two peer-reviewed studies that have investigated the impact of persulfate on the population and activity of indigenous microorganisms in the laboratory. In a series of batch

experiments, Tsitonaki et al. (2008) exposed aquifer material contaminated with landfill leachate to various doses of heat-activated persulfate (0.02 to 2 g/kg) and monitored the change in cell density and activity of the indigenous aerobic communities, as well as a laboratory strain Pseudomonas putida KT2440 (*P.putida*). They used a standard viability assay (microscopic enumeration) and ^{14}C-acetate mineralization to measure the population and activity of the microorganisms, respectively. They observed that persulfate concentrations up to 10 g/L did not have any adverse impact on the population and metabolic activity of either the indigenous or *P.putida* microcosms. Their study reported the inhibition of microbial activity at persulfate concentration of 10 g/L; however, it was shown that compared to other oxidants (iron catalyzed hydrogen peroxide, and permanganate) heat-activated persulfate had the least deteriorating impact on the indigenous microorganisms. The same observation was reported by Cassidy et al. (2009) who compared the effect of ozone, modified Fenton reagent, and iron-activated sodium persulfate on subsequent aerobic biodegradation of 2,4-dinitrotoluene (DNT) in batch slurry reactors. They also found that persulfate had the lowest adverse impact on the population of DNT degraders, and thus led to highest overall treatment efficiency compared to other oxidants.

In the other study, Richardson et al. (2011) investigated the impact of persulfate on the abundance and activity of the indigenous microbial community, and of a specific PAH-degrading bacteria present in contaminated soil from a former manufactured gas plant (MGP) site. They used molecular biology techniques to measure the population and activity of the total microbial community and those of the PAH-degrading bacterium following the injection of 20 g/L persulfate in a column experiment. Their findings showed that exposure to persulfate initially led to reduction in total bacterial communities, inhibition of microbial activity, and decrease in community diversity; however, a rapid recovery was observed. In the grey literature, the impact of persulfate on the population and diversity of SRB communities has been documented in a few laboratory experiments (Bou-Nasr et al. 2006; Gallagher and Crimi 2007; Cassidy 2008) and observed at field sites contaminated with chlorinated hydrocarbons (Droste et al. 2002; Marley et al. 2006; Sessa et al. 2008; Studer et al. 2009).

Unfortunately none of these studies are representative of an engineered persulfate/EBR treatment train and at best provide some information on the temporal (but not the spatial) separation of chemical and biological treatment zones. Moreover, they do not provide detailed characterization of the

intertwined processes involved in a persulfate/EBR treatment train, and no previous effort has investigated the impact of persulfate on the subsequent BTEX-degrading microbial processes.

To improve our understanding of the treatment of a groundwater system impacted with PHCs using persulfate coupled with sulfate reducing biodegradation, a pilot-scale experiment was designed and executed. A unique design approach was used to spatially separate the chemical oxidation and enhanced bioremediation zones. The main objectives of this field effort were to characterize the processes involved in a persulfate/EBR treatment train, to identify the temporal and spatial boundaries and transitional points between the various processes, and finally to assess the impact of persulfate on the subsequent microbial processes (e.g., biodegradation under sulfate reducing condition).

2.2 GENERAL METHODOLOGY

Figure 2.2 illustrates the conceptual approach adopted for this pilot-scale trial. Initially, a dissolved (quasi steady-state) plume of selected PHC compounds was generated using a diffusive source to develop a fully anaerobic aquifer system, and to provide favorable conditions for the acclimation and growth of indigenous SRB (Figure 2.2(a)). Next, two sequential persulfate injection episodes were executed to trap a portion of the dissolved phase plume (Figure 2.2(b and c)). Due to longitudinal dispersion, the two persulfate slugs were expected to mix with the confined portion of the PHC plume as they migrated downgradient (Figure 2.2(c)) to form a chemical oxidation (ChemOx) zone. As the PHC and persulfate mass was depleted due to chemical oxidation, a sulfate plume was expected to form (Figure 2.2(d)) and the ChemOx zone was expected to transition into an EBR zone. It was postulated that the migration of the sulfate plume would stimulate the growth and activity of the indigenous SRB, within the EBR zone (Figure 2.2(e)). PHC mass removal in the ChemOx zone was expected to be dominated by oxidation and in EBR zone by enhanced microbial sulfate reduction.

To monitor the fate of the “ChemOx zone” and the “EBR zone”, and to detect the biogeochemical shifts prior to, during and following the persulfate injection, a host of parameters were monitored in groundwater. These included BTX and methane concentrations, selected inorganic (e.g. SO_4^{2-}, Na^+, Ca^{2+}, S^{2-}) concentrations, dissolved inorganic carbon (DIC) content, and geochemical indicators including dissolved oxygen (DO), electrical conductivity (EC), redox potential (Eh), and pH. However, evaluating the impact of persulfate oxidation on the subsequent microbial processes only

through concentration patterns of sulfate, sulfide and/or changes of DIC content was considered to be a challenge due to the system dynamics (resulted from the ongoing transport) and the potential dilution, dispersion, sorption, and abiotic processes (e.g., mineral precipitation).

To aid in this characterization effort, a number of advanced methods under the general title of environmental molecular diagnostic (EMD) tools were employed along with conventional methods (e.g., use of concentration profiles and geochemical indicators). EMD tools refer to a group of emerging techniques developed to analyze the biological and chemical characteristics of groundwater. Over the last decade, EMD tools have been increasingly applied to improve site characterization and remediation (e.g., Bolliger et al. 2000; Griebler et al. 2004; Beller et al. 2008; Kleikemper et al. 2004). Examples of such methods include compound specific isotope analysis (CSIA), polymerase chain reaction (PCR), quantitative PCR (qPCR), microbial fingerprinting methods, specific metabolite detection, microarrays, stable isotope probing (SIP), enzyme activity probes (EAPs), and fluorescence *in situ* hybridization (FISH). Among these methods, isotopes (CSIA and sulfate) and qPCR methods along with specific metabolite detection were utilized in this study to: (1) evaluate the successful delivery and effectiveness of persulfate as the first step of the treatment train, (2) understand the short- and long-term impact of persulfate on the intrinsic microbial processes, and (3) distinguish microbial sulfate reduction from other biotic and/or abiotic degradation pathways (e.g., methanogenesis). The fundamentals of the isotopes and molecular biology tools are described in the following sub-sections.

2.2.1 Isotope Analyses

The rationale for application of isotope tools in biodegradation and remediation studies of organic contaminants in groundwater is based on the process of isotope fractionation that affect compounds involved in biological and chemical reactions. In general, the lighter isotopes (e.g., ^{12}C) form weaker chemical bonds compared to heavier isotopes (e.g., ^{13}C). Therefore, during a mass removal process (e.g., chemical oxidation or biodegradation), the lighter isotopes react faster than the heavier isotopes. As the reaction proceeds and contaminants/electron acceptors are degraded, the ratio of the heavy to light isotopes is expected to increase in the residual pool of reacting compounds (Meckenstock et al. 2004; ITRC 2011; Marchesi et al. 2013). The isotopic evolution of compound *x* (e.g., carbon) in substrate *s* (e.g., benzene) during degradation reactions can be modeled using a simple Rayleigh equation which is expressed by:

$$\delta^{13}C_s = \delta^{13}C_{s0} + \varepsilon \ln f \quad (2.1)$$

where ε is the isotopic fractionation factor, f is the fraction of substrate (i.e., benzene) remaining, and $\delta^{13}C_s$ and $\delta^{13}C_{s0}$ are the isotope composition of the sample and standard, respectively.

It has been demonstrated that each specific degradation process results in a distinct isotopic fractionation (Hunkeler et al. 2008; Aelion et al. 2009; Marchesi et al. 2013). Application of carbon and hydrogen (C/H) isotope fractionation as a complementary tool to assess the efficiency of in situ remediation technologies has been increasing in the recent years (Hunkeler et al. 1999; Schmidt et al. 2004; Hunkeler et al. 2008; Meckenstock et al. 2004; Wilkes et al. 2000). The carbon and hydrogen (C/H) isotopic fractionation caused by various chemical and biological mass removal processes (e.g., aerobic/anaerobic biodegradation and permanganate oxidation) have been investigated for many organic contaminants including BTX (Meckenstock et al. 1999; Morasch et al. 2001; Poulson & Naraoka 2002; Mancini et al. 2003; Hunkeler et al. 2003; Marchesi et al. 2013). Solano et al. (2014) were the first to characterize C and H isotope fractionation during the oxidation of BTEX compounds by persulfate. Also, the use of isotope fractionation of sulfur (S) and oxygen (O) for assessment of microbial sulfate reduction has been reported in the literature (Strebel et al. 1990; Bolliger et al. 2001; Schroth et al. 2001; Detmers et al. 2001; Canfield 2001; Song et al. 2002; Knöller et al. 2006).

In the present study, carbon and hydrogen isotopic data (δ^{13}C and δ^{2}H) were used to characterize the fate of the BTX compounds and to identify the dominant mass removal process during the experiment. For this purpose, the isotope data in BTX were evaluated using the isotopic fractionation factors reported in the literature for oxidation of BTX by persulfate and for biodegradation of BTX. To investigate the occurrence and extent of the subsequent microbial sulfate reduction process, the evolution of oxygen and sulfur isotopes (δ^{18}O and δ^{34}S) in sulfate were also tracked.

2.2.2 Molecular Biology Tools

Molecular biology-based EMDs are a collection of analytical techniques that provide information on the biodegradation activity of the indigenous microorganisms. To biodegrade a certain contaminant, microorganisms need to have specific genetic information (genes) that encode a particular biochemical activity. Gene expression is the process by which information from a gene is used to synthesize proteins/enzymes that define the functionality of that microorganism. Genetic information flows from cell DNA (Deoxyribonucleic acid) into proteins/enzymes, which define the function of a

given microorganism. This flow of information occurs through the sequential processes of transcription (DNA to RNA (Ribonucleic acid)) and translation (RNA to proteins/enzymes). Various EMD techniques are available to detect and quantify either the existence of the genes themselves (e.g., qPCR technique) or the products of the genes when they are expressed and lead to a biodegradation activity (e.g., enzymes and/or metabolite detection technique) (ITRC 2011). In this study, the qPCR technique and specific metabolite detection were utilized to investigate the evolution of microbial processes in the persulfate/EBR treatment train.

2.2.2.1 Detection of Functional Genes using qPCR Technique

qPCR is a technique that selectively amplifies and quantifies the abundance of targeted microorganisms or expressed genes by extracting the DNA or RNA (Ribonucleic acid) from a groundwater sample (RNA is the transcribed form of the DNA). RNA translation into specific enzymes enables the microbial cells to degrade specific contaminants under specific redox conditions. The advantage of the RNA-based qPCR (also known as RT-qPCR) over the DNA-based qPCR is that the former can distinguish the active cells from the dead cells which, despite containing the target gene, are not transcribing the gene (i.e., are not metabolically active). Only the transcribed cells are metabolically active and capable of a specific biodegrading activity. The resulting metric from qPCR is the number of copies of specific genes or DNA/RNA targets present in a liter of groundwater (ITRC 2011). The key target genes need to be carefully selected based on the contaminant type and expected biodegradation pathway as the qPCR technique requires specific primers to selectively amplify and detect the low-abundance target genes in a sample containing millions of other genes.

Development of qPCR techniques for the detection and quantification of the genes associated with the anaerobic degradation of BTEX compounds is still emerging. Only a limited number of such genes have been sufficiently characterized to qualify as robust genetic biomarkers (Beller et al. 1999; Beller et al. 2002; Hosoda et al. 2005; Sun et al. 2014). Beller et al. (2002) were the first to report on the use of qPCR to assess the anaerobic biodegradation of BTEX compounds. They developed a qPCR method to detect and quantify the catabolic gene Benzylsuccinate Synthase (bssA) which encodes a key enzyme known to initiate anaerobic degradation of benzene, toluene and xylene. The bssA gene has been detected in BTX degrading cultures under a wide variety of anaerobic electron accepting conditions, including but not limited to sulfate-reducing conditions (Beller et al. 1996;

Beller & Spormann 1999; Rabus & Heider 1998; Kane et al. 2002). Hence, bssA was selected as an important catabolic biomarker gene for assessing anaerobic biodegradation of BTX in this study.

The qPCR technique was also used in this study to also quantify the following four other functional genes which are highly specific to the degradation of BTX (Table 2.2(a)): (1) toluene dioxygenase (todC) which is associated with BTX aerobic degradation, (2) anaerobic benzene carboxylase (abcA) which is associated with benzene anaerobic degradation, and (3) dissimilatory sulfate reductase (dsrA, dsrB) which are genes associated with the microorganism exclusively consuming sulfate for their activity and growth (Spormann & Widdel 2000; Williams & Sayers 1994; Weelink 2008; Beller et al. 2008; Piskonen et al. 2008; Abu Laban 2009; Plugge et al. 2011; Chin et al. 2008; Villanueva et al. 2008). In pure culture studies, it has been shown that the abundance of the dsrA and dsrB genes is directly correlated to the rates of toluene sulfate reduction (Chin et al. 2008; Kazy et al. 2010; Neretin et al. 2003). Thus, the evolution of these particular genes was used to quantify the impact of persulfate on the population and activity of BTX-degrading sulfate reducers

2.2.2.2 Specific Metabolite Detection

Biodegradation of the organic compounds is a multi-step metabolic process that is facilitated by specific proteins and enzymes encoded in a cell DNA. Under various redox conditions, different microorganisms produce different enzymes according to their genetic information, and each enzyme leads to production of specific metabolites. Therefore, during biodegradation and before complete mineralization, several intermediate metabolites may form. The primary metabolite of any biodegradation pathway (aerobic or anaerobic) appears in the early stages of metabolism and is generally compound-specific. The detection of known primary metabolites indicates active biodegradation of a specific compound under a specific redox condition (ITRC 2011). The key metabolites monitored in this study are listed in Table 2.2(b). Benzene-1, 2-cis-dihydrodial and toluene-cis-dihydrodial are the major metabolites that are expected to form during aerobic BTX biodegradation (Junca & Pieper 2005; Gülensoy & Alvarez 1999; Mikesell et al. 1993). Benzylsuccinate and 2-Methylbenzyl succinate (2-MeBS) are the common metabolic by-products from biodegradation of benzene, toluene and xylene under various anaerobic conditions (Oka 2009; Hess 1988; Beller et al. 1992 (a,b); Beller & Spormann 1999; Kane et al. 2002; Lee et al. 1995; Spormann & Widdel 2000; Agrawal & Gieg 2013). Association of the anaerobic metabolites Benzylsuccinate and (2-MeBS) with biodegradation of toluene and o-xylene under sulfate reducing

conditions have been reported (Beller et al. 1992(a,b); Junca & Pieper 2005; Suflita et al. 2004). Other monitored metabolites (Benzoate, Phenol, 2,3-dimethylphenol, o-, m- and p-Cresol, and Benzyl alcohol (aerobic/anaerobic toluene and xylene) were categorized as ambiguous, implying they could form as a result of more than one specific enzymatic pathway of BTX biodegradation (Smith 1990; Yerushalmi et al. 2001; Junca & Pieper 2005). In combination with geochemical data (e.g., DO levels and/or Eh) and isotope analysis, monitoring of these metabolites can also provide important information about the ongoing microbial pathways.

2.3 SITE DESCRIPTION

This pilot-scale experiment was conducted in a sheet pile-walled gate at the University of Waterloo Groundwater Research Facility at the Canadian Forces Base (CFB) Borden located near Alliston, ON. As shown in Figure 2.3(a, b, c), the experimental gate used was 2 m wide and 24 m long, and was enclosed on three (3) sides by sheet piling driven 3 m below the ground surface (bgs) into the underlying aquitard. The fourth side was open to allow ambient groundwater to enter. Four (4) source wells installed at the gate entrance (fully screened, 25.4 cm diameter) were used to introduce a source of PHCs into the system. A pump was installed in the well at the downgradient closed end of the gate (fully screened, 5.1 cm diameter) to control the groundwater flow rate.

The monitoring network consisted of six (6) fence lines at various locations along the length of the gate (identified as Row 1 to Row 6). Each row consisted of three (3) multilevel monitoring wells (identified as left, middle and right). The wells in each row were spaced 0.65 m apart and each was equipped with four (4) multilevel sampling points spaced vertically at 0.7 m intervals. For persulfate delivery, three (3) wells (fully screened, internal diameter of 5.1 cm) were installed between Row 1 and Row 2 (Figure 2.3(a, e)).

The unconfined Borden aquifer is a surficial, well-sorted fine to medium-grained sandy aquifer with a hydraulic conductivity of 6.0×10^{-6} to 2.0×10^{-4} m/s. Micro-scale heterogeneities exist in the form of silty sand and coarse sand lenses (Mackay et al. 1986). General hydrogeological properties and background geochemistry of the Borden aquifer have been extensively characterized (e.g., MacFarlane et al. 1983; Nicholson et al. 1983; Mackay et al. 1986). The fraction of organic carbon (f_{oc}) of the aquifer sand is 0.0002, and the aquifer porosity is approximately 0.33. The background

concentration of SO_4^{2-}, Na^+, Ca^{2+}, and H_2S varies from 10 to 30 mg/L, 1 to 2 mg/L, 50 to110 mg/L, and <0.002 to 0.1mg/L, respectively. The groundwater pH is in the range of 7 to 8.

2.4 EXPERIMENT PHASES

2.4.1 Plume Generation (Phase 1)

To facilitate the controlled release of the selected PHC compounds at the gate entrance, a series of Waterloo Emitters™ (Solinst® Model 703) were placed into the source wells (Figure 2.3(d)). Each emitter device consisted of 46 m of low-density polyethylene (LDPE) tubing (6.4 mm in diameter) coiled around a central PVC frame (130 cm in length, 15 cm in diameter). The mass transfer from an emitter is controlled by molecular diffusion (driven by the concentration gradient between the source solution circulating inside the emitter tubing and the by-passing ambient water) and advection (driven by the flow rate of the by-passing water) (Arildskov & Devlin 2000; Wilson & Mackay 1995). The purpose of the passive emitters was to maintain a continuous transfer of PHC compounds from the source solution into the groundwater passing through the wells.

A Waterloo Emitter™ was initially tested in the laboratory to determine a suitable composition for the PHC source solution and to estimate the potential concentration of the selected PHC compounds in the surrounding groundwater under field conditions. As a result of this testing effort, benzene, toluene and xylene (BTX) were selected as the constituents in the source solution. It was observed that large organic molecules, such as ethylbenzene, naphthalene, ethanol and Methyl tert-butyl ether (MTBE), could not diffuse out of the emitters at a measurable rate. Also the tests showed that with a BTX-saturated source solution (i.e., BTXs concentration in the solubility range), the concentrations of BTX in the surrounding well water were in the range of 5-20 mg/L. To achieve a BTX-saturated source solution, ethanol (10%) was mixed as a co-solvent in the source solution.

Within the experiment gate, eight (8) Waterloo Emitters® were placed inside the four (4) source wells (two emitters per well stacked on top of each other) to create a semi-uniform steady source of dissolved BTX compounds. To recirculate the source solution, each pair of emitters was connected to a 3.2 mm diameter stainless steel tube which in turn was connected to a corresponding source tank. Each source tank contained 90 L of water and 10 L of ethanol spiked with the BTX mixture. The initial concentration of benzene, toluene and xylene in the source tanks was 380, 320 and 70 mg/L, respectively. The source solution was pumped at a rate of ~50 mL/min through the emitters on a

timed cycle of six (6) hours circulation followed by six (6) hours no circulation. The source tanks were sealed, and the stock solution was stirred periodically with a drill-adapted mixing rod. As the stock solution was re-circulated, the BTX concentration in the source tanks would deplete over time due to the loss of BTX mass into the source wells. To maintain the BTX concentration at a quasi-constant level in the source wells, the tanks were occasionally replenished by adding 10 L of the ethanol/BTX mixture to each tank (replenishment frequency was about 50 days).

The groundwater flow rate was controlled by the extraction well located at the closed end of the experimental gate. To estimate the groundwater velocity, a tracer test was conducted by injecting a slug of a sodium chloride (NaCl) solution directly into the four source wells to reach a target chloride (Cl^-) concentration of 100 mg/L. The transport of chloride was monitored downgradient of the source wells, and the resulting breakthrough data were used.

2.4.2 Chemical Oxidation (Phase 2)

Phase 2 of the experiment involved two injections of sodium persulfate into the BTX plume using a modified cross-injection system (CIS) (Devlin & Barker 1996; Gierczak et al. 2007; Critchley 2010), installed between Row 1 and Row 2 (Figure 2.3(a,e)). The persulfate solution was injected into the two outside CIS wells while groundwater was simultaneously extracted from the central CIS well and transferred to a polyethylene (PE) waste tank. Each injection episode was used to create a persulfate slug a short distance downgradient of the CIS wells. The extent of the ChemOx zone, confined between the two persulfate pulses, depends on the groundwater flow rate. An interval of 10 days between each injection episode was selected so that the fate of the ChemOx zone (e.g., depletion of persulfate and BTX, production of sulfate, and geochemical shifts) could be captured in the first monitoring row downgradient of the CIS wells (i.e., Row 2).

An intended outcome of Phase 2 was to partially destroy the BTX mass in the ChemOx zone, so that the remaining substrate would serve as the carbon/energy source for the subsequent microbial activities. To estimate the amount of persulfate required to destroy ~50% of the mass confined in the ChemOx zone, the BTX mass in this zone was estimated from the BTX mass discharge across Row 1 and using reaction stoichiometry between persulfate and the individual compounds.

A series of simulations using the MODFLOW (McDonald & Harbaugh 1988) and MT3DMS (Zheng & Wang 1998) numerical engines were performed to aid in the selection of

injection/extraction rates and the duration of each injection episode. Representative transport parameters for the Borden aquifer (e.g., hydraulic conductivity, porosity, longitudinal/transverse dispersivity, etc.) were obtained from the available literature (Schirmer et al. 2000; MacQuarrie et al. 1990; Devlin et al. 2002). The rate of persulfate decomposition due to reactions with aquifer material was derived from Sra et al. (2013a). The modelling results suggested that for a semi-uniform persulfate distribution between the CIS injection and extraction wells, a pulsing duration of three hours, an injection rate of 0.5 L/min at each injection well, and an extraction rate of 1 L/min at the CIS extraction well were required.

The injection solution (10 g/L unactivated sodium persulfate ($Na_2S_2O_8$)) was prepared by mixing sodium persulfate (Sigma-Aldrich, St. Louis, MO) with uncontaminated groundwater. The solution was stored in a polyethylene tank and was mechanically stirred using an electric drill mixer to enhance dissolution. The injection/extraction pumps were equipped with a ball-valve flow controller. A manifold was used to distribute the injection solution into two Teflon tubes connected to the injection wells. Each of these outlets was equipped with a flow control gate valve, a vent valve and a pressure gauge to enable flow control during injection. PE pipes were used to connect the manifold outlets to the riser pipes of the three CIS wells.

2.4.3 Extended Monitoring (Phase 3)

The performance assessment of the combined treatment system was continued for long term following the persulfate injection. The purpose of the extended monitoring phase was to monitor the fate of the ChemOx and EBR zones, to evaluate the long-term impact of persulfate on the subsequent microbial processes and to identify the dominant mass removal process long after persulfate treatment. As mentioned earlier, a host of parameters were monitored in groundwater samples collected from the network of the monitoring rows throughout the three phases of this experiment. These included BTX and methane concentrations, selected inorganic (e.g. SO_4^{2-}, Na^+, Ca^{2+}, S^{2-}) concentrations, dissolved inorganic carbon (DIC) content, and geochemical indicators. Moreover, samples were collected for isotopes (CSIA and sulfate) and molecular biology analyses.

2.5 SAMPLING METHODS

Groundwater samples were collected at multilevel locations using a peristaltic pump and a sampling manifold (Mackey et al., 1986). Prior to collecting samples, each sampling point was purged ~80 mL

to flush the water inside the tubing and the sampling manifold to ensure the collected samples represent the groundwater adjacent to the sampling point. Samples for persulfate analysis were collected in 25 mL glass vials and those for inorganic analyses were stored in 20 mL polypropylene vials. Samples collected for cation analyses were filtered with a 0.45 µm Acrodisc® syringe membrane filter, and acidified with nitric acid (Sigma-Aldrich, St. Louis, MO) to a pH < 2. Samples for VOC analysis and samples for C/H isotopic analyses were collected in 40 mL glass vials and were preserved with 0.4 mL of a 10% sodium azide solution (Acros Organics). Samples for isotope analysis of sulfate were collected in 1 L glass bottles without addition of preservatives. Samples for analysis of metabolites were collected in two, 500 mL glass bottles at each sampling point. The metabolite samples were immediately preserved by adding HCl (J.T.Baker) to one of the bottles with a pH target of < 2, and NaOH (Fisher Scientific) to the other bottle with a pH target of ~8. All samples were stored at 4°C and held for up to 14 days prior to analyses. The sample for qPCR analyses was collected by passing 2 L of groundwater through a 0.2 µm Sterivex® filter. The filter was then frozen immediately, and stored at -80°C until further processing.

2.6 ANALYTICAL METHODS

2.6.1 Organic/Inorganic Analyses

BTX concentrations were determined using a micro-extraction gas chromatographic technique first proposed by Henderson et al. (1976). The sample (5 mL) was solvent extracted (by addition of 2 mL methylene chloride) before being injected into a HP 5890 capillary gas chromatograph (GC) equipped with a HP 7673A autosampler, a flame ionization detector (FID) and DB-5 capillary column. Three (3) µL of methylene chloride was injected in splitless mode (purge on 0.5 min, purge off 10.0 min) onto a 0.25 mm (Ø) × 30 m (L), DB5 capillary column with a stationary phase film thickness of 0.25 µm. The helium column flow rate was 2 mL/min with a make-up gas flow rate of 30 mL/min. The injection temperature was 275 ºC while the detector temperature was 325 ºC. The initial column oven temperature was 35 ºC held for 0.5 min, then ramped at 15 ºC/min to a final temperature of 300 ºC and held for 2 min. The chromatographic run time was 10 minutes. Data integration was completed using Peak Simple® software. The method detection limit (MDL) for benzene, toluene and xylene was 1.1, 0.83 and 0.37 µg/L, respectively. Calibration and quality control/assurance (QC/QA) was

based on the methods described elsewhere (Henderson et al. 1976; Longbottom & Lichtenberg 1982; Glaze et al. 1983). Precision was estimated by comparing the analyses of duplicates.

Methane was analyzed using a Varian 3800 gas chromatograph equipped with a FID and a 30-m Megabore® GS-Q capillary injector. The GC was equipped with a 2 mL sample loop, a 30 m Megabore® GS-Q capillary column (with helium flowing at 12 mL/min serving as the carrier gas) and an oven temperature of 100 ºC. The injector temperature was 100 ºC, and the FID temperature was 200 ºC. Sample preparation/analysis, calibration and QA/QC were performed following methods described elsewhere (Wilhelm et al. 1977; Kampbell et al. 1989; Kampbell & Vandegrift 1998). The MDL for methane was 0.3 µg/L. Data integration was completed with the Varian Star chromatography workstation software®.

Persulfate was measured following the approach of Huang et al. (2002) and also described by Sra (2010). Analytical reagents were prepared by adding a 0.1 mL solution of 0.4 N ACS grade ferrous ammonium sulfate (FAS) (EMD, Gibbstown, NJ), 0.6 N ammonium thiocyanate (NH_4SCN) (J.T.Baker, Phillipsbourgh, NJ) and sulfuric acid (H_2SO_4) (EMD, Gibbstown, NJ) into 0.9 mL of Milli-Q water. The absorbance was read with a spectrophotometer at a wavelength of 450 nm. The MDL for persulfate was 250 mg/L.

Anions/cations were analyzed using a Dionex® ICS2000 Ion Chromatograph equipped with an ion-eluent generator and conductivity detector. For anions, a 25-µL sample was injected using a Dionex AS-40 Autosampler onto a Dionex® Ion Pac AS11-HC (4 × 250 mm) column. The mobile phase was 30 mM potassium hydroxide (KOH) at a flow rate of 1.0 mL/min. For cations, a 25 µL sample was injected using a Dionex IonPac® CS-12A column (4 × 250 mm). The mobile phase used was a 22.5 mM methanesulfonic Acid (MSA) at a flow rate of 1.0 mL/min. The chromatograph was obtained using Dionex Chromeleon software®. The MDL for anions was 0.5 mg/L, while for cations it ranged from 0.8 to 1.1 mg/L. Precision was estimated by comparing the analyses of duplicates. A YSI® Pro Plus Multi parameter meter was used to simultaneously measure DO, EC, Eh, pH and temperature. The device was calibrated prior to each monitoring event according to the manufacturer instructions. Field measurements of dissolved sulfide (methylene blue method, Hach method 8131) were conducted on a Hach® DR/2400 portable spectrophotometer.

Dissolved $CO_{2\,(aq)}$ was estimated based on the total alkalinity test (results reported as mg/L $CaCO_3$). The method involved titration of a 5 mL groundwater sample with 0.02 N sulfuric acid (J.T.Baker,

Phillipsbourgh, NJ) and a few drops of bromocerosel green reagent until the blue color changed to green. The dissolved inorganic carbon (DIC, sum of H_2CO_3, HCO_3^- and CO_3^{2-}) concentration was estimated from alkalinity and pH (Stumm and Morgan, 1981).

2.6.2 Isotope Analysis

2.6.2.1 Carbon Isotope Ratio ($^{13}C/ ^{12}C$)

Carbon isotope ratios for BTX were analyzed using an Agilent™ 7890a GC coupled to an Isoprime™100 isotope ratio mass spectrometer (IRMS) via an Isoprime® GC5 combustion interface. A pre-concentration step was performed using a purge-and-trap module (Stratum Teledyne Tekmar). Twenty-five (25) mL of the sample was purged with gas-phase N_2 (40 mL/min) and the degassing volatile organic carbon (VOC) was accumulating on a Vocarb® 3000 adsorbing matrix (VICI). Ten (10) min after the purge step, the VOC was transferred into a cryogenic trap (Tekmar Dohrmann) installed at the entry of the GC column. Once the transfer was completed, a sudden increase in temperature (from -80°C to 180 °C) was applied to release the concentrated mass of VOC in the column (DB-VRX, 60 m, 0.25 mm, 1.4 μm). The initial temperature of the GC oven was set to 90 °C followed by ramping at 7 °C/min to reach a final temperature of 200 °C and held for 2 minutes. Helium was use as the gas carrier (1.2 mL/min). Each sample was analyzed in duplicate. The analytical error for carbon isotopes analysis was ± 0.2 ‰.

2.6.2.2 Hydrogen Isotope Ratio ($^2H/^1H$)

The hydrogen isotope ratio of BTX was analyzed using a purge and trap (P&T) module (Tekmar Velocity, USA) connected to a TRACE® gas GC which in turn was coupled to a ThermoFinnigan Delta® Plus XP isotope-ratio mass spectrometer via a ThermoFinnigan® GC combustion III interface. A cryogenic trap device (Atas) was used to concentrate the analyte into a narrow band. The column used in this analysis was a DB-VMS (30 m, 0.25 mm, 1.4 μm). The initial temperature of the GC oven was set to 50 °C and held for 3 minutes, followed by increasing at a rate of 5 °C/min to reach 130 °C. Helium was used as the carrier gas (1.7 mL/min). Each sample was analyzed in duplicate. The analytical error for hydrogen isotope analysis was ± 4 ‰.

2.6.2.3 Sulfur ($^{34}S/^{32}S$) and Oxygen ($^{18}O/^{16}O$) Isotope Ratio

To determine the sulfur and oxygen isotope signatures of the remaining sulfate (SO_4^{2-}), the dissolved sulfate in a sample was precipitated as $BaSO_4$ with the addition of 1.0 M $BaCl_2$+2H_2O in an acid media (pH < 2) to prevent $BaCO_3$ precipitation. The purified $BaSO_4$ was then weighed (300- 400 mg) and poured into a tin capsule along with a 10-fold excess of Nb_2O_5 and combusted at 1000 °C in a Costech® element analyzer (EA) to produce SO_2. The produced SO_2 was carried with a helium stream to a Micromass® IsoChrom-IRMS for $\delta^{34}S$ analyses (±0.3‰). For analysis of $\delta^{18}O$ (±0.5‰), the purified $BaSO_4$ was weighed into a tin capsule and combusted in a HEKAtech® Pyrolysis furnace (with the temperature of 1350 °C) to produce CO and then carried with a helium stream to a GVI® IsoPrime-IRMS. The analytical errors for ^{34}S and ^{18}O analysis are ± 0.3 and ±0.5 ‰.

The isotope data are expressed using the delta per mil notation δ (‰) and mathematically described by:

$$\delta_x(‰) = \left(\frac{R_x}{R_{reference}} - 1 \right) \times 1000 \qquad (2.2)$$

where R_x is the isotopic ratio of element x (eg. $^{13}C/^{12}C$ or $^{2}H/^{1}H$) and $R_{reference}$ is the isotopic ratio of an internationally agreed-upon standard.

2.6.3 Molecular Biology Analysis

2.6.3.1 Extraction and Analysis of RNA/DNA using the qPCR Technique

A modified phenol-chloroform/bead-beating method described by Griffiths et al. (2000) was used to simultaneously extract DNA and RNA from groundwater biomass. All vessels and reagents used for RNA processing were either certified ribonuclease (RNase)-free, treated with RNase ZAP (Ambion, Austin, TX), or treated with diethyl pyrocarbonate (DEPC) for inactivation of RNase.

The frozen filters were aseptically transferred to 2-mL Lysing® Matrix E tubes along with a 0.5-mL hexadecyltrimethylammonium bromide (CTAB) buffer (including 10% CTAB in 0.7 M NaCl, 240 mM potassium phosphate buffer, pH 8) and a 0.5-mL phenol:chloroform:isoamylalcohol (25:24:1). The tubes were homogenized for 30 sec in a Mini-Bead Beater-8 instrument (Biospec Products), and then centrifuged at 16,000 g for 5 minutes at 4 °C. The aqueous layer was then transferred to a new

1.5-mL Eppendorf® tube containing an equal volume of chloroform:isoamylalcohol (24:1), vortexed and then centrifuged again. The aqueous layer was transferred again to a new tube containing two volumes of 30% (wt/vol) polyethylene glycol 6000/1.6 M NaCl. RNA/DNA was precipitated at 4 °C overnight and their pellets were collected by centrifugation (10 min, 16,000 g, 4 °C), washed with ice-cold 70% ethanol, air-dried, and resuspended in 30 µl DNAse/RNAse-free water. Total nucleic acid concentration was determined using a Nano Drop Spectrophotometer (Thermo Scientific, Waltham, MA). The DNA/RNA extracts were stored at -80°C prior to further processing.

To analyze the RNA extracts for quantifying the abundance of the target genes, the qPCR analytical technique described by Yagi et al. (2010) was used. The extracts were adjusted to 1 µg total nucleic acid. The DNA was removed by DNase I treatment (Invitrogen), and RNA was reverse transcribed to complementary DNA (cDNA) using the SuperScript® III First-Strand Synthesis System for RT-PCR (Invitrogen) according to the manufacturer instructions. Control PCRs with no RT were performed using primers and PCR conditions described below to ensure complete removal of contaminating DNA. The DNA fragments associated with the target genes bssA, todC, abcA, and dsrB were quantified in 25 µL reactions using an AB7300 Real-Time PCR system and either a Power SYBR® Master Mix or SYBR® Select Master Mix (Applied Biosystems). The list of primers for each specific gene and the amplification factors used in this study are presented in Appendix A. Finally, the standard curves were prepared from purified gene standards and "no template controls" were included for each analysis. A melting curve analysis was performed to verify target amplification.

2.6.3.2 Specific Metabolite Detection

To determine the concentration of metabolites present in a groundwater sample, 200 mL of the sample was filtered (Whatman® No. 1) and then processed using Supelclean® Envi-Chrom P solid-phase extraction (SPE) tubes (Supelco, Inc., Bellefonte, PA) at a flow rate of ~50 mL/min to concentrate the metabolites. Prior to processing the sample, all the tubes were conditioned with 5 mL of ethyl acetate and methanol and then were water rinsed. Aliquots of these extracts (100 mL) were derivatized with either a 10 µL solution of 10 mg of 1-butaneboronic acid/mL of acid-free ethyl acetate, or a 25 µL of a BSTFA solution (N,O-Bis(trimethylsilyl)trifluoroacetamide).

The extracted sample (1 µL) was then injected into a Hewlett-Packard® Model 6890 GC equipped with a fused silica capillary column (30 m × 0.25 mm × 0.25 µm (film thickness)) HP-5 (5% phenylmethyl silicone; Hewlett-Packard). The column was connected to a Hewlett-Packard Model

5973 quadrupole mass selective detector operated at an electron energy of 70 eV and a detector voltage of 2000-3000 V. A splitless injection was used with a 1-min delay before septum purge. The carrier gas was helium at a linear gas velocity of 30 cm/s. The injector and detector temperatures were 250 and 300 °C, respectively. The ion source pressure was maintained at 1.33×10^{-3} Pa. The oven temperature program began at 40 °C and increased to 250 °C at a rate of 10 ºC/min. Metabolites were identified by co-elution with reference compounds and by comparison of mass spectra with published data. De-ionized water served as a negative control and was processed and analyzed identically to the groundwater samples.

2.7 RESULTS AND DISCUSSION

Figure 2.4 shows a detailed timeline of the pilot-scale experiment, and the various groundwater sampling events. The generation of the BTX plumes began on Day 0 by turning on the extraction pump and allowing the transport of BTX compounds from the source tanks to flow into the emitters installed in the source wells. The two persulfate pulsing episodes were conducted on Day 170 and Day 180. Due to the onset of winter conditions, the system was shut-down on Day 221 by turning off the extraction pump and the flow to the emitters. Extended monitoring was continued until Day 391.

2.7.1 Phase 1- Plume Generation

On Day 0, the groundwater extraction rate was set to 125 mL/min to establish a theoretical Darcy groundwater velocity of 9 cm/day (equal to the ambient groundwater velocity in the Borden aquifer) based on the extraction rate and aquifer properties (e.g., porosity and aquifer thickness). The conservative tracer test which was performed by adding NaCl into the source wells over a two-week period (Days 5, 14 and 20) created a slug of tracer downgradient. Chloride concentrations were monitored at 12 points in Row 1, and the groundwater velocity was back-calculated based on the observed travel time of the chloride peak and distance between source wells and Row 1. The estimated groundwater velocity from the observed tracer breakthroughs ranged from 7 to 12 cm/day across the 12 monitoring points. Since the theoretical Darcy velocity approach was consistent with the estimate from the tracer test data, it was used during the course of this experiment to estimate the theoretical velocity in the gate.

Figure 2.5 shows the groundwater depth and the corresponding theoretical velocity as well as the evolution of total BTX concentration in the source tanks and source wells during the plume

generation phase. The concentration data used are the average BTX concentration in the four source wells and four source tanks. The observed concentrations in each individual source tank and well did not show significant variation from the average values. The average concentration of benzene, toluene and xylene in the source wells during the plume generation phase was approximately 55 mg/L, 40 mg/L and 10 mg/L, respectively.

The development of the BTX plumes until Day 156 (before persulfate injection) is shown in Figure 2.6. The non-uniform distribution of BTX concentrations across the gate cross-section, which was also observed for the chloride plume (data not shown here), indicates the existence of preferential flow pathways which result from the mildly heterogeneous nature of the aquifer (Mackay et al. 1986; Cherry et al. 1996; King & Barker 1999; Devlin et al. 2002). By Day 97 the front of the BTX plume had only reached Row 2 (located only 4 m downgradient of the source wells, while based on the average groundwater velocity the expected advective front was expected to be ~9 m from source wells (past Row 3). The stalled plume development between Day 57 and Day 97 was confirmed by (see also Figure 2.7): (1) decreased BTX concentrations at Row 1 (between Day 57-71) while the source well concentrations were continually increasing, (2) decreased BTX concentration at Row 2 (between Day 71-97) while the mass discharge from Row 1 was continuing, and (3) no detected BTX mass at Row 3 located 7.5 m downgradient the source wells. Early plume development was being hindered by sorption and biodegradation. The BTX retardation factors (R) for the Borden aquifer range from 1.2 to 2 (Schirmer et al. 2000; MacQuarrie et al. 1990) and thus slowed the development of plume. In addition, substantial biodegradation in the vicinity of Row 1 and Row 2 was confirmed by the decreased DO and Eh levels (Figure 2.8(a, e)), and supported by the detection of metabolites specific to both aerobic and anaerobic BTX biodegradation (e.g. benzene- and toluene-cis dihydrodiol (CDHD), m- and o-Cresol, 2-MeBS and phenol) (Figure 2.9(a-f)). The presence of both aerobic and anaerobic metabolites at Row 1 on Day 97 suggests that aerobic degradation dominated the BTX mass removal initially and once oxygen was depleted, anaerobic biodegradation prevailed.

Since the intended result from the plume generation phase was to develop a quasi steady-state BTX plume and establish anaerobic conditions throughout the experimental gate, the groundwater extraction rate was increased to 425 mL/min on Day 110 to counterbalance the impact of biodegradation processes on plume development. As a result, the migration of the plume was significantly enhanced, and by Day 126 the BTX plume had reached Row 4 (Figure 2.6). On Day

140, the extraction rate was reduced to ~150 mL/min (15 cm/day) and held constant until Day 221, at which point the groundwater flow was permanently stopped.

By Day 156 (the last sampling event before persulfate injection) the BTX plume had reached Row 5 (Figure 2.6), dissolved oxygen was depleted (DO < 2 mg/L) and reducing redox conditions prevailed through the entire the experimental gate (-200 mV < Eh < -50 mV) (Figure 2.8). The increased BTX concentrations at Row 4 and Row 5 on Day 156 (Figure 2.7) is attributed to the increased mass discharge from the upgradient rows following the increase in flow rate; however, a decrease in BTX concentration was observed at Rows 1, 2 and 3 after Day 110. This decrease is attributed to the mixed effect of decreased mass transport from the source wells and increased microbial activities as explained in the following. The occurrence of anaerobic biodegradation at Rows 1 to 3 after Day 110 and prior to persulfate injection was confirmed by the detection of a high concentration of anaerobic metabolites (e.g., benzylsuccinate and 2-MeBS, Phenol and benzoate) at as well as detection of bssA-mRNA transcripts associated with anaerobic BTX biodegradation at Row 2 on Day 156 (see Table A2 in Appendix A). In addition, apparent sulfate reducing conditions were present in the vicinity of Rows 2 and 3 as suggested by the concurrent depletion of the background sulfate and the production of sulfide by Day 156 (Figure 2.8(b, h)).

The above observations demonstrate the development of a quasi steady-state BTX plume, the establishment of anaerobic conditions and manifestation of mass removal due to biodegradation processes across the experimental gate prior to first persulfate injection on Day 170. The benzene plume had migrated beyond Row 5 (~18 m downgradient) while the toluene and xylene plumes lagged behind likely due to their higher sorption and biodegradability relative to benzene (Schirmer et al. 2000; Schirmer & Butler 2004).

2.7.2 Chemical Oxidation Phase

The first persulfate pulsing episode was conducted on Day 170. During this 3 h episode, groundwater samples were collected and EC measurements were taken every 20 min. EC was elevated in all the CIS wells, however, the increase was much more pronounced (~20 times higher) in the injection wells than in the central extraction well. The persulfate concentration in the injection wells was much higher than that in the extraction well (10.3 g/L vs <1 g/L). To decrease this gap and create a more uniform persulfate slug, the duration of the second episode (executed on Day 180) was increased to 5 h. An interval of 10 days was selected between the two injection episodes to ensure that the ChemOx

zone was of sufficient length by the time it reached Row 2. This interval was based on the estimated groundwater velocity at the time of persulfate injections (15 cm/day), the distance between the CIS wells and Row 2 (1.5 m), and assuming negligible retardation for persulfate and sulfate.

As a result of the two injection episodes, a total of ~4.7 kg of persulfate was estimated to have being present initially in the gate in two slugs (considering the extracted persulfate mass from the middle CIS well). The increased EC and Eh levels at Row 2 following persulfate injection (Figure 2.8(c, e)) as well as the observed breakthroughs of persulfate and Na^+ (Figure 2.10) demonstrates the extent of the ChemOx zone as it passed across Row 2. Only persulfate peak (on Day 196) and sodium peak (on Day 208) was observed at Row 2 suggesting that the two persulfate slugs had coalesced before reaching Row 2 as designed. The retardation of Na^+ compared to persulfate (Figure 2.10) is attributed to the cation exchange capacity of the Borden aquifer material which results to Na^+ attenuation (Sra et al. 2013a).

The maximum fence-averaged persulfate and sodium concentrations observed at Row 2 were ~0.5 g/L for both. The maximum concentration observed at a single sampling point was ~3 g/L for persulfate and ~0.8 g/L for Na^+. The much lower persulfate and sodium concentration observed at Row 2 compared to the averaged concentrations observed in the CIS wells (8.3 g/L for persulfate and 1.8 g/L for sodium) indicates that significant mixing occurred between the injected solution and ambient groundwater, and perhaps for persulfate some decomposition as a result of ongoing reactions with BTX compounds and aquifer materials. By Day 221, the persulfate concentration at Row 2 (Figure 2.8(f)) was non-detectable indicating that the ChemOx zone had dissipated.

The persulfate decomposition in the ChemOx zone led to a significant increase in the fence-averaged sulfate (SO_4^{2-}) concentrations at Row 2 shortly after persulfate injection (Figure 2.8(g)). The increased sulfate concentration at Row 2 was first observed on Day 180 and peaked on Day 208. The produced sulfate plume passed Row 2 and reached Row 3 by Day 221. The mass ratio between SO_4^{2-} and Na^+ was estimated based on the peak fence-averaged concentration of these two compounds at Row 2. The consistency between the estimated ratio (~4) and the theoretical stoichiometry (4.2 g SO_4^{2-} per 1 g of Na^+) confirms the near complete decomposition of the injected sodium persulfate.

Oxidation of BTX by persulfate, if it proceeds to complete mineralization, leads to production of dissolved $CO_{2(aq)}$ and hydrogen ions (H^+), which in turn is expected to elevate DIC concentrations and decrease pH. Figure 2.8 (i, d) shows an increased DIC concentration and a decreased pH at Row 2

which supports the occurrence of chemical oxidation. The pH at Row 2 returned to levels prior to persulfate injection by Day 221 (Figure 2.8(d)) due to the high buffering capacity of the calcite-rich Borden aquifer. The increased Ca^{2+} concentrations at Row 2, as shown in Figure 2.8(j), illustrates that the pH drop enhanced calcite dissolution, which led to buffering of the pH. Thus, it is likely that the observed peak in the DIC concentration at Row 2 on Day 196 (Figure 2.8(i)) is the mixed effect of $CO_{2(aq)}$ production during BTX mineralization as well as the increased $CO_{2(aq)}$ during pH-buffering. In summary, the decreased BTX concentrations (Figure 2.7), depletion of persulfate and production of sulfate (Figure 2.8(f, g)), significant increase of Eh, EC and DIC (Figure 2.8(e, c)), as well as the drop of pH (Figure 2.8(d)), are all the geochemical indicators of persulfate oxidation of BTX at Row 2.

Unlike Row 2, the persulfate concentration at Row 3 was negligible (i.e., < MDL). Elevated Na^{+} was not observed at Row 3 until Day 208 at a concentration much lower (10-20 times) than that observed at Row 2, likely due to mixing with low Na^{+} concentration groundwater (dilution) and/or its loss in cation exchange reactions (Dance & Reardon 1983). The changes in EC, Eh and pH were also minimal at Row 3 (Figure 2.8(c, d, e)) indicating that persulfate and thus the ChemOx zone did not reach Row 3. Instead, Row 3 captured the EBR zone as expected in the conceptual design. The increased sulfate concentration at Row 3 which started on Day 208 and peaked on Day 221 confirmed the initiation of the EBR zone by Row 3. Since there was no pre-existing persulfate at Row 3, the slight delayed shifts observed in the geochemical indicators (e.g., pH, EC and Ca^{2+}) at this row (Figure 2.8(c, d, j)) is attributed to groundwater migration from Row 2, which also caused the transport of the sulfate plume to Row 3 (Figure 2.8(g)). There is a good agreement between the observed delay and the expected travel time between Row 2 and Row 3.

2.7.2.1 Impact on Microbial Processes

Between Day 170 to Day 208, while persulfate was present at Row 2, the concentration of the majority of metabolites and the number of copies of bssA genes associated with anaerobic biodegradation of BTX compounds decreased (Figure 2.9(e, f), Table A1). There was also a reduction in the concentration of sulfide (the primary by-product of microbial sulfate reduction) during this period (Figure 2.8(h)). These observations indicate the inhibitory effect of persulfate on the population and biodegradation activity of indigenous microbial communities. The initial inhibition of the microbial processes at Row 2 was short term as the concentration of metabolites and number of the bssA functional gene copies started to rebound by Day 221, when persulfate was depleted in the

gate. The concentration of some metabolites (e.g., phenol, benzoate, benzyl alcohol, o-, p- and m-Cresol) increased to levels even higher than before being exposed to persulfate (Figure 2.9 and Table A1). Although these metabolites were categorized as ambiguous, their presence under low DO levels (< 1 mg/L; Figure 2.8(a)) and simultaneous existence of transcribed bssA gene (associated with anaerobic BTX degradation) strongly suggested that such metabolites were produced through anaerobic pathways. The rebound and stimulation of anaerobic microbial processes at Row 2 was concurrent with a rise in the sulfide concentration (Figure 2.8(h)) and DIC levels (Figure 2.8(i)), all occurring in the between Day 208 to 221. These observations suggest that the consumption of the by-product sulfate through microbial sulfate reduction contributes to the apparent reduction in sulfate concentration during this period (Figure 2.8(g)). Due to the dynamic nature of the system, however, it was not feasible to quantify the contribution of the ongoing processes (i.e., transport and BTX biodegradation) to the observed reduction of sulfate at Row 2.

In summary, it was demonstrated that at Row 2 the microbial processes were temporarily inhibited when initially exposed to persulfate, and rebounded only after ~40 days when the persulfate was completely depleted. The initial inhibition is attributed to the highly oxidized redox condition created after persulfate injection (Figure 2.8(e)) and the biogeochemical shifts following the change of pH (Figure 2.8(d)) that could affect the microbial growth and activity. The enhanced microbial activity (including sulfate reduction) at Row 2 is attributed to: (1) the rebound of subsurface geochemical conditions (e.g., pH, EC and Eh) to levels observed before persulfate exposure (2) incomplete inhibition of microbial processes due to the low dosage and short duration of the persulfate treatment, (3) existence of subsurface heterogeneities and persistence/ growth of indigenous microbes in the dead-end pores, (4) re-inoculation of microbial communities by groundwater flow, (5) increased sulfate concentrations and (6) enhanced biodegradability of the remaining contaminant pool following persulfate treatment (breakdown of BTX compounds into simpler organic substrates following persulfate injections was demonstrated by the additional peaks in gas chromatograms of samples from Row 2, suggesting the formation of simple by-products, potentially low molecular weight acids, in the ChemOx zone). The enhanced microbial activity could also be attributed to the increased nutrient concentrations following persulfate injection. Chemical oxidation has been shown to increase nutrient release in the system through oxidizing the soil organic matter (Sirguey et al. 2008; Westersund et al. 2006).

The evolution of the anaerobic metabolites and functional genes at Row 3 (contained within the EBR zone) was completely different from that in Row 2 (contained within the ChemOx zone). In the period between Day 180 and Day 221 the number of copies of the bssA and dsrB genes, which are associated with the degradation of toluene and xylene under sulfate reducing conditions, significantly increased at Row 3 while apparently being inhibited at Row 2 (Figure 2.9(e, i), Table A2). This confirms the stimulation of microbial sulfate reduction downgradient of the ChemOx zone at Row 3 which resulted in a reduction in the concentration of sulfate observed at Row 3 as compared to Row 2. However, the reduction of the maximum sulfate concentration at Row 3 is not entirely associated with sulfate reduction as mixing (dilution) with low sulfate ambient groundwater or abiotic geochemical processes (e.g., gypsum ($CaSO_4$) precipitation) could also be responsible for this difference.

The maximum population of dsrB and bssA genes observed at Row 3 (888 copies/L and 762 copies/L, respectively) occurred between Day 190 and 196 which corresponds to the height of sulfate reduction activities. However, it is worthwhile noting that the concentration of sulfate continued to remain near zero at Row 3 prior to Day 196 despite the occurrence of microbial sulfate reduction perhaps due to the simultaneous transport and consumption of sulfate at almost equal rates.

Besides detection of bssA and dsrB genes, consumption of sulfate, and elevated sulfide concentrations, the stimulated activity of SRB communities and the formation of the EBR zone at Row 3 was also confirmed by elevated concentrations of anaerobic metabolites such as phenol, p-Cresol and 2-MeBS (Figure 2.9(h, i)), which are reported to be associated with degradation of toluene and xylene under sulfate reducing condition (Junca & Pieper 2005). The enhanced microbial sulfate reduction at Row 3 was attributed to the transport of the excess by-product sulfate and the absence of persulfate, which kept the geochemical conditions (e.g., redox condition and pH) relatively undisturbed at Row 3 compared to Row 2.

2.7.2.2 Reactive Zone Characterization Using CSIA Data

The geochemical and molecular biology data clearly show the occurrence of the two successive reactive zones: chemical oxidation controls mass reduction in the ChemOx zone, while enhanced microbial sulfate reduction dominates the mass loss in the downgradient EBR zone. In many other dynamic systems, however, this may not be easily achievable. Due to the ongoing transport, many of the changes occurring in the ChemOx zone could be reflected in the EBR zone with a lag-time

(controlled by groundwater velocity) which alters the signature of the distinct processes occurring in the downgradient EBR zone. To overcome such difficulties, the coupling of $\delta^{13}C$ and $\delta^{2}H$ data provided complementary information to evaluate the occurrence and differentiate the two reactive zones. To illustrate, the $\delta^{13}C$ and $\delta^{2}H$ data for benzene were compared at two arbitrary points in the ChemOx and EBR zones (i.e., in Rows 2 and Row 3, respectively). Similar $\delta^{13}C$ and $\delta^{2}H$ data for toluene and xylene are presented in Appendix A. As shown in Figure 2.11(a,b), the evolution of $\delta^{13}C$ and $\delta^{2}H$ data between Day 170 and Day 221 at Row 2 was quite different from that at Row 3. A significant enrichment of $\delta^{13}C$ with no major shift in $\delta^{2}H$ was observed at Row 2 where persulfate oxidation was occurring; however, at Row 3, where biodegradation was the main reaction, the isotope data showed a slight enrichment in both $\delta^{13}C$ and $\delta^{2}H$.

The isotope data were further evaluated using the dual isotope approach that provides a picture of the main processes that could be responsible for the degradation of benzene. Based on the isotopic fractionation factors for carbon and hydrogen reported in the literature for persulfate oxidation, and aerobic and anaerobic biodegradation of benzene (Aelion et al., 2009; Hunkeler et al., 2008), Figure 2.12 was prepared and the field data were added. In this figure, $\Delta\delta^{13}C$ and $\Delta\delta^{2}H$ respectively represent the change in the isotopic fractionation of carbon and hydrogen from time zero (in the source solution) to time *t*. The $\Delta\delta^{13}C$ and $\Delta\delta^{2}H$ data clearly demonstrate the distinct evolution of the isotopic fractionation pattern at Row 2 and Row 3. At Row 2, the observed $\Delta\delta^{13}C$/ $\Delta\delta^{2}H$ data from Day 170 to Day 208 are close to the line representing the isotopic fractionation of benzene associated with persulfate oxidation (Solano 2014). This observation confirms that persulfate oxidation was the dominant mass removal process at Row 2 during this period. Starting from Day 221, a deviation from the persulfate oxidation line towards the anaerobic biodegradation area is observed which is due to the depletion of persulfate and enhanced microbial sulfate reduction. For Row 3 however, the clustering of $\Delta\delta^{13}C/\Delta\delta^{2}H$ data in the area representing anaerobic biodegradation suggests that anaerobic biodegradation had been the predominant mass removal process at this row since persulfate injection (the slightly depleted isotope signature observed at Row 3 on Day 190 corresponds to the arrival of oxidized groundwater from Row 2 due to the ongoing transport). In summary, the distinct isotopic patterns observed at Row 2 and Row 3 are consistently within the expected ranges as previously reported for the corresponding dominant mass removal process taking place at each row as the groundwater system migrates downgradient. Persulfate oxidation was the main process at Row 2 prior to persulfate depletion, and enhanced anaerobic biodegradation was dominant at Row 3.

2.7.2.3 Mass Loss Estimation

To evaluate the treatment effectiveness following persulfate addition between Rows 1 and 2 (ChemOx zone) and between Rows 2 and 3 (EBR zone), the BTEX mass loss was estimated between Day 156 to Day 221. First, the cumulative mass loading at Rows 1, 2 and 3 was estimated by integrating the product of the row-averaged BTX concentrations, Darcy flux and the cross-sectional area of the gate. Second, the cumulative mass loading profiles for Row 2 and Row 3 were translated in time to account for the transport between rows. Finally, assuming no mass accumulation occurred between rows, the difference between the mass loading profiles was used to estimate the mass lost. For these calculations, a velocity of 15 cm/day was used or a travel time of 20 days between rows. Quantifying the uncertainties and interpolation errors associated with this mass loss estimate is difficult but they are thought to be about ±50% according to Schirmer et al. (2000).

The cumulative mass loss and the mass loss rate (i.e., mass loss per unit time) in the ChemOx and EBR zones are presented in Figure 2.13(a, b). Based on these estimates, the rate of BTX mass removal at Row 2 appears to be doubled after each persulfate injection episode, with a jump from 0.015 kg/day to 0.03 kg/day (the cumulative BTX mass loss between Day 156 and Day 221 is ~1.2 kg). The highest mass loss was for toluene (~0.7 kg), followed by benzene (0.4 kg) and xylene (0.1 kg). This trend is most likely due to the higher oxidation rate coefficient of toluene compared to benzene and xylene (Sra et al. 2013b; Liang et al. 2008; Huang et al. 2005). The mass loss estimates suggests that about 50% of the total mass loss between Row 1 and 2 (1.2 kg of the total 2.4 kg mass loss) occurred immediately after the two persulfate injection episodes. This mass loss estimate approach cannot differentiate the contribution of individual mass removal processes (e.g., persulfate oxidation, biodegradation) to the total mass loss. However, according to the molecular biology data, microbial processes were inhibited at Row 2 due to presence of persulfate, and chemical oxidation was identified by CSIA as the dominant mass removal process in the vicinity of Row 2. Therefore, BTX mass loss in the ChemOx zone is mainly attributed to persulfate oxidation. The estimated fraction of mass loss prior to persulfate injection is partially attributed to the biodegradation processes established during the plume development phase and partially to dilution.

Figure 2.13(b) shows the rate of mass loss and the cumulative mass loss in the EBR zone (i.e., between Row 2 and Row 3) between Day 156 and Day 221. According to these estimates, the rate of mass loss increased substantially at Row 3 on Day 190 and corresponds to the time that the sulfate

plume was estimated to have reached Row 3. The rate of mass loss in the EBR zone, which is primarily controlled by microbial processes as confirmed by metabolite data and CSIA, significantly increased from ~0.005 kg/day on Day 156 to ~0.022 kg/day on Day 190 and continued to increase to ~0.03 kg/day on Day 221. This six-fold increase in the mass removal rate is attributed to the microbial processes enhanced by increased sulfate concentration. The estimated total BTX mass loss in the EBR zone was about 0.5 kg. Again toluene was degraded fastest compared to benzene and xylene, which is consistent with the higher anaerobic biodegradation kinetic rates reported for the toluene (Schirmer et al. 2000; Borden et al. 1997; Rifai & Newell 1998; Shim et al. 2005).

2.7.3 Extended Monitoring Phase

Groundwater extraction and the feed to the source wells were stopped on Day 221 due to unfavorable winter conditions; however, monitoring and sampling were performed on Day 293 and Day 391. The stopped flow condition was expected to: (1) decrease BTX concentrations due to the system shutdown and ongoing biodegradation, and (2) prevent further migration of the elevated sulfate plume. Thus, the flow shutdown would limit the spatial extent of the enhanced sulfate reduction zone and consequently lead to biodegradation pathways other than sulfate reduction. When the system was shutdown, the advective front of the EBR zone was estimated to be between Row 3 and Row 4 and hence no significant enhanced biogeochemical changes were observed at Rows 4 to 6 (Figure 2.8). The observed sulfate breakthrough at Row 4 on Day 293 is attributed to dispersion and then diffusion of sulfate. By Day 391, due to the source shut down and sustained microbial processes, toluene and xylene were completely removed from the gate while benzene remained in trace amounts due to its lower biodegradation rate (Figure 2.7). Between Day 221 and Day 391, the geochemical indicators (e.g., ORP, pH, EC and DO) remained unchanged but sulfate, sulfide, Ca^{2+} and DIC concentrations decreased at both Row 2 and Row 3 (Figure 2.8).

The evolution of hydrogen and carbon isotope composition for benzene at Row 2 (Figure 2.11(a)) shows that after persulfate depletion on Day 221, hydrogen was enriched much faster than carbon; the opposite trend compared to the isotopic shift during exposure to persulfate. No significant change is observed in carbon and hydrogen isotopic fractionation for benzene at Row 3 prior to and after Day 221 (Figure 2.11(b)). These observations suggest that the dominant mass removal process had shifted at Row 2, but was unchanged at Row 3. The 2D-CSIA figures (Figure 2.12(a, b)) clearly show the shift of the dominant mass removal process from chemical oxidation (before Day 221) to anaerobic

biodegradation (after Day 221) at Row 2, while anaerobic biodegradation remained the primary mass removal process at Row 3.

To investigate the long-term impact of persulfate on the microbial sulfate reduction process, it was important to distinguish this microbial process from other anaerobic biodegradation processes such as methanogenesis. Although the carbon and hydrogen CSIA data confirmed the occurrence of anaerobic biodegradation at both Row 2 and Row 3, they cannot discern which anaerobic pathway prevailed. Also, the sulfide concentration data is not sufficient to characterize the microbial sulfate reduction process because the *in situ* sulfide concentrations are most likely obscured by the potential precipitation of amorphous Fe-S minerals such as pyrite (Drever 1988; Benner et al. 2002; Miao et al. 2012). Therefore we used $\delta^{34}S$ and $\delta^{18}O$ data for sulfate to investigate the occurrence of microbial sulfate reduction.

Microbial sulfate reduction is expected to cause an isotopic fractionation in both sulfur and oxygen isotopes as the reaction proceeds. The concurrent decrease of sulfate concentration and enrichment of sulfur and oxygen isotopes would provide strong evidence for the continued microbial sulfate reduction. Figure 2.14(a) shows a significant enrichment of $\delta^{34}S$ and $\delta^{18}O$ at Row 2 between Day 221 and Day 391. The greatest enrichment of both sulfur and oxygen isotopes was observed on Day 293 at which time the sulfate was completely depleted at Row 2 (Figure 2.8(g)). The coincident decrease of sulfate concentration (from ~400 to ~10 mg/L) and significant enrichment of both sulfur and oxygen isotopes ($\Delta\delta^{34}S$, $\Delta\delta^{18}O > 15$) indicates the continued microbial sulfate reduction at Row 2 up to Day 293. The decrease in $\Delta\delta^{34}S$ and $\Delta\delta^{18}O$ between Day 293 and Day 391 is attributed to the mixing of sulfate affected and non-affected by sulfate reduction, as well as the decreased sulfate concentration (i.e., redistribution of sulfate) which may have hindered microbial sulfate reduction at Row 2.

As seen in Figure 2.14(a), a reduction in the $\delta^{34}S$ value was also observed earlier between Day 156 and Day 208 (when persulfate was present at Row 2). This reduction occurred in spite of a high concentration of sulfate at that time and location. The type of depletion in $\delta^{34}S$ observed at Row 2 during this period, however, is different from that observed later between Day 293 and Day 391. The depleted $\delta^{34}S$ at the earlier stages of the experiment is attributed to the isotopic composition of the sulfate produced from persulfate decomposition. The produced sulfate seems to have a depleted isotopic signature which causes a reduction in the observed $\delta^{34}S$ valuesBetween Day 156 to Day 208

the enrichment of $\delta^{34}S$ and $\delta^{18}O$ at Row 3 was much higher than the enrichment observed at Row 2 (Figure 2.14(b)), due to the apparent microbial sulfate reduction at this row suggested by the molecular biology data. The primary reason for the lower enrichment at Row 3after Day 208 is the lower sulfate mass at Row 3 compared to what existed at Row 2. Also, it is speculated that the dynamic nature of this experiment (caused by the ongoing transport up to Day 221) may have affected the isotope values at Row 3. The isotopic fractionation induced by microbial sulfate reduction at Row 3 may be masked due to dispersive mixing with the transported sulfate with a depleted $\delta^{34}S$ and $\delta^{18}O$ pattern from Row 2 to Row 3. The depleted sulfate is associated with that generated as the by-product of persulfate decomposition. As a result of the simultaneous presence of both depleted and enriched sulfate (due to sulfate reduction), the observed $\delta^{34}S$ and $\delta^{18}O$ values at Row 3 were not found to be indicative of sulfate reduction, particularly before Day 221. The different isotopic patterns at Row 2 and Row 3 after Day 221, suggests that different microbial processes may have dominated the mass removal at these two rows following the system shutdown.

It appeared that stopping the groundwater flow on Day 221 affected the microbial processes by limiting the delivery/mixing of sulfate, substrates (BTX) and nutrients (e.g. nitrogen and phosphorus) required for the activity and growth of the SRB community. According to Struchtemeyer et al. (2005), under sulfate-limiting conditions, incomplete BTX degradation may occur which results in acetate production. That in turn creates an ideal condition for a certain group of methanogens (i.e. aceticlastic) to compete with sulfate reducing bacteria. A number of site-specific factors (e.g., pH, sulfide toxicity, substrate type, sulfate limitation, kinetic factors, and substrate threshold concentration) control which type of bacteria (methanogens or sulfate-reducing) degrade the remaining BTX compounds (Vroblesky et al. 1996; Al-zuhair et al. 2008).

To identify the active biodegradation pathways (e.g., sulfate reduction or methanogenesis) and to investigate the long-term impact of persulfate on the population and activity of the indigenous microorganisms, the use of molecular biology data was critical. Between Day 221 and Day 391, a substantial increase in the number of copies of anaerobic transcripts bssA (from 181.9 to 3461 copies/L between Day 221 to Day 293) and dsrB (from 153.5 copies/L on Day 221 to 11.5×10^{6} copies/L on Day 293 and 5.5×10^{6} copies/L on Day 391) was observed at Row 2. The concentration of the anaerobic metabolite 2-methylbenzyl succinate (2-MeBS) also increased at this row (Figure 2.9(e, f) and Table A1). As mentioned, the functional gene dsrB and metabolites benzylsuccinate and 2-

methylbenzylsuccinate (2-MeBS) are known to be highly associated with toluene and o-xylene biodegradation mediated by sulfate reduction (Junca & Pieper 2005; Suflita et al. 2004). During the extended monitoring phase the concentration of benzylsuccinate was always lower than 2-MeBS. The reason could be due to further metallization of benzylsuccinate to benzoate and other downstream metabolites such as carboxylates (fowler et al., 2012). The increased benzoate concentration was observed at both Row 2 and also Row 3 during the extended monitoring phase (Figure 2.9(e, h)). Therefore, the molecular biology data strongly confirm the significant growth of the SRB community and enhancement of microbial sulfate reducers at Row 2 during the period between Day 221 and Day 293 under system shutdown conditions.

In contrast to Row 2, the abundance of the dsrB and bssA communities decreased at Row 3 during the extended monitoring phase, whereas the number of copies of both these genes thrived between Day 180 to 221 (Figure 2.9(h, i) and Table A1). The maximum population of dsrB and bssA genes (highly associated with microbial sulfate reduction) observed at Row 3 were ~900 copies/L which occurred on Day 190 and Day196, respectively. However, the copies of these functional genes dropped to zero on Day 221 and remained at zero until Day 391, indicating the cessation of microbial sulfate reduction at Row 3 under system shutdown conditions. This was confirmed by the decreased concentration of the metabolic by-product 2-MeBS associated with microbial sulfate reduction, at Row 3 between Day 293 and 390. The significant change in molecular biology data at Row 3 under system shutdown conditions was associated with the increased concentration of metabolites such as 2,3-dimethylphenol (2,3-DMP) and o-cresol and benzyl alcohol (Figure 2.9(h, i)). One of the known pathways that may have resulted in the formation of 2,3-DMP and o-cresol is the degradation of toluene and xylene under methanogenic condition (Fowler et al. 2012; Evans et al. 1992; Grbić-Galić & Vogel 1987).

The elevated methane concentrations at Row 3 on Day 293 and Day 391 (from the background concentration of ~20 μg/L to ~100 μg/L) confirm the establishment of methanogenic conditions at Row 3. Methane concentration at Row 2 also showed an increase on Day 391 (~50 μg/L), but remained lower than its corresponding value in Row 3 (see Appendix A). The increased methane concentration at Row 2, which was concurrent with the drastic decrease in the number of copies of dsrB and bssA genes between Day 293 and Day 391, suggests that methanogenesis outcompeted sulfate reduction at Row 2 between Day 293 and Day 391 (Figure 2.9(h, i)). The increased

concentration of 2,3-DMP and o-cresol metabolites at Row 2 indicates the establishment of methanogenic conditions at Row 2 on Day 391.

The molecular biology data confirmed that the distinct pattern for the isotope composition of the sulfate at Row 2 and Row 3 was partly due to dominance of different microbial processes at these rows (sulfate reduction vs. methanogenesis). The higher concentration of methane and methanogenesis metabolites at Row 3 compared to those at Row 2 on both Day 293 and Day 391 indicates the more significant role of methanogenesis over sulfate reduction at Row 3. Therefore, the continued BTX mass loss at Row 2 and Row 3 was associated with methanogenesis.

2.8 SUMMARY AND CONCLUSION

A pilot-scale field experiment was conducted in a sheet pile-walled gate at CFB Borden to investigate and characterize the processes involved in a persulfate/EBR treatment train. A quasi steady-state BTX plume and an associated anaerobic aquifer system (low DO, and reducing conditions) were developed prior to persulfate injection. Then, two (2) sequential persulfate injection episodes were conducted to generate two persulfate slugs using a cross-borehole injection system (CIS). About 480 L of 10 g/L unactivated sodium persulfate solution was injected for a total duration of eight (8) hours at a rate of 0.5 L/min into two outside CIS wells, while groundwater was simultaneously extracted from the central CIS well at a rate of 1 L/min. The mixing between persulfate and BTX led to formation of a chemical oxidation (ChemOx) zone in the portion of the plume confined between the two persulfate slugs. As the BTX and persulfate mass was depleted due to chemical oxidation, a sulfate plume formed and the ChemOx zone was transitioned into an enhanced bioremediation (EBR) zone, which propagated downgradient as the groundwater system migrated along the experimental gate.

The evolution of the ChemOx and EBR zones was monitored for >13 months, even after the groundwater flow was stopped due to unfavorable winter conditions. An extensive monitoring plan including the combined application of conventional and emerging site characterization tools (e.g., isotope analysis and molecular biology) was used to distinguish the dominant mass removal processes in the course of the treatment train and to investigate the impact of persulfate on the subsequent microbial processes. Concentration data showed that the BTX plume was successfully degraded with this persulfate/EBR treatment train (>70% BTX mass removal). The highest mass loss was for toluene, with higher chemical and biological degradation rate coefficients compared to benzene and

xylene. Multiple lines of evidence from this experiment demonstrated that chemical oxidation was the dominant mass removal process in the vicinity of the persulfate injections (i.e., ChemOx zone), while enhanced bioremediation (including enhanced microbial sulfate reduction and methanogenesis) dominated BTX degradation in the downgradient portions of the plume (i.e., EBR zone).

Stable isotope analysis of BTX and sulfate and monitoring of process-specific functional genes and intermediate metabolites proved to be powerful tools for identifying the dominant degradation pathway at various stages of this experiment. CSIA data clearly indicated the spatial and temporal separation of the ChemOx and EBR zones. The coupling of $\delta^{13}C$ and $\delta^{2}H$ data demonstrated a distinct and specific isotopic trend for chemical oxidation and anaerobic biodegradation processes, which respectively dominated the mass removal in the ChemOx and EBR zones. The sulfur and oxygen isotope data for sulfate qualitatively confirmed the occurrence of microbial sulfate reduction in the EBR zone and highlighted the evolution of the dominant biodegradation pathway (sulfate reduction vs. methanogenesis) during the no-flow condition.

Molecular biology data successfully demonstrated the short- and long-term impact of persulfate on the population and biodegradation activity of indigenous microbial communities including SRB. The decreased concentration of anaerobic metabolites such as benzylsuccinate, 2-MeBS and benzoate, and reduced number of the expressed bssA genes associated with BTX anaerobic biodegradation indicated that persulfate, even at low concentrations (<10 g/L), caused a temporary inhibition of microbial processes in the ChemOx zone. However, the concentration of metabolites and the number of copies of the bssA and dsrB genes (the latter is particular associated with BTX degradation under sulfate reduction) started to rebound and increased significantly after persulfate depletion. For example, the number of copies of dsrB genes at Row 2 (enclosed in the ChemOx zone) was increased by three (3) orders of magnitude in about 120 days following persulfate injection. The incomplete inhibition of microbial processes due to the low dosage and low duration of the persulfate treatment, existence of subsurface heterogeneities and persistence/growth of indigenous microbes in the dead-end pores, re-inoculation of microbial communities by groundwater flow, increased sulfate and nutrients concentration and the enhanced biodegradability of the remaining contaminant pool contributed to the observed enhancement of the microbial sulfate reduction following persulfate treatment. The MBT data, however, demonstrated that the microbial sulfate reduction established in the EBR zone eventually stalled during the period of no-flow condition. The flow stoppage hindered

further transport of sulfate, substrates and nutrients and subsequently decreased the biodegradation activity of sulfate reducing bacteria. Instead, an accumulation of the metabolites associated with biodegradation of BTX compounds under methanogenic conditions suggested that methanogenesis biodegradation maintained BTX mass removal long after persulfate treatment.

This pilot-scale trial illustrated that the geochemical conditions established after persulfate oxidation (reduced and sulfate-rich environment) were conducive for both SRB and methanogens communities, and eventually the competition between the two communities dictated which biological pathway would control the mass removal in the longer term. It was demonstrated that when a carefully designed ISCO treatment (i.e., low dosage, short duration and small exposure area) is implemented, the initial inhibitory impact of persulfate on the population and activity of indigenous microbial communities (including SRB) would be short term, and followed by a substantial enhancement. Moreover, this study revealed the major role of the flow and transport processes on the performance of the treatment train. Transport of microbial communities, sulfate, nutrients and bioavailable substrates from upgradient, not only facilitates the natural rebound/multiplication of indigenous microbial communities at the experimental gate following persulfate application, but also define the dominant biological pathway over the long term.

The general conclusion that can be drawn based on this study is that a persulfate/EBR treatment train can be a feasible technique for treatment of dissolved BTX plumes. However, finding the balance between persulfate oxidation and enhanced bioremediation is the key design criteria for a combined remedy which is more efficient and time/cost effective than each of the individual techniques. A limited persulfate treatment step can improve the overall performance of the persulfate/EBR treatment train by minimizing the contact between the oxidant and indigenous microbial communities, preventing the permanent inhibition of microbial processes and providing sulfate and bioavailable substrates for stimulating the subsequent microbial processes as the polishing step.

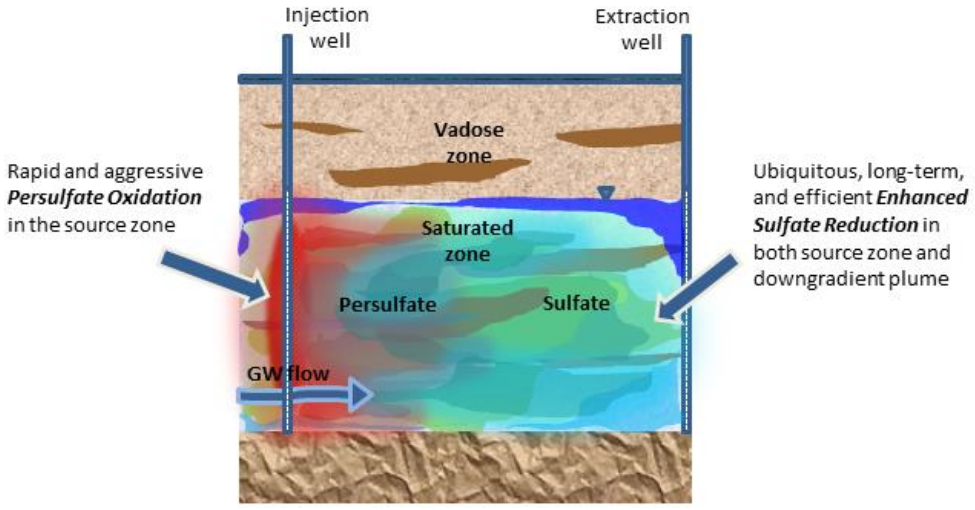

Figure 2.1 Schematic illustration of a persulfate/EBR treatment train.

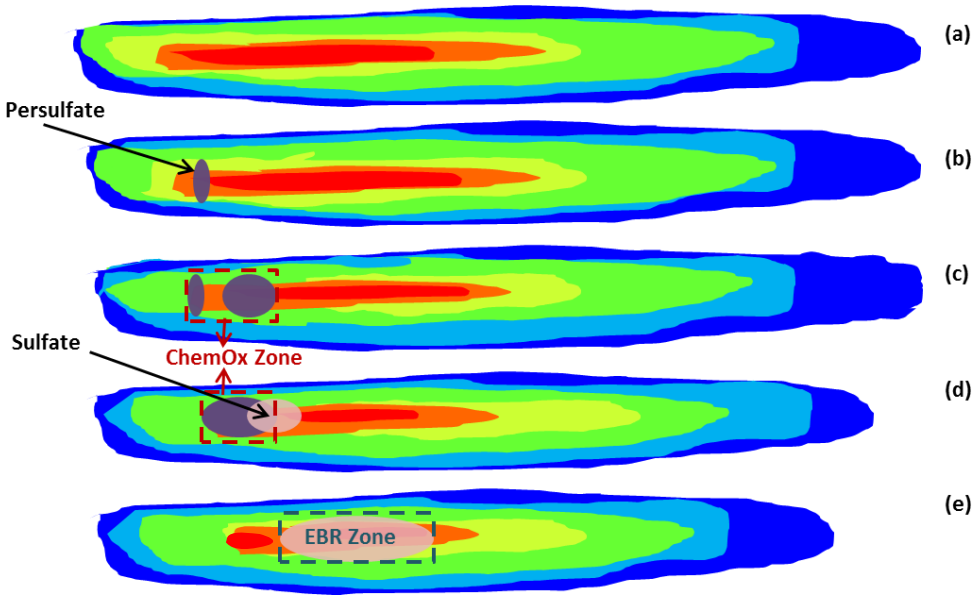

Figure 2.2 Conceptual representation of the pilot-scale experiment: (a) the generated quasi steady-state PHC plume, (b) first persulfate injection adjacent to the plume source, (c) second persulfate injection and formation of the ChemOx zone between the two persulfate slugs where mixing and the reaction between persulfate and the PHC mass occurs, (d) depletion of ChemOx zone due to persulfate decomposition and generation of a sulfate plume, and (e) migration of sulfate plume and the establishment of the EBR zone where enhanced microbial sulfate reduction is expected to occur.

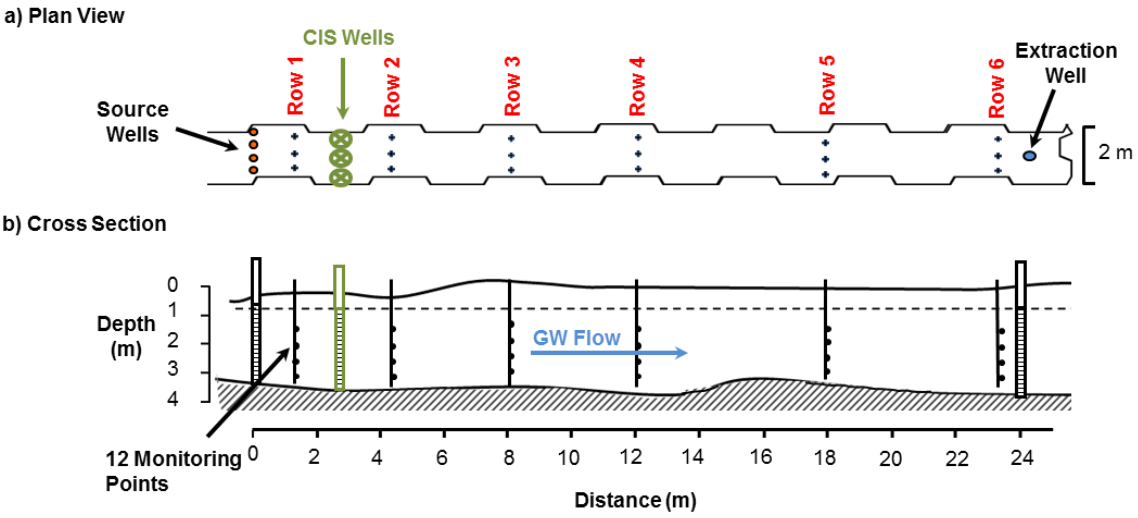

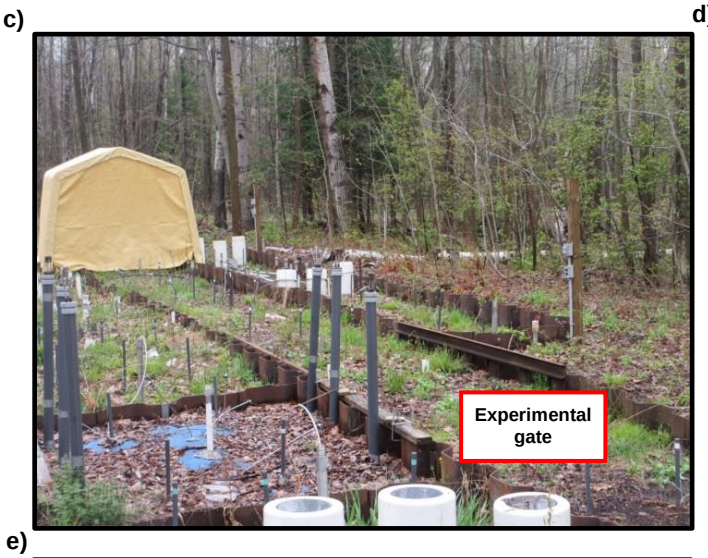

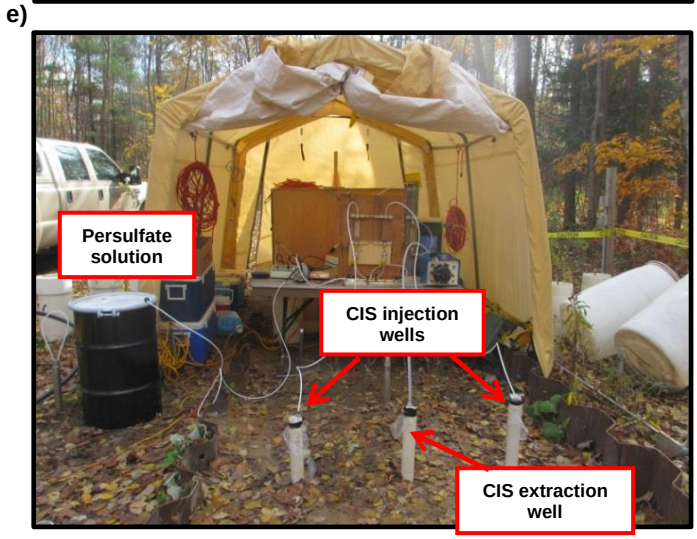

Figure 2.3 (a) Plan view, (b) cross sectional view, and (c) image of the experimental gate; (d) installation of Waterloo Emitters™ inside the source wells; and (e) CIS wells located between Row 1 and Row 2.

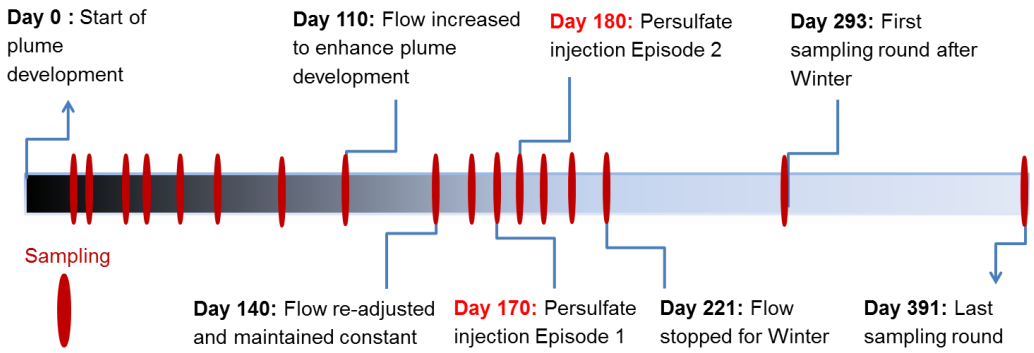

Figure 2.4 Timeline of the pilot-scale experiment, and the frequency of monitoring and groundwater sampling.

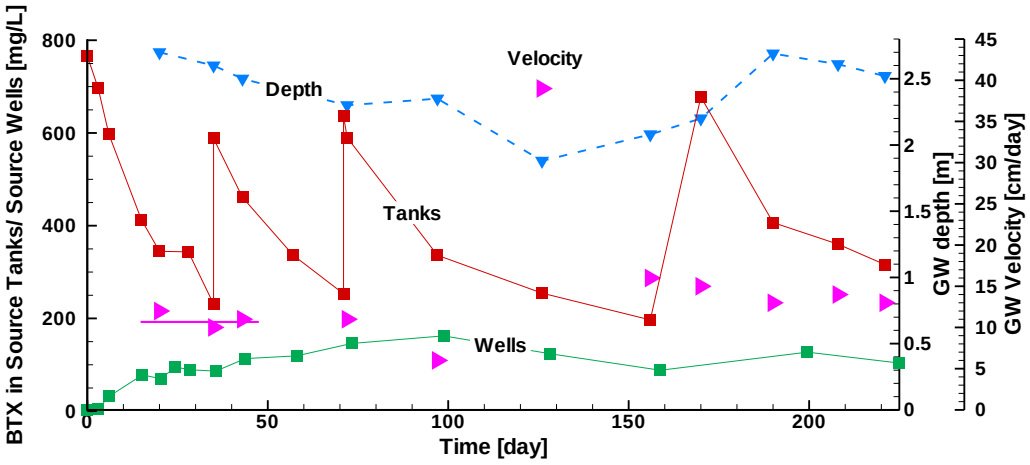

Figure 2.5 Temporal evolution of groundwater depth and velocity in the experimental gate, and the average total BTX concentration in the source tanks and wells. The solid pink line indicates the average velocity supported by the tracer test data.

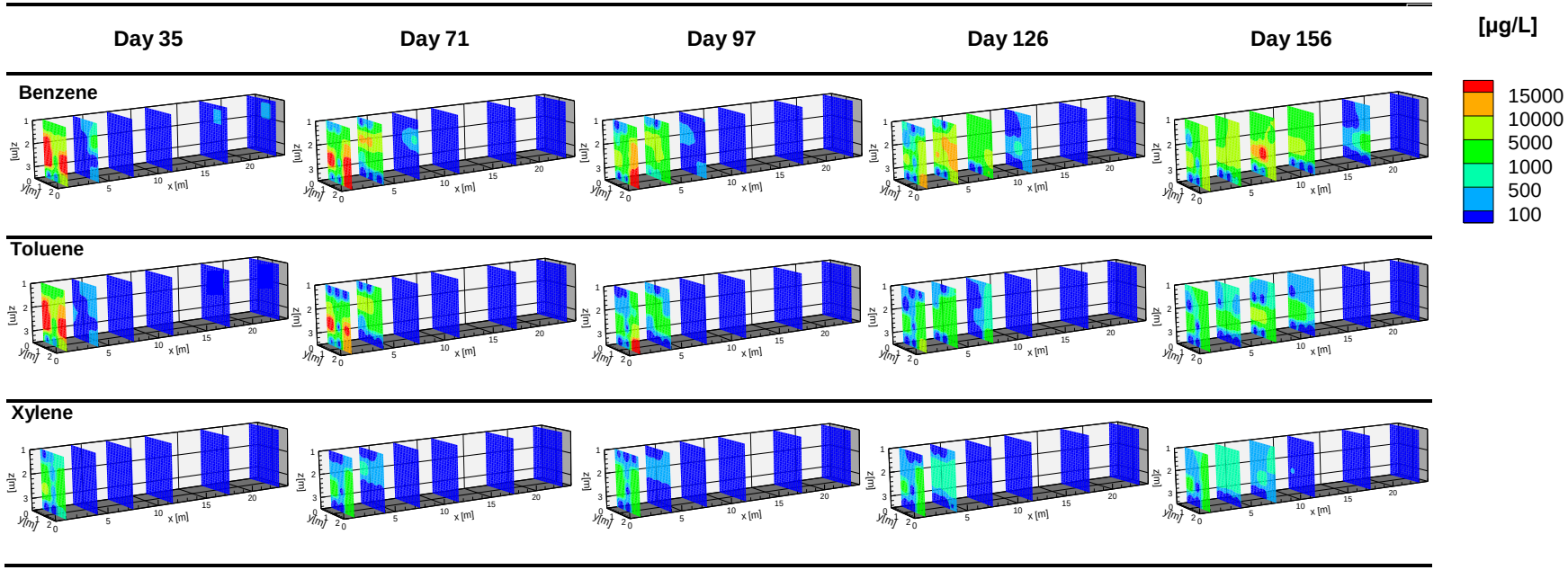

Figure 2.6 Development of benzene, toluene and xylene plumes during the plume generation phase. All three plumes followed the same general pattern; however, the slower migration of toluene and xylene compared to benzene is attributed to a higher sorption capacity and biodegradation rate. Between Day 72 and 97 plume development appeared to stop as a result of natural attenuation processes and hence the groundwater velocity was increased on Day 110 to encourage the plume to migrate further downgradient as seen on Day 156.

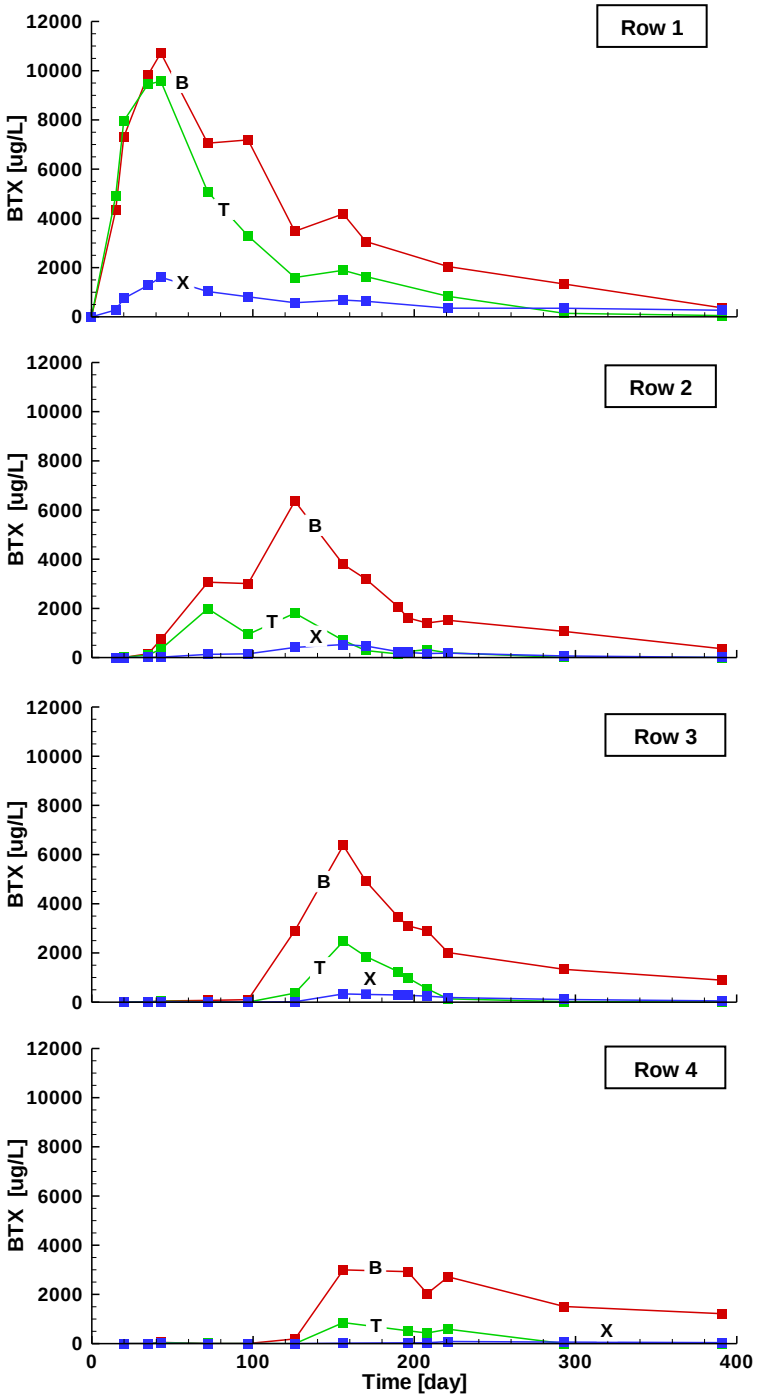

Figure 2.7 Row-averaged (based on weighted area)BTX breakthrough curves at the first four monitoring rows. The two (2) persulfate injections were conducted on Day 170 and Day 180 between Row 1 and Row 2. The decreased BTX concentration after Day 156 is the integrated impact of persulfate oxidation, enhanced microbial sulfate reduction, and the system shut down on Day 221.

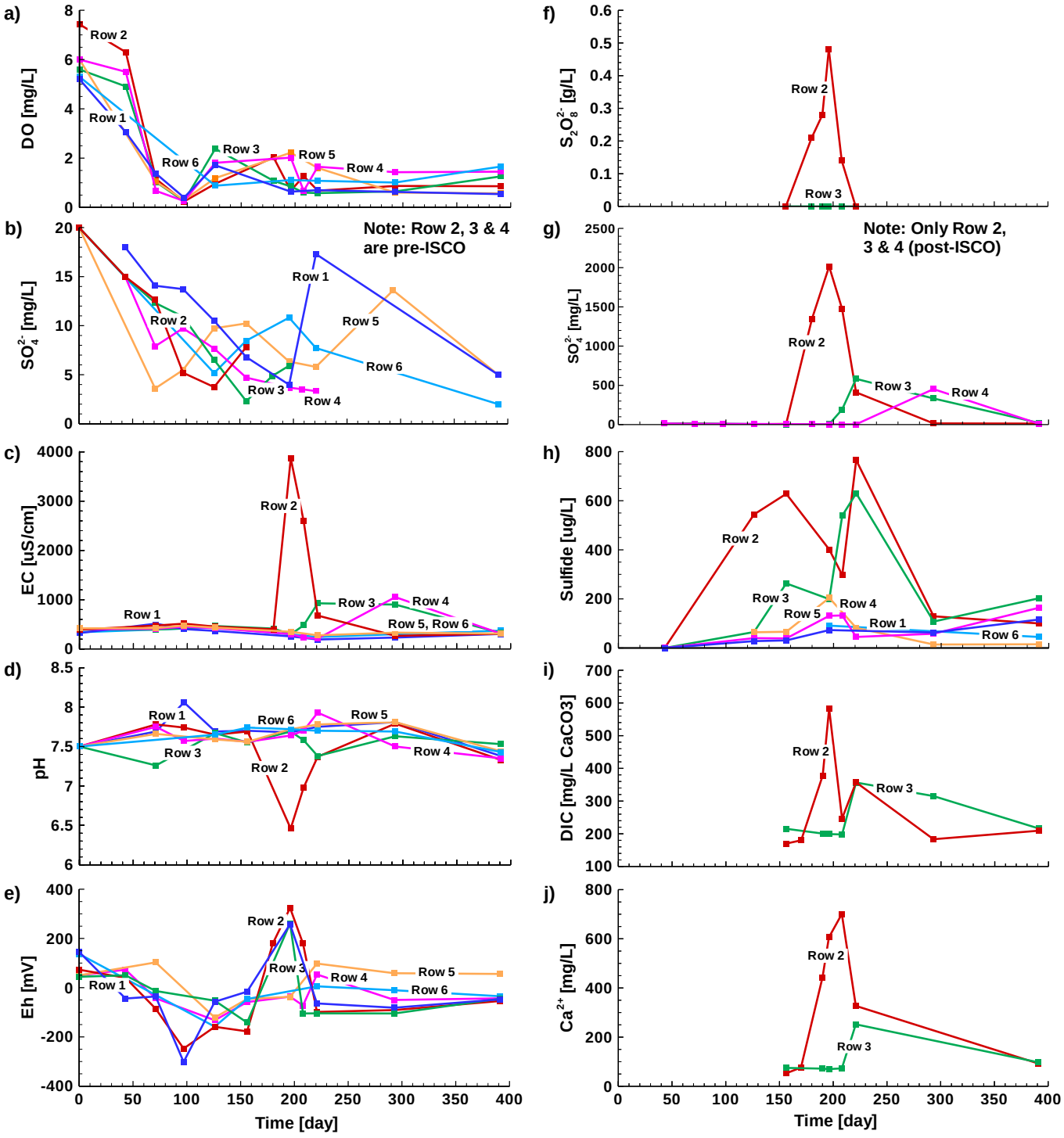

Figure 2.8 Temporal evolution of geochemical indicators (row-averaged based on weighted area): (a) dissolved oxygen, (b,g) pre- and post-persulfate injection sulfate concentration, (c) electrical conductivity, (d) pH, (e) oxidation-reduction potential (Eh), (h) sulfide concentration, (i) dissolved inorganic carbon content as mg/L $CaCO_3$, and (j) calcium concentration.

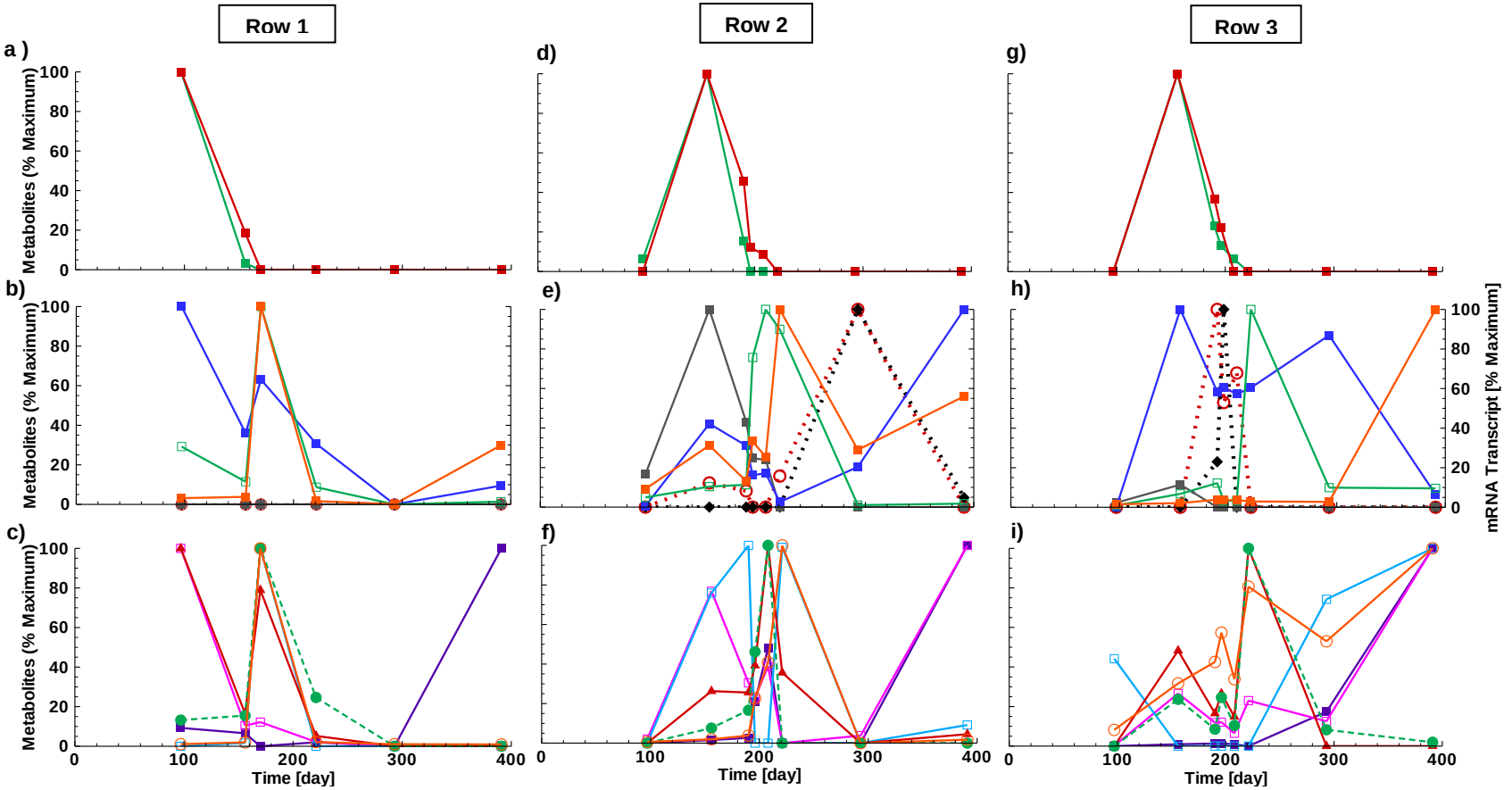

Figure 2.9 Temporal evolution of the key intermediate metabolites (aerobic (a,d,g), anaerobic (b,e,h) and ambiguous (c,f,i)), and mRNA transcripts associated with BTX biodegradation under anaerobic/sulfate reducing condition at Row 1 (ML1-L3), Row 2 (ML2-L3) and Row 3 (ML3-M3).

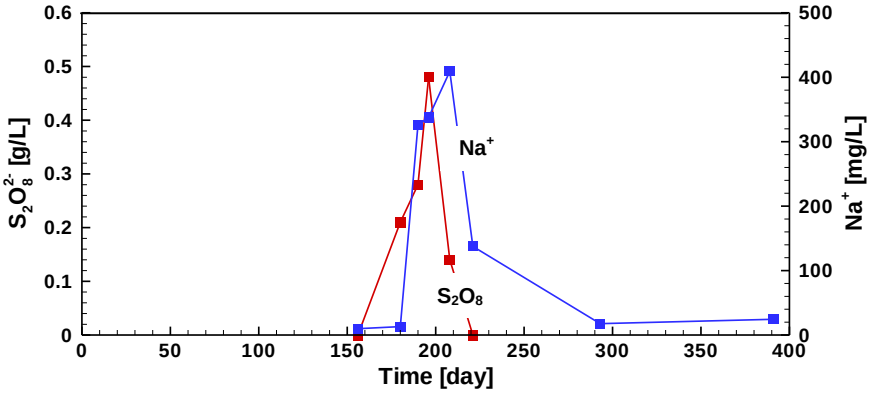

Figure 2.10 Row-averaged (based on weighted area) persulfate and sodium concentrations at Row 2.

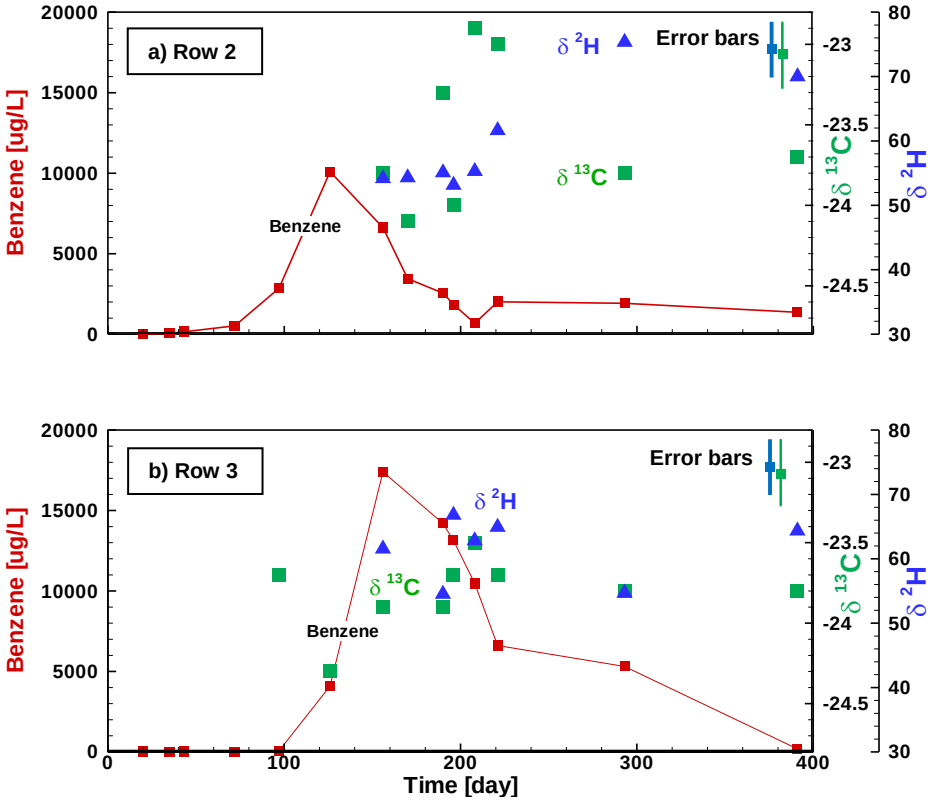

Figure 2.11 Carbon and hydrogen isotope data of benzene from two arbitrary sampling points (ML2-L3 and ML3-M3) located, respectively at (a) Row 2 (i.e., the ChemOx zone) and (b) Row 3 (i.e., the EBR zone).

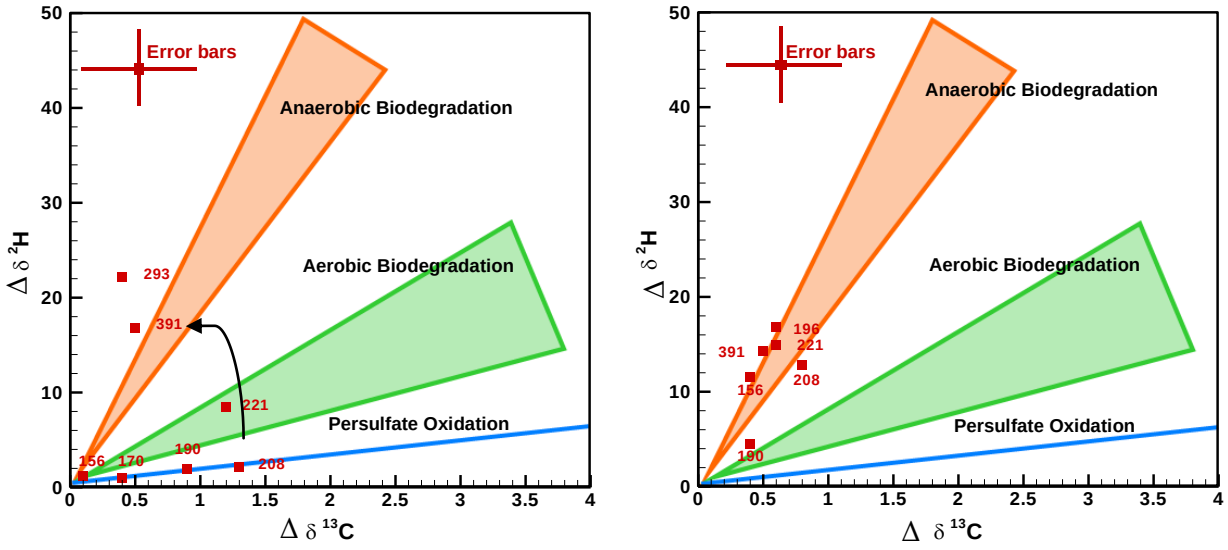

Figure 2.12 Two-dimensional CSIA representation of the C/H isotope fractionation data for benzene at (a) Row 2 (ML2-L3) and (b) Row 3 (ML3-M3). The corresponding sampling time (Day) is beside data point. The green and orange areas respectively represent the range of $\Delta\delta^{13}C$-$\Delta\delta^{2}H$ values reported in the literature for aerobic and anaerobic biodegradation of benzene (Hunkeler et al. 2008; Aelion et al. 2009). The blue line represents the $\Delta\delta^{13}C$-$\Delta\delta^{2}H$ value corresponding to benzene oxidation by persulfate (Solano

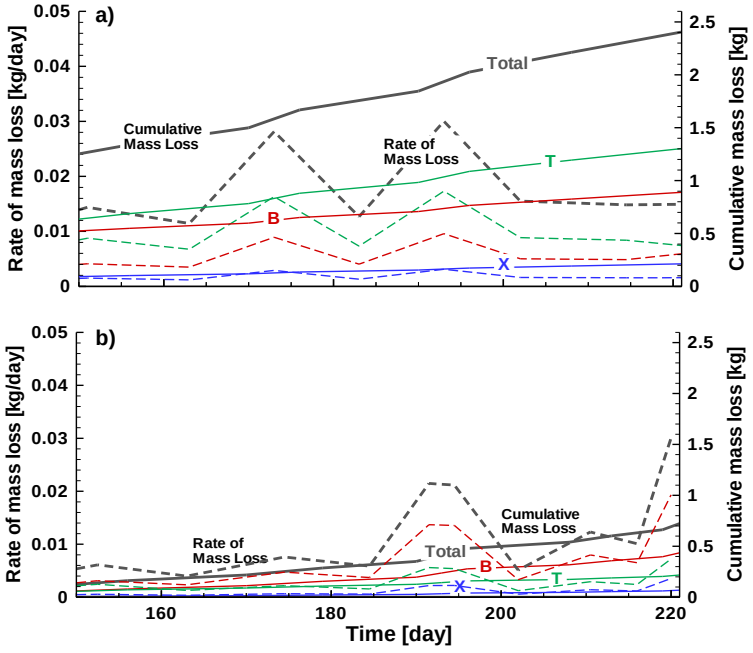

Figure 2.13 Cumulative mass loss (solid line) and mass loss rate (dashed line) in the (a) ChemOx zone (Row 2) and (b) the EBR zone (Row 3) between Day 156 and Day 221.

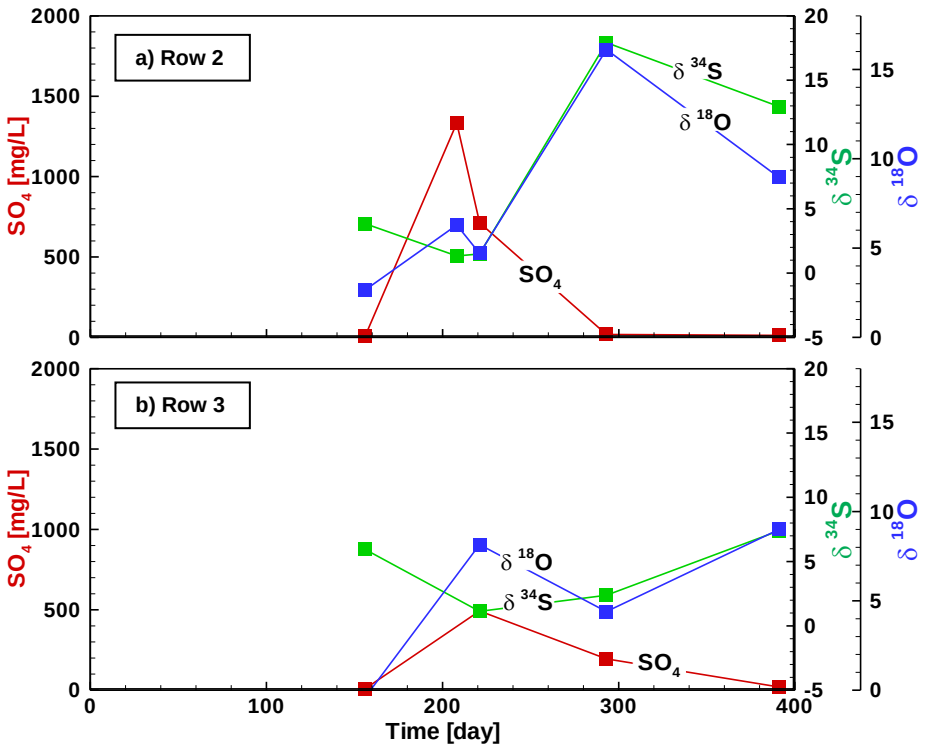

Figure 2.14 $\delta^{34}S$ and $\delta^{18}O$ values between Day 221 and Day 391 at (a) Row 2 (ML2-L3) and (b) Row 3 (ML3-M3). The different isotope patterns observed at both rows suggests distinct mass removal processes prevails in the two locations over the course of this experiment.

Table 2.1 The key advantages and limitations of persulfate and sulfate reduction, and benefits of using them in a combined remedy.

Technology	Advantages	Limitations	Advantage in a combined remedy
Persulfate Oxidation	- Aggressive and rapid - Suitable for a range of PHCs - Persistent	- Oxidant delivery - Rebound - Not cost effective for treatment of low concentrations	- Breakdown of complex organic compounds - Generation of sulfate - Stimulation of subsequent microbial sulfate reduction
Microbial Sulfate Reduction	- Ubiquitous - long-term efficacy - Inexpensive	- Slow degradation rates - Site-specific - Not suitable for complex compounds in high concentrations - Inhibits in the absence of electron acceptors and nutrients	- SRB are abundant at PHC impacted sites - Ideal to degrade residual plume

Table 2.2 (a) The key intermediate metabolites and (b) process-specific functional genes monitored.

(a)

Compound	Encoded enzyme	Redox condition
Benzene	Anaerobic Benzene Carboxylase (abcA)	Anaerobic
Benzene, Toluene	Toluene dioxygenase (todA)	Aerobic
Benzene, Toluene, xylene	Benzylsuccinate Synthase (bssA)	Anaerobic
Sulfate	Dissimilatory sulfate reductase (dsrA, dsrB)	Anaerobic

(b)

Process	Metabolite
Aerobic	Benzene-1,2-cis-dihydrodiol, Toluene-cis-dihydrodiol
Anaerobic	Benzylsuccinate, 2-Methylbenzyl succinate
Either	Benzoate (anaerobic benzene, aerobic toluene), Phenol (aerobic/anaerobic benzene, anaerobic toluene), 2,3-dimethylphenol,o-, m- and p-Cresol, Benzyl alcohol, 2-Methylbenzylalcohol

Chapter 3

Simulation of Persulfate Oxidation Combined with Enhanced Bioremediation as a Combined Remedy

Abstract

The coupling or sequential use of different remediation technologies, also referred to as a "treatment train", is an emerging remediation strategy that combines the strengths of each individual remediation technology to improve the overall treatment efficiency and minimize clean-up cost and time. Combining *in situ* chemical oxidation (ISCO) with persulfate and enhanced bioremediation (EBR) under sulfate reducing condition is an example of a plausible treatment train for application at PHC-contaminated sites. A modelling tool (BIONAPL/PS) was developed to simulate the intertwined physical, chemical and biological processes involved in a persulfate/EBR treatment train and to quantify the impact of various parameters on the performance of this treatment system. The key processes captured in this model include transient groundwater flow, multi-component advective-dispersive transport, multicomponent dissolution, persulfate decomposition, chemical oxidation of dissolved PHCs, and biodegradation under various redox conditions. The model can also simulate the inhibitory impact of persulfate on subsequent sulfate reduction, and can quantify the role of the intertwined mass removal processes. The formulation of BIONAPL/PS was validated against an analytical solution, and observations from a series of laboratory column experiments designed to mimic a persulfate/EBR treatment train. Data from a pilot-scale experiment conducted at the University of Waterloo Groundwater Research Facility at the Canadian Forces Base (CFB) Borden near Alliston, ON, Canada were used in a model benchmarking effort. Simulating the pilot-scale experiment, which investigated the coupled processes involved in a persulfate/EBR treatment train, was aimed to evaluate the model capability to simulate a complex system with multiple components within a dynamic flow system. Also, the modelling tool was used to evaluate options for performance optimization. Reaction kinetics, flow regime and design parameters (e.g., persulfate dosage, and injection period/interval and rate) were identified as the key factors which influence the overall performance of the persulfate/EBR treatment train. It was found that a less aggressive persulfate treatment step (i.e., lower dosage, duration and extent) improves the overall treatment efficiency by minimizing the inhibitory effect of persulfate on the subsequent microbial processes.

Keywords: In situ chemical oxidation, Biodegradation, Persulfate, Sulfate reduction, Dissolved plume, BTEX, Numerical modelling

3.1 INTRODUCTION

Groundwater contamination by petroleum hydrocarbon (PHC) compounds, including the high impact, toxic and persistent monoaromatic compounds such as benzene, toluene, ethylbenzene and xylene (BTEX) poses a serious risk to human health and the environment (WHO 2005). Innovative and efficient remediation strategies are required to mitigate such risks in a smart, and cost and time effective manner. The coupling or sequential use of different remediation technologies, also referred to as a "treatment train", is an emerging remediation strategy that combines the strengths of each individual remediation technology to improve the overall treatment efficiency and minimize clean-up cost and time (Yang et al. 2005; Tsitonaki 2008). Coupling *in situ* chemical oxidation (ISCO) and enhanced bioremediation (EBR) is an example of a plausible treatment train for the application at PHC-contaminated sites (Sutton et al. 2010; Munakata-Marr et al. 2011; Richardson et al. 2011).

Persulfate is an aggressive oxidant that has been successfully used in the treatment of BTEX-contaminated sites (Huling & Pivetz 2006), and it also has a significant inherent advantage in the context of being an integral part in an ISCO/EBR treatment train (see Chapter 2). The reaction of persulfate with organic compounds leads to the production of sulfate, which along with the breakdown of complex organic compounds into simpler and more bioavailable organic substrates can lead to enhanced biodegradation activity of sulfate reducing bacteria (SRB) (Kulik et al. 2006; Miller et al. 1996; Nam et al. 2000; Sutton et al., 2010). Subsequently, the enhanced bioremediation under sulfate reducing conditions is expected to dominate the removal of the remaining contaminant mass following persulfate treatment.

As demonstrated in Chapter 2, a persulfate/EBR treatment train can serve as a viable and effective remediation approach. The results from the pilot-scale study confirmed the enhancement of the SRB community following persulfate application, and sustained degradation of organic compounds long after persulfate had disappeared from the system. A combined application of conventional and emerging site characterization tools (e.g., stable isotope analysis of BTX and sulfate, and monitoring of the process-specific functional genes and intermediate metabolites) were used in the field trial to evaluate the short- and long-term impact of persulfate on microbial activity. The results illustrated

that when a carefully designed ISCO system is implemented, the initial inhibitory impact of persulfate on the population and activity of indigenous microbial communities (including SRB) is short-term and is followed by substantial enhancement.

The effectiveness of a persulfate/EBR treatment train is dependent on the delivery and mixing of persulfate *in situ* and therefore site-specific transport processes (e.g., advection, dispersion and diffusion) have a major impact on the performance of this combined remedy. Moreover, the kinetics of chemical oxidation and sulfate reduction, as well as the interaction between the two processes can influence the overall treatment performance. Application of a modelling tool capable of simulating the intertwined physical, chemical and biological processes involved in a persulfate/EBR treatment train is useful to understand the influence of the key processes on treatment effectiveness and to examine options to optimize the performance of the combined remedy.

To date, there has been no reported effort made to simulate a persulfate-based ISCO treatment system or an ISCO/EBR treatment train. Over the last two decades, the focus of numerical tool developments in the field of *in situ* groundwater remediation has been primarily on the simulation of individual treatment processes such as natural attenuation and/or *in situ* bioremediation of organic contaminants (Lu et al. 1999; Rifai & Rittaler 2005; Schirmer et al. 2000; Barry et al. 2002; Clement et al. 1998; MacQuarrie et al. 1990; Essaid et al. 1995; Nicol et al. 1994; Ballarini et al. 2013; Geng et al. 2013), or on permanganate-based ISCO treatment. A review of the latest ISCO related modelling studies is provided by Heiderscheidt et al. (2011).

Conceptual Design for ISCO (CDISCO) developed by Borden et al. (2009) is a one-dimensional model formulated for permanganate-based ISCO. CDISCO is capable of modelling transport and decomposition of permanganate only during the injection period, and can only simulate oxidant interaction with the aquifer materials and not with any target contaminant. CDISCO is not capable of simulating transport and natural attenuation processes including biodegradation. CORT3D (Heiderscheidt 2005; Heiderscheidt et al. 2008) is a three-dimensional reactive transport model that can simulate the reactive transport of permanganate, contaminant species and associated oxidation by-products. However, similar to CDISCO, CORT3D does not simulate biodegradation processes. Henderson et al. (2009) enhanced the MIN3P model (Mayer et al. 2002) to simulate the density-dependent flow and multicomponent reactive transport processes involved in the oxidation of chlorinated solvents by permanganate. The enhanced model (MIN3PD) provides a direct coupling

between fluid flow, dissolution of a non-aqueous phase liquid (NAPL), solute transport, biodegradation and geochemical reactions. However, similar to other models, the formulation of the MIN3PD model was limited to permanganate-based ISCO. None of these models are capable of simulating a coupled ISCO/EBR treatment train or to evaluate the impact of chemical oxidation (particularly by persulfate) on the subsequent biological processes.

The main objective of this study was to develop and evaluate a modelling tool to simulate the processes involved in a persulfate/EBR treatment train. An existing model was selected and enhanced to capture the key first-order processes involved in the persulfate/EBR treatment train. The formulation of the enhanced model was validated against an analytical solution and observations from a laboratory column experiment designed to mimic a persulfate/EBR treatment train. The model was then benchmarked against results from a pilot-scale experiment that investigated the coupled processes involved in a persulfate/EBR treatment train. The latter effort was used to characterize the impact of persulfate on sulfate reduction, and to evaluate the temporal and spatial contribution of individual mass removal processes.

3.2 MODEL SELECTION

BIONAPL/3D (Molson 2014) was selected as the basis of the present model development effort because of its capability to simulate the majority of the processes involved in the persulfate/EBR treatment train and also because of the feasibility of making enhancements to the source code. BIONAPL/3D is a three-dimensional model that can be used to simulate multi-component reactive transport processes in porous or fractured media. The model architecture involves a transient groundwater flow model coupled to a multi-component advective-dispersive transport model. BIONAPL/3D can simulate a variety of processes such as NAPL dissolution, equilibrium or rate-limited sorption, and first-order or Monod type degradation. Moreover, multi-component sources, multiple electron acceptors as well as the growth of multiple microbial communities can be simulated.

In BIONAPL/3D, the source of organic compounds and electron acceptors can be either set as initial conditions, boundary conditions, or internal sources. Additionally, a residual (immobile) NAPL source can be specified. A rectangular prism (3D brick) mesh generator is built within BIONAPL/3D, although externally-generated deformed rectangular meshes can also be used. Further details on the model capabilities and sample applications are provided by Molson (2014). BIONAPL/3D has been

successfully used to simulate a variety of groundwater field experiments and contaminated sites (Frind et al. 1999; Molson et al. 2002; Molson et al. 2008; Greer et al. 2010; Vaezihir et al. 2012).

3.3 ENHANCED MODEL FORMULATION

To simulate the processes involved in a persulfate/EBR treatment train, the formulation of BIONAPL was enhanced and the resulting code was named BIONAPL/PS (PS stands for persulfate). One of the required model enhancements included adding second-order reaction kinetics to simulate chemical oxidation of the organic compounds. The chemical oxidation reaction has been demonstrated to be dependent on the concentration of both oxidant and the contaminant of concern (CoC) (Sra et al. 2013b). Another major enhancement was the ability to simulate the generation of sulfate resulting from persulfate decomposition during reactions with CoCs and the aquifer material (AM)). In summary, the processes captured in BIONAPL/PS include:

- Transient groundwater flow
- Advective-dispersive transport of multiple organic compounds, and persulfate
- Dissolution of multicomponent NAPLs
- Degradation of organic compounds due to persulfate oxidation
- Decomposition of persulfate due to reactions with organic compounds and the aquifer material
- Production and advective-dispersive transport of the by-product sulfate
- Consumption of sulfate due to degradation of organic compounds by microbial sulfate reduction
- Biodegradation under various redox conditions
- Microbial growth and decay

Although most of the key processes involved in a persulfate/EBR treatment train are captured in the initial version of BIONAPL/PS, relevant geochemical interactions (e.g., mineral dissolution/precipitation and carbonate system) are not simulated. The governing equations and mathematical representation of the processes involved in BIONAPL/PS are presented in the following sections. These coupled equations for density-dependent groundwater flow and reactive transport are

solved using Picard iteration. Iteration between the solution of the flow and reactive transport equations continues until the concentration differences between iterations falls below a user-specified tolerance. These coupled equations also require initial and boundary conditions for their solution. The description of the three types of boundary conditions (i.e., Dirichlet, Neumann and Cauchy), and further details on the BIONAPL/3D model have been provided in the model user guide (Molson 2014).

3.3.1 Density-dependent groundwater flow

The continuity equation for flow in a porous medium is expressed as (Molson 2014)

$$\frac{\partial}{\partial x_i}\left[K_{i,j}k_{rw}\left(\frac{\partial \psi}{\partial x_j}+\gamma c_j\right)\right] \mp \sum_{k=1}^{N} Q_k(t)(x_k, y_k, z_k) = S_w S_s \frac{\partial \psi}{\partial t} + \theta \frac{\partial Sw}{\partial t} \quad (3.\ 1)$$

where x_i are the 3D spatial coordinates, $K_{i,j}$ is the hydraulic conductivity tensor (m/d), ψ is the equivalent freshwater head (m), $\gamma c_j = \rho_r$ is the concentration-dependent relative density of water (c_j is the total concentration of component being transported), Q_k is the fluid volume flux for a source or sink (m^3/day) located at (x_k, y_k, z_k), S_w is the water saturation (dimensionless), S_s is the specific storage (m^{-1}), θ is porosity (dimensionless) and t is time (day). The relative permeability k_{rw} (dimensionless) is defined as a function of S_w, using (Corey, 1986)

$$k_{rw} = \left(\frac{S_w - S_{rw}}{1 - S_{rw}}\right)^4 \quad (3.\ 2)$$

where S_{rw} is the irreducible water saturation. Boundary conditions for Eq. (3.1) can be either first type (fixed head) or second type (fixed head gradient).

3.3.2 Multi-component Advective-Dispersive Transport

The general equation for advective-dispersive reactive transport of a particular reactant component (α) is expressed as

$$R^{(\alpha)}\theta S_w \frac{\partial C^{(\alpha)}}{\partial t} = \frac{\partial}{\partial x_i}\left[\theta S_w D_{ij} \frac{\partial C^{(\alpha)}}{\partial x_j}\right] - q_i \frac{\partial C^{(\alpha)}}{\partial x_i} + \Gamma^{(\alpha)} \quad (3.\ 3)$$

where $C^{(\alpha)}$ is the concentration of the aqueous component α (kg/m^3), q_i is the Darcy flux (m/d), D_{ij} is the hydrodynamic dispersion tensor (m^2/d), $R^{(\alpha)}$ is the linear retardation coefficient of component α

(dimensionless), and $\Gamma^{(\alpha)}$ is the reaction term which is different for various aqueous components as described below for the different components involved in a persulfate/EBR system.

3.3.2.1 Reaction Term for PHC Compounds

The reaction of each PHC compound (α) is comprised by a dissolution term ($\Gamma_{DIS}^{(\alpha,PHC)}$), a biodegradation term ($\Gamma_{BIO}^{(\alpha,PHC)}$) and a chemical oxidation term ($\Gamma_{ChemOx}^{(\alpha,PHC)}$) as given by

$$\Gamma^{(\alpha,PHC)} = \Gamma_{DIS}^{(\alpha,PHC)} - \Gamma_{BIO}^{(\alpha,PHC)} - \Gamma_{ChemOx}^{(\alpha,PHC)} = \theta S_w \lambda_{DIS}^{(\alpha,PHC)} \left(C_S^{(\alpha,PHC)} - \frac{C^{(\alpha,PHC)}}{E} \right) - \theta S_w \lambda_{BIO}^{(\alpha,PHC)} C^{(\alpha,PHC)} - \theta S_w \lambda_{ChemOx}^{(\alpha,PHC)} C^{(\alpha,PHC)} \quad (3.4)$$

with

$$\lambda_{DIS}^{(\alpha,PHC)} = \frac{Sh^{(\alpha)}\, D^{(\alpha)}}{(d_{50})^2} \left(\frac{f^{(\alpha)} S_n^{(\alpha)}}{S_{n,0}^{(\alpha)}} \right)^{\beta}, \quad (3.5)$$

$$C_S^{(\alpha,PHC)} = C_0^{(\alpha,PHC)} X^{(\alpha)}, \quad (3.6)$$

$$\lambda_{BIO}^{(\alpha,PHC)} = \sum_{\beta=1}^{N_A} k_{max}^{(\alpha,\beta)} M^{(\beta)} \left(\frac{1}{K_c^{(\alpha,\beta)} + C^{(\alpha,PHC)} + \sum_{j=1}^{N_c} K_{II}^{(\alpha,j)} C^{(j,PHC)}} \right) * \left(\frac{A^{(\beta)}}{K_A^{(\alpha,\beta)} + A^{(\beta)}} \cdot I^{(\beta)} \right), \text{ and} \quad (3.7)$$

$$\lambda_{ChemOx}^{(\alpha,PHC)} = k''_{\alpha,PHC}\, C^{(oxidant)} \quad (3.8)$$

where $C^{(\alpha,PHC)}$ is the concentration of PHC compound α (kg/m^3), $\lambda_{DIS}^{(\alpha,PHC)}$ is the dissolution rate coefficient (day^{-1}), E is the dissolution enhancement factor, $Sh^{(\alpha)}$ is the Sherwood number, d_{50} is the mean grain diameter (m), $D^{(\alpha)}$ is the aqueous diffusion coefficient, $S_n^{(\alpha)}$ is the NAPL saturation, $S_{n,0}^{(\alpha)}$ is the initial NAPL saturation, $f^{(\alpha)}$ is the local volume fraction of NAPL component α, $C_0^{(\alpha,PHC)}$ is the pure phase solubility of the organic compound α (kg/m^3), $X^{(\alpha)}$ is the mole fraction of the organic component α, N_A is the number of electron acceptors, N_c is the number of organic compounds, $A^{(\beta)}$ is the concentration of the electron acceptor β (kg/m^3), $M^{(\beta)}$ is the concentration of microbes which are consuming electron acceptor β (kg/m^3), $k_{max}^{(\alpha,\beta)}$ is the maximum substrate utilization rate (kgS/kgM/day), $K_c^{(\alpha,\beta)}$ is the organic half-utilization-rate concentration (kg/m^3), $K_A^{(\alpha,\beta)}$ is the electron acceptor half-utilization-rate concentration (kg/m^3), $K_{II}^{(\alpha,j)}$ is the inter-component inhibition constant of organic α by component j, $I^{(\beta)}$ is the electron acceptor inhibition constant (represented by

$I^{(\beta=1)} = 1;\ I^{(\beta>1)} = \coprod_{i=2}^{\beta}\left[\frac{1}{1+\frac{A^{(i-1)}}{K_{IA}^{i-1}}}\right]$, where K_{IA} is the inhibition coefficient for electron acceptor β), $k''_{\alpha,PHC}$ is the second-order oxidation rate coefficient for component α (m^3/kg/day or $Lg^{-1}day^{-1}$), and $C^{(oxidant)}$ is the oxidant concentration (kg/m^3). The second-order formulation, used to simulate persulfate oxidation of organic compounds (Eq. 3.8), was verified against an analytical solution (details provided in Appendix B).

3.3.2.2 Reaction Terms for Persulfate

The reaction term for persulfate (oxidant) consists of a term representing the persulfate reaction with PHC compounds ($\Gamma_{ChemOx,PHC}^{(oxidant)}$) and a term which represents persulfate decomposition due to reactions with aquifer material ($\Gamma_{ChemOx,AM}^{(oxidant,EA)}$). Decomposition of persulfate due to reactions with PHC compounds is represented by

$$\Gamma_{ChemOx,PHC}^{(oxidant)} = -\theta S_w \sum_{\alpha=1}^{N_c} X^{(\alpha,oxidant)}\, k''_{\alpha,PHC} C^{(oxidant)}\, C^{(\alpha,PHC)} \quad (3.9)$$

where $X^{(\alpha,oxidant)}$ is the stoichiometric mass ratio between persulfate and the organic compound. To simulate persulfate decomposition due to interaction with an aquifer material, the kinetic model developed by Sra et al (2013 (a)) was adopted as given by

$$\Gamma_{ChemOx,AM}^{(oxidant)} = -\theta S_w(k_1 + \gamma_{\text{oxidant}}\{\gamma_{H^+}k_2[H^+] + (\gamma_{cat})^{n_{cat}}k_{cat}(C_{cat})^{n_{cat}} + (\gamma_{NOM})^{n_{NOM}}k_{NOM}(C_{NOM})^{n_{NOM}}\})C^{(oxidant)} \quad (3.10)$$

with

$$C_{cat} = C_{cat}^{(solids)} m_{solids}/V_m \quad (3.11)$$

$$C_{NOM} = C_{NOM}^{(solids)} m_{solids}/V_m \quad (3.12)$$

where k_1 is the first-order reaction rate coefficient for uncatalyzed persulfate degradation, k_2 is the second-order reaction rate coefficient for acid-catalyzed persulfate degradation (which can usually be neglected in highly buffered aquifers), k_{cat} is the mineral-catalyzed degradation rate, k_{NOM} is the rate coefficient of the persulfate reaction with aquifer natural organic matter (NOM), and n_{cat} and n_{NOM} are the reaction orders with respect to mineral catalysts (represented by Fe^{2+}) and NOM. The terms $\gamma_{oxidant}$, γ_{H^+}, γ_{cat} and γ_{NOM} are respectively the activity coefficients for $S_2O_8^{2-}$, H^+, Fe^{2+} and NOM

in the system; $C_{cat}^{(solids)}$ is the concentration of Fe^{2+} and $C_{NOM}^{(solids)}$ is the solid NOM concentration represented by TOC concentration; m_{solids} and V_m are the mass of solids and aqueous volume, respectively. Sra et al (2013a) argued that with some simplification and using site-specific information, Eq. (3.10) can be written in the form of a first-order reaction and hence the decomposition of persulfate as a result of the interaction with an aquifer material can be written as

$$\Gamma_{ChemOx,AM}^{(oxidant)} = -\theta S_w k'_{AM,oxidant} C^{(oxidant)} \quad (3.\ 13)$$

where $k'_{AM,persulfate}$ is the first-order rate coefficient.

3.3.2.3 Reaction Term for Electron Acceptors

The reaction of each electron acceptor compound (β) is comprised of a biodegradation term ($\Gamma_{BIO}^{(\beta,EA)}$) and a chemical oxidation term ($\Gamma_{ChemOx}^{(\beta,EA)}$) as given by

$$\Gamma^{(\beta,EA)} = -\Gamma_{BIO}^{(\beta,EA)} + \Gamma_{ChemOx}^{(\beta,EA)} \quad (3.\ 14)$$

Oxygen, nitrate, manganese, iron, and sulfate are examples of terminal electron acceptors that can be simulated by BIONAPL/PS. Consumption of electron acceptor β during reaction with PHC compound α is given by

$$\Gamma_{BIO}^{(\beta,EA)} = -\theta S_w \lambda_{BIO}^{(\beta,EA)} C^{(\beta,EA)} \quad (3.\ 15)$$

with

$$\lambda_{BIO}^{(\beta,EA)} = \sum_{\alpha=1}^{N_c} k_{max}^{(\alpha,\beta)} M^{(\beta)} X^{(\alpha,\beta)} \left(\frac{C^{(\alpha,PHC)}}{K_c^{(\alpha,\beta)} + C^{(\alpha,PHC)} + \sum_{j=1}^{N_c} K_{II}^{(\alpha,j)} C^{(j,PHC)}} \right) * \left(\frac{1}{K_A^{(\alpha,\beta)} + A^{(\beta)}} \cdot I^{(\beta)} \right) \quad (3.\ 16)$$

where $C^{(\beta,EA)}$ is the concentration of the electron acceptor β (kg/m^3) and $X^{(\alpha,\beta)}$ is the stoichiometric molar mass ratio between the electron acceptor β and the PHC compound α which is consumed by the corresponding microbial community ($M^{(\beta)}$). The term $\Gamma_{ChemOx}^{(\beta,EA)}$ is used to simulate the generation of electron acceptor β during the chemical oxidation process. Hence, sulfate production as the result of persulfate decomposition is represented by

$$\Gamma_{CHE}^{(sulfate,EA)} = +\theta S_w \lambda_{CHE}^{(sulfate,EA)} C^{(sulfate,EA)} \quad (3.\ 17)$$

with

$$\lambda_{CHE}^{(sulfate,EA)} = X^{(sulfate/oxidant)}\left[\left(\sum_{\alpha=1}^{N_c} k_{\alpha}''.C^{(oxidant)}.\ C^{(\alpha,PHC)}\right) + k'_{AM,oxidant}C^{(oxidant)}\right] \quad (3.\ 18)$$

where $X^{(sulfate/oxidant)}$ is the stoichiometric molar mass ratio between sulfate and persulfate.

3.3.3 Microbial population growth and decay

The growth and decay of microbial communities such as SRB is represented by

$$\frac{\partial M^{(\beta)}}{\partial t} = \left[\sum_{\alpha=1}^{N_c} Y^{\alpha,\beta} M^{(\beta)} k_{max}^{(\alpha,\beta)} \left(\frac{C^{(\alpha,PHC)}}{K_c^{(\alpha,\beta)} + C^{(\alpha,PHC)} + \sum_{j=1}^{N_c} K_{II}^{(\alpha,j)} C^{(j,PHC)}}\right) * \left(\frac{A^{(\beta)}}{K_A^{(\alpha,\beta)} + A^{(\beta)}} \cdot I^{(\beta)}\right)\right] - bM^{(\beta)} \quad (3.\ 19)$$

where $Y^{\alpha,\beta}$ is the microbial yield coefficient (kg cell/ kg substrate, dimensionless) of microbial biomass $M^{(\beta)}$ (kg/m^3), and b is the linear decay rate (day^{-1}). The microbial yield coefficient ($Y^{\alpha,\beta}$) is the ratio of produced microbial biomass $M^{(\beta)}$ (corresponding to electron acceptor, β) per consumed mass of substrate α.

3.4 SIMULATING A COLUMN EXPERIMENT

BIONAPL/PS was used to simulate a series of stop-flow column experiments that were executed to mimic a persulfate/EBR treatment train. In these experiments, toluene was the only PHC compound and sulfate was the only electron acceptor. The validity of the BIONAPL/PS model formulation was evaluated by comparing the model results with the observed persulfate, toluene, sulfate and sulfide concentration data from three distinct experimental systems:

- ChemOx/EBR system which involved persulfate oxidation and microbial sulfate reduction. The comparison between the model results and observations from this column was used to estimate the second-order rate coefficient of toluene degradation by persulfate.
- EBR system which involved only microbial sulfate reduction. Through curve-fitting the model results to the observed concentration data from this column, the dual-Monod kinetic parameters for toluene biodegradation under sulfate reducing conditions were estimated. Comparing the concentration data of ChemOx/EBR and EBR column (i.e., the "reactive columns") was expected to provide insight into the impact of persulfate on the subsequent microbial sulfate reduction.
- Control system which was conducted to identify the possible effect of abiotic processes (e.g. dilution, sorption, precipitation, etc.) on the toluene concentration profile.

3.4.1 Experimental Design

Three (3) plexiglas columns (length 50 cm, internal diameter 3.8 cm) were packed with air-dried Borden sand mixed with a small fraction of granular carbon (0.2% v/v) to provide favorable conditions for the attachment and growth of bacterial communities. After packing, the columns were kept under anaerobic conditions (DO < 1) to create an ideal condition for the activity and growth of sulfate reducing bacteria. CO_2 was initially flushed through each column, followed by the injection of nitrogen-purged simulated groundwater (contained ~90 mg/L of $CaCO_3$ and ~50 mg/L of sulfate) for ten (10) pore volumes (PVs) in an up-flow mode (flow rate of 0.09 mL/min, column PV of 220 mL).

Following the water saturation process, an inoculum of anaerobic digester sludge (containing SRB) was injected into the reactive columns (1% v/v of the column soil). Then, ten (10) PVs of a 10 mg/L toluene solution (neat toluene mixed with the anoxic simulated groundwater) was injected at a flow rate of 0.12 mL/min to establish a steady and uniform toluene concentration in each column system. The steady-state toluene concentration observed in the effluent from all three columns was ~7.4 mg/L. After the toluene concentration reached steady-state, persulfate (230 mg/L) and sulfate (230 mg/L) solutions were co-injected with toluene, respectively into the ChemOx/EBR and EBR columns for three (3) PVs at a flow rate of 4 mL/min. The concentration of persulfate in the solution injected into the ChemOx/EBR column was deemed sufficient to oxidize 50% of the toluene mass in the system based on the persulfate/toluene stoichiometry. The remaining toluene mass would then be available for degradation by sulfate reduction. The sulfate mass added to the EBR column was the stoichiometric equivalent of the amount of sulfate expected to be generated in the ChemOx /EBR column due to persulfate decomposition. Sodium azide (NaN_3, Acros Organics) at 10% v/v was added to the injected toluene solution for the control column (for three (3) PVs) as a biocide. The uniform distribution of reactants along the length of each column were demonstrated by analyzing the samples collected from the 7 sampling ports located at 2.5, 5, 10, 15, 20, 30 and 40 cm from the inflow end (results not shown).

Following the injection of three (3) PVs, the flow was stopped to allow all systems sufficient time to react. Samples were collected from the effluent of each column by the injection of Milli-Q water (27 mL) at the influent. Given the column PV and the minimum sample volume required, only eight (8) samples could be collected from each column. Samples were analyzed for persulfate, toluene, sulfate, and sulfide using the same analytical methods as described in Chapter 2.

3.4.2 Model Parameters

Each 50 cm long column (discretized into 100 × 1 × 1 elements) was simulated under a no-flow condition. The observed concentrations of toluene, sulfate and persulfate observed just prior to flow shutdown conditions were assigned as the initial conditions (see Table 3.1).

There are only two peer-reviewed studies that have reported on the pseudo-first order rate coefficients for persulfate oxidation of BTEX compounds (Huang et al. 2005; Sra et al. 2013b), and only one study that has investigated the rate of persulfate decomposition due to the interaction with aquifer materials (Sra et al. 2013a). The pseudo-first order rate coefficients along with the appropriate persulfate concentrations were used to estimate second-order rate coefficients required for BIONAPL/PS. For toluene, the estimated second-order rate coefficient was 0.005 $Lg^{-1}day^{-1}$ for a reaction with naturally activated persulfate (Sra et al. 2013b), and 2.0 $Lg^{-1}day^{-1}$ for a reaction under heat-activated persulfate conditions (Huang et al. 2005). These second-order rate coefficients provide some context, but in this study, the second-order rate coefficient was determined by matching the toluene simulation results with the observed data from the ChemOx/EBR column. The first-order rate coefficient representing persulfate decomposition in the presence of Borden aquifer materials as reported by Sra et al (2013a) ranged from 2.82×10^{-3} to 2.82×10^{-2} day^{-1}.

The dual Monod kinetic model (Kissel et al. 1985; MacQuarrie et al. 1990) which is used in BIONAPL/PS is considered the most suitable mathematical representation of intrinsic biodegradation processes since the rate of reaction is dependent on the availability of both electron acceptors and electron donors (Adriano, 1994). However, the dual Monod kinetic parameters for biodegradation of BTEX compounds under sulfate-reducing conditions (e.g., maximum utilization rates, biomass yield coefficient and half utilization constants for both electron donor and acceptor) are not directly available from the literature. The number of studies which have investigated the kinetics of BTEX biodegradation under natural conditions is limited and primarily focused on aerobic biodegradation (e.g., MacQuarrie et al. 1990, Alvarez et al. 1991; Rifai & Newell 1998; Schirmer et al. 1999; Schirmer et al. 2000).

For BTEX degradation under microbial sulfate reduction, most of the previous studies have reported first-order or single Monod kinetic parameters (Roychoudhury & McCormick 2006; Roychoudhury et al. 2003; Oude Elferink 1998; Fukui & Takii 1994; Edwards et al. 1992; Ingvorsen et al. 1984). There are only a few investigations on the dual Monod kinetic parameters for

degradation of simple organic compounds (e.g., acetate) under sulfate reducing condition (Zacatenco et al. 2013; Van Wageningen et al. 2006; Poinapen & Ekama 2010; Fedorovich et al. 2003; Kalyuzhnyi et al. 1998). These existing literature data provide some context, but in this study, the dual Monod parameters were determined by fitting the toluene simulation results with the observed data from the EBR column. According to Schirmer et al. (2000), who conducted an extensive sensitivity analysis to determine the effect of uncertain dual Monod kinetic parameters on BTEX biodegradation under aerobic conditions, the maximum utilization rate (k_{max}) has the most significant influence on the modelling results, compared to other Monod parameters (e.g., microbial growth and decay rate and half utilization constants). Therefore, in this study the value of k_{max} was adjusted through trial and error to achieve the best fit between the simulated toluene concentration and the observed data from the EBR column.

3.4.3 Results

The main goal of simulating the column experiment was to test the BIONAPL/PS model formulation and assess the model capability to reproduce the observed laboratory data. After adjusting the persulfate oxidation second-order rate coefficient and the sulfate reduction maximum utilization rate coefficient in the ChemOx/EBR and EBR column respectively, BIONAPL/PS was able to re-produce the observed toluene and sulfate concentrations in these systems (Figure 3.1). The parameters which created the best-fit between the simulation results and observed data are listed in Table 3.1. As expected, no significant change in the toluene and sulfate concentration was observed or predicted in the control column. The small decrease of toluene concentration (~0.8 mg/L) in this column was most likely a result of the occurrence of microbial activity in spite of the addition of sodium azide. The minor decrease in sulfate concentration (~5 mg/L) in the control column corresponds to the amount predicted by the stoichiometry of the toluene biodegradation coupled with sulfate reduction. Microbial sulfate reduction was likely established in the control column prior to addition of sodium azide due to the presence of the background sulfate and indigenous soil microbes (soil was not autoclaved and occurrence of tiny black spots was indicative of sulfide precipitates in this column).

In both reactive columns (i.e., ChemOx/EBR and EBR) the toluene concentration decreased from 7.4 mg/L to MDL in less than 20 days (Figure 3.1(a)). The greater toluene degradation was observed for the ChemOx/EBR column compared to the EBR column at early time, as the result of the faster kinetics associated with persulfate oxidation compared to microbial sulfate reduction (Note: the same

parameters associated with toluene sulfate reduction were used for both the ChemOx/EBR and EBR systems). The simulation results and experimental data show the generation of sulfate following persulfate decomposition for the ChemOx/EBR system, and consumption of sulfate during microbial sulfate reduction for the EBR system (Figure 3.1 (b)).

The similar toluene mass removal in the EBR and ChemOx/EBR experiments (except at the early treatment times when persulfate oxidation resulted in greater toluene degradation in the ChemOx/EBR system) is most likely associated with the ideal conditions for the stimulation of microbial processes (including sulfate reduction) in the EBR column. The optimized conditions included the existence of reducing conditions and excess availability of sulfate, organic substrates and the amendment of the columns with granular carbon and inoculum of anaerobic digester sludge (containing SRB), which is not a general practice at contaminated sites. Therefore, the above-mentioned observation may not be valid under most site conditions (e.g., multi-component contamination, higher concentrations of organics, lower background sulfate, etc.). The comparison between the performance of the combined ChemOx/EBR and EBR treatment systems was further investigated in the next phase of this modelling study.

3.4.3.1 Sensitivity of the ChemOx/EBR System Parameters

Figure 3.2(a) shows the model prediction of toluene concentration in the ChemOx/EBR system for different second-order rate coefficients. The adjusted value (0.8 $Lg^{-1}day^{-1}$) was within the range of the rates estimated based on the literature (0.005-2 $Lg^{-1}day^{-1}$). However, there is a two-order of magnitude difference between the rate coefficient obtained from the best-fit model and that reported by Sra et al. (2013b) for toluene oxidation with naturally activated persulfate based on a series of laboratory batch experiments using Borden aquifer material (0.005 $Lg^{-1}day^{-1}$). This discrepancy may be due to a combination of possible factors including:

1. A higher soil/water ratio in the columns compared to the batch experiments which can enhance the natural activation of persulfate by increasing the concentration of natural catalysts (i.e., trace metals) and organic matter (Anipsitakis & Dionysiou 2004; Teel et al. 2011; Sra 2010), and thus increase the rate of toluene oxidation .
2. The amount of contact (mixing) between the oxidant, organic compounds and aquifer material was minimal in the batch experiments, due to lack of continual shaking (K. Sra,

personal communication, September 18, 2014). Hence, the higher rate of oxidation in the column experiment could be attributed to the enhanced mixing/contact between the reactants in comparison to a batch reactor.

3. The oxidation rate obtained from the batch experiment corresponds to reaction of persulfate with a mixture of several different organic compounds. The inter-component competition for the available persulfate in the batch systems, could lead to lower oxidation rate for each of the individual compounds (including toluene), compared to that obtained from this column experiment in which persulfate reacted only with toluene.

4. Both the columns in this experiment and the batch reactors in the study by Sra et al. (2013b) were packed with Borden aquifer materials. However, as mentioned earlier, Borden sand in the columns was mixed with added granular carbon and organic matter contained in the anaerobic digester sludge (i.e., the activated sludge). The significant source of added organic matter might have activated persulfate (Elloy et al. 2014; Ahmad et al. 2013; Ocampo 2009) and led to increased reaction rates in the ChemOx/EBR system compared to that obtained based on the batch experiment.

As seen in Figure 3.1(b), the observed sulfate concentration in the ChemOx/EBR system increased from 50 mg/L (initial concentration) to ~280 mg/L over 20 days using the best-fit parameters. This increase was consistent with that expected from the stoichiometry of sulfate production during the reaction between toluene and persulfate; however, there is a difference between the predicted sulfate generated and that observed. To decrease the discrepancy at early time (< 5 days), the first-order decay rate coefficient representing persulfate interaction with aquifer material was increased by an order of magnitude from the initial value (2.8×10^{-2} day^{-1}) which was based on the available literature (Sra et al. 2013a). This increased persulfate decomposition rate enhances the rate of sulfate generation (Figure 3.3 (a)) and also the rate of persulfate decomposition in the ChemOx/EBR column (Figure 3.4) (Note: in the ChemOx/EBR system, persulfate was below the minimum detection limit (i.e., 250 mg/L) over the entire course of the experiment, and thus due to lack of observed persulfate data, the model prediction of persulfate decomposition could not be verified).

The increased first-order persulfate decomposition rate at early simulation time can be justified since the column was packed with granular carbon which was initially flushed with organic matter from the activated sludge. This may have altered the persulfate decomposition pathway (e.g.,

persulfate activation can initiate free radical-based reactions) and enhanced the rate of persulfate consumption, which in turn, may have led to increased sulfate generation in the ChemOx/EBR column. Moreover, there may be additional sources of sulfate production (e.g., geochemical processes such as oxidation of sulfide by persulfate (USEPA, 2004; Huling ant Pivetz, 2006)) that are not considered in the BIONAPL/PS model. However, as see in Figure 3.3(a), adjusting the persulfate decomposition rate could not reduce the discrepancy between the simulated and observed sulfate concentrations observed at later simulation times (> 5 days). A number of additional simulations were performed by varying different model parameters (e.g., dual-Monod kinetic parameters such as half-utilization rate constants, microbial yield and concentration, etc.) to decrease the observed discrepancy between the simulated and observed sulfate data in the ChemOx/EBR system. However, the results (not shown here) showed that changing individual model parameters did not imporove the overall fit between the observed and simulated sulfate and toluene data. In general, the lower sulfate consumption observed in the ChemOx/EBR column compared to that predicted by BIONAPL/PS (based on the stoichiometry) could be the mixed effect of the following factors:

1. the rate of sulfate consumption by microorganisms (specially following exposure to persulfate) may not be precisely represented by the stoichiometry ratios; since the rate of sulfate uptake depends mainly on the type, diversity and growth conditions of the existing sulfate reducers.

2. microbial communities may only transform toluene to other compounds and may not completely mineralize it to carbon dioxide, and thus less sulfate would be used per unit of toluene being transformed than being completely mineralized.

3. inhibition of microbial sulfate reduction due to the presence of persulfate along the entire length of the column. In this scenario, the decreased toluene concentration in the column at later simulation times can be attributed to the activity of microbial communities other than SRB which are also present in the activated sludge (e.g., methanogenic bacteria). The inhibitory effect of persulfate was not accounted for in simulating the ChemOx/EBR system.

To date were insufficient data to examine any of the above hypotheses for the ChemOx/EBR column.

3.4.3.2 Sensitivity of the EBR System Parameters

Figure 3.1 depicts the match between the simulated and observed toluene and sulfate concentrations in the EBR column using the best fit parameters (Table 3.1). As discussed earlier, the dual Monod parameters were selected within the bounds of the reported literature values (e.g., Kalyuzhnyi et al. 1998; Fedorovich et al. 2003; López-Pérez et al. 2013), and the maximum utilization rate (k_{max}) was adjusted to acquire the best-fit between the simulated and observed toluene and sulfate concentrations in the EBR system. Figure 3.2(b) shows the simulated toluene concentration in the EBR system using different maximum utilization rate coefficients.

The result of the best-fit scenario shows a reduction of sulfate from 230 mg/L to ~170 mg/L which is consistent with the stoichiometry of toluene degradation under sulfate reducing conditions. However, as seen in Figure 3.1(b), more sulfate was consumed in the EBR column compared to what was predicted by the model. Simulation of additional modelling scenarios again showed that the inconsistency between the simulated and observed sulfate concentration in the EBR column could not be rectified by changing individual dual-Monod kinetic parameters and ensuring consistency between the simulated and observed toluene concentration. For example, using a slightly increased maximum utilization rate to increase sulfate consumption in the model (Figure 3.3 (b)) led to much more toluene degradation than what was observed in the EBR system (see Figure 3.2(b)).

The greater sulfate consumption observed in the EBR column compared to that predicted by BIONAPL/PS could be as result of (1) additional consumption of sulfate by SRB communities for cellular maintenance and growth without any impact on organic mass (Jin & Bethke 2009); (2) increased activity of the SRB microbial community due to presence of carbon/energy sources other than toluene (e.g., the granular carbon); and (3) existing uncertainty regarding the Monod kinetic parameters used in the model (discussed later in the text) and (4) the occurrence of geochemical processes which might affect the observed sulfate concentration. For example precipitation and dissolution of solid minerals, such as iron sulfide, calcium sulfate or calcium carbonate can confound the concentrations of the primary reaction byproducts such as sulfate, sulfide and dissolved inorganic carbon (Maurer & Rittmann 2004).

3.4.3.3 Microbial Sulfate Reduction in ChemOx/EBR and EBR Systems

The occurrence of microbial sulfate reduction can be indicated by the detection of sulfide as the primary reaction by-product. Figure 3.5 compares the observed sulfide concentrations in the two reactive columns as measured during this experiment. Higher sulfide concentrations in the EBR system compared to the ChemOx/EBR system confirms the inhibitory effect of persulfate on the activity of sulfate reducers (also discussed on Chapter 2). The sulfide data, however, could not be used to estimate the rate of sulfate reduction because sulfide concentrations are most likely masked by the precipitation of Fe-S minerals, the loss of volatile hydrogen sulfide gas and by measurement errors. This lower sulfide concentration observed in the EBR column compared to what was expected based on the stoichiometry can be readily linked to the precipitation of sulfide which was inferred from the black spots clearly visible inside the EBR column. Sulfide production and precipitation are not captured by BIONAPL/PS; however, it can simulate the inhibition of microbial sulfate reduction in the presence of persulfate. This capability of the model was enabled and examined in the next phase of this modelling effort, where BIONAPL/PS was used to simulate a controlled pilot-scale field system with multiple contaminants, multiple electron acceptors, a complex flow system, and no additional microbial populations or carbon sources.

3.5 SIMULATING A CONTROLLED FIELD TRIAL

In the next phase of this modelling study, BIONAPL/PS was used to simulate a controlled pilot-scale field trial with multiple components within a complex flow system. As opposed to the column experiment, there was no addition of microbial communities or carbon sources in this system. The pilot-scale trial was conducted to investigate the coupled processes involved in a persulfate/EBR treatment train and to characterize the impact of persulfate on indigenous microbial processes. The pilot-scale experiment was divided into two distinct phases:

Phase 1) this phase involved the development of a quasi steady-state BTX plume and an associated anaerobic aquifer system (low DO, and reducing conditions) prior to persulfate injection. To facilitate the controlled release of the BTX compounds, a series of Waterloo Emitters™ were used to maintain a continuous transfer of BTX into the groundwater. The maximum BTX concentration in the experimental gate was approximately 25 mg/L.

Phases 2) in this phase, two (2) sequential persulfate injection episodes using a cross-borehole injection system (CIS) were conducted to generate two persulfate slugs. About 480 L of a 10 g/L sodium persulfate solution was injected at a rate of 0.5 L/min into two outside CIS wells, while groundwater was simultaneously extracted from the central CIS well at a rate of 1 L/min. Mixing between persulfate and BTX was expected to form a chemical oxidation zone (ChemOx zone) in the portion of the plume confined between the two persulfate slugs. Based on stoichiometry, the injected persulfate mass would be sufficient to oxidize 50% of the BTX mass confined between the persulfate slugs. As sulfate was generated as a result of persulfate decomposition, the ChemOx zone would be transformed into the "EBR zone". Microbial sulfate reduction was enhanced in the EBR zone due to the increased sulfate concentration (source of electron acceptor) and degradation of BTX into simpler/more bioavailable substrates following persulfate oxidation. Microbial sulfate reduction then dominated BTX mass removal in the EBR zone.

The fate of the "ChemOx zone" and the "EBR zone" was monitored for >13 months as the groundwater migrated along the experimental gate and continued even after the groundwater flow was stopped (on Day 221) due to unfavorable winter conditions. An extensive monitoring plan including the combined application of conventional and emerging site characterization tools (e.g., isotope analysis and molecular biology) was used to distinguish the dominant mass removal process and to investigate the impact of persulfate on the subsequent microbial processes. Additional details of this pilot-scale experiment can be found in Chapter 2. The main objective of this modelling effort was to evaluate the capability of BIONAPL/PS to:

- reproduce the distribution and migration of the BTX plumes;
- reproduce the temporal and spatial distributions of the injected persulfate slug and the produced sulfate plume resulting from persulfate decomposition;
- obtain an estimate of the reaction kinetics for BTX through an exploratory benchmarking effort;
- explore options to optimize the efficiency of this treatment train system; and
- investigate the advantages of persulfate/EBR treatment train over EBR treatment alone.

3.5.1 Site Description and Infrastructure

The pilot-scale experiment was conducted in a sheet pile-walled gate at the University of Waterloo Groundwater Research Facility at the Canadian Forces Base (CFB) Borden located near Alliston, ON. The experimental gate was 2 m wide and 24 m long, and was enclosed on three sides using sheet piling driven into the underlying aquitard located 3 m below the ground surface (bgs) (Figure 3.6). The fourth side was left open to allow ambient groundwater to enter. Four wells installed at the gate entrance were used to introduce dissolved PHCs into the subsurface. A pumping well at the closed end of the gate was used to control the groundwater flow rate in the experimental gate.

The monitoring network in the gate consisted of six fence lines installed at various distances along the length of the gate (identified as Row 1 to Row 6). Each row consisted of three multilevel monitoring wells (identified as left, middle and right looking downgradient). The wells in each row were spaced 0.65 m apart and each was equipped with four multilevel sampling points spaced at 0.7 m. The three CIS wells installed between Row 1 and Row 2 (Figure 3.6) were used to deliver persulfate into the system.

The unconfined Borden aquifer is a surficial, well-sorted fine to medium-grained sandy aquifer with a hydraulic conductivity of 6.0×10^{-6} to 2.0×10^{-4} m/s, underlain by a clay deposit. Micro-scale heterogeneities exist in the form of silty sand and coarse sand lenses (Mackay et al. 1986). General hydrogeological properties and background geochemistry of the Borden aquifer have been extensively characterized (e.g., MacFarlane et al. 1983; Nicholson et al. 1983; Mackay et al. 1986). The fraction of organic carbon (f_{oc}) of the aquifer sand is 0.0002, and the aquifer porosity is ~0.33. The background concentrations of the major ions are: 10 to 30 mg/L SO_4^{2-}, 1 to 2 mg/L Na^+, 50 to 110 mg/L Ca^{2+}, and <0.002 to 0.1mg/L H_2S. Groundwater pH is in the range of 7 to 8.

3.5.2 Modelling Approach

A two-dimensional (depth-averaged) simulation of the pilot-scale experiment was performed using BIONAPL/PS. The rectangular domain (26 m × 2 m × 2.5 m) representing the experimental gate was discretized with 260 × 20 × 1 elements. The flow boundary conditions included a fixed head at the left (inflow) boundary, a recharge flux across the top, four internal fixed-head nodes representing the PHC source wells and no-flow (zero-gradient type) conditions along the remaining boundaries (bottom and sides) representing the sheet pilings and the underlying clay deposit. The extraction well

was simulated by defining a point sink and assigning the corresponding pumping (extraction) rates at each time interval. Temporal changes in the groundwater flow rate due to changes in the extraction rate were captured by assigning a different extraction rate.

The transport boundary conditions included a first-type (fixed concentration) boundary condition for all components at the left inflow boundary, a third-type (Cauchy mass flux) boundary condition along the top, and internal nodes with specified concentrations representing the source wells. To capture the variation of source well concentrations with time, the concentrations assigned to the source well nodes were equal to the averaged BTX concentrations observed in the source wells. A dilution factor was used to represent the decreased BTX concentrations outside the source wells compared to the in-well concentrations. Fixed ambient inflow concentrations were specified for organic compounds and electron acceptors, and the same concentration values were used to define the initial conditions throughout the domain. The time step varied from 0.01 to 0.05 days, which satisfied the Courant stability criterion.

To simulate persulfate injection, the three CIS wells were defined as point sources/sinks at the corresponding nodes located between Row 1 and Row 2 (Figure 3.6). The concentration of persulfate and dissolved oxygen in the uncontaminated injected solution (10 g/L and 4 mg/L, respectively) as well as the corresponding injection/extraction rates were assigned to each location. Consistent with the experiment, the persulfate solution was injected into the two outside CIS wells (injection rate 0.5 L/min) while groundwater was extracted from the middle CIS well (extraction rate 1 L/min).

In this modelling effort, the inhibition of microbial sulfate reduction in the presence of persulfate was simulated which in turn limits the consumption of sulfate in the system. This was accomplished using the electron-acceptor inhibition term ($I^{(\beta)}$) in the BIONAPL/PS model formulation (see Eq. 3.10 and Section3.3.2.1). The inhibition term allows a gradual change between persulfate oxidation to microbial sulfate reduction if the inhibition coefficient (K_{IA}) is set to a very small value for persulfate (for details see BIONAPL/3D user guide). As such sulfate would be utilized only after the persulfate is almost completely consumed. The basis for using the inhibition feature was the information obtained from the column experiments as well as the pilot-scale field experiment, in which the decreased population and activity of SRB in the presence of persulfate were demonstrated using molecular biology tools (see Chapter 2).

Similar to the column simulations, the model input parameters were initially selected within the existing ranges reported in the literature. Model parameters including maximum utilization rates, microbial yield and concentration as well as second-order chemical oxidation rate coefficients were manually adjusted through a trial-and-error process to match the model output with the observed field data. Table 3.2 lists the model parameters and initial conditions used in the simulation scenario which led to the best-fit between the model results and the observed field data (i.e., the "best-fit scenario"). To benchmark the flow model, the bulk hydraulic conductivity was adjusted so that a good fit between the simulated and observed heads and velocities was obtained. The transport model was benchmarked through adjusting parameters such as porosity, dispersivity, and kinetic rate coefficients for chemical oxidation and biodegradation of the BTX compounds to obtain the best fit between the simulated and observed BTX concentrations. The model integrity was further evaluated by comparing the BTX mass loading and mass loss rates determined by BIONAPL/PS, with the estimates based on the observed row-averaged BTX concentrations and corresponding Darcy flux.

3.5.3 Results

The exact reproduction of the observed data from such a complex field system with dynamic flow conditions, multiple contaminants/electron acceptors, and inter-component competition and inhibitions was not anticipated, given the modelling assumptions and simplifications (e.g., neglecting the existing heterogeneities and geochemical reactions), and uncertainties regarding the model input parameters, and the inevitable errors associated with the field data measurements. The complexities of this experiment system make it virtually impossible to claim the uniqueness of the obtained model parameters which are basically the by-product of benchmarking the model outputs against the observed field data. However, the main objective of this model benchmarking effort was to evaluate the capability of BIONAPL/PS to capture the observations from this complex field system, and then explore options for performance optimization.

Figure 3.7 shows the consistency between the observed groundwater depth and velocity at a monitoring point in Row 5 with the results of the best-fit scenario simulation. Figure 3.8 demonstrates a good agreement between the simulated and observed BTX breakthrough at Row 2 and Row 3 which represent the ChemOx and EBR zones, respectively (see Appendix C for comparison between the simulated and observed BTX plume profiles). In scenarios with higher persulfate decomposition or higher oxidation rate coefficients compared to the best fit scenario (with rates lower than that used in

column simulations, but yet, higher than that extracted from the literature), a better match was obtained between the observed and simulated BTX concentrations at Row 3. However, these changes had a negative impact on the match between the simulated and observed BTX and sulfate concentrations at Row 2 (results not shown).

BIONAPL/PS underestimated the persulfate concentrations at Row 2 compared to the observed row-averaged concentrations (Figure 3.9a). In contrast, the model overestimated the persulfate concentration at Row 3 despite the use of higher rate coefficients for persulfate (in reaction with both BTX and aquifer material) compared to those extracted from the literature. This higher persulfate concentrations at Row 3 caused the overestimation of the role of persulfate oxidation in the EBR zone by the model, which in turn, led to greater BTX removal at Row 3 compared to the observed field data (Figure 3.8(b)).

The formation of the sulfate plume as predicted by the model is consistent with the observed trends with corresponding concentration values being of the same order of magnitude (except for Row 2 with higher deviation)(Figure 3.9(b)). However, similar to the column simulation, the model predicted less sulfate production during the persulfate decomposition in the ChemOx zone (i.e., Row 2) and less sulfate consumption during the microbial sulfate reduction in the EBR zone (i.e., Row 3 and 4). The lower sulfate consumption predicted at Row 3 can be partly caused by the overestimated persulfate concentrations at this location, which prevent microbial sulfate reduction to proceed through the inhibition term in the model.

The possible underlying mechanisms contributing to the discrepancy between the simulated and observed sulfate concentrations in both the ChemOx and EBR zones have been briefly discussed in Section 3.4.3. In general, the variations between the simulated and observed sulfate and persulfate concentrations in this modelling effort can be caused by the uncertainties regarding the initial microbial population and the chosen stoichiometric ratios and kinetic parameters associated with both persulfate oxidation and microbial sulfate reduction. Also the discrepancies can be attributed to model simplifications and assumptions such as: (1) neglecting the existing heterogeneities, (2) neglecting the effect of temperature variations (between 7-15 ºC) and other ambient conditions (e.g., enhanced bioavailability of the remaining substrate) on the growth and activity of microbial communities and (3) neglecting the effect of other biotic/abiotic processes such as geochemical processes or other possible biological pathways (e.g., methanogenesis or fermentation) on the observed field data. For

instance, the dual-Monod mathematical model used in e BIONAPL/PS is one of the most representative, but as mentioned earlier, is one of the least-studied kinetic models. Due to data scarcity in the literature, in this study the Monod kinetic parameters such as maximum substrate utilization, background microbial concentration and microbial yield were obtained through curve-fitting the model results to the observed field data. The non-uniqueness of the fitted Monod kinetic parameters is the major obstacle in obtaining reliable kinetic parameters (Kim et al. 2005). According to Schirmer et al. (1999), different combinations of $k_{max}/K_S/K_A$ could fit the measured concentration of a substrate. The problem becomes even more complex when the uncertainty of chemical oxidation reaction rates is added. Nevertheless, evaluating the effect of uncertain chemical and biological kinetic parameters on BTX degradation was beyond the scope of this study.

3.5.3.1 Quantifying the Role of Mass Removal Processes

The BIONAPL/PS model could successfully reproduce the general evolutionary trend of the observed field data. The model integrity was further evaluated by comparing the cumulative BTX mass loss and mass loss rates determined by BIONAPL/PS, with the estimates based on the observed BTX concentrations and corresponding Darcy flux (see chapter 2 for details). The mass loss estimates were used to identify the dominant mass removal processes in the ChemOx and EBR zones and also to quantify the contribution of the various mass removal processes (i.e., aerobic biodegradation, sulfate reduction, persulfate oxidation).

Figure 3.10 shows the BTX mass loss and mass loss rate calculated between Day 156 and Day 221 (flow shutdown) for both the ChemOx zone and the downgradient EBR zone. It can be seen that the results from the best fit scenario are consistent with the calculations based on the observed field data. The observed peaks in the mass removal rate in the ChemOx zone correspond to two persulfate injection episodes on Day 170 and Day 180 (Figure 3.10 (a)), demonstrating the dominant role of chemical oxidation in this zone. However, the higher rates calculated by the model led to higher cumulative BTX mass loss compared to the estimates based on the observed field data (1.5 kg vs 1.1 kg). In the EBR zone, results from both calculations showed that the enhanced rate of mass loss in this location occurred after persulfate application (Figure 3.10 (b)). In calculations based on the observed field data, the increased rate of mass loss is correlated with the time that high sulfate concentrations reach Row 3, and in contrast to the model estimates, the rate of mass removal continually increases until Day 221. The main cause of the observed inconsistency between the two

calculations in the EBR zone is again the overestimated persulfate concentrations at Row 3, which inhibits the role of microbial sulfate reduction in this zone.

The BIONAPL/PS mass loss estimates were also used to quantify the contribution of individual mass removal processes in both reaction zones. Figure 3.11(a,b) shows the model prediction for the rate of mass loss associated with aerobic biodegradation, microbial sulfate reduction and persulfate oxidation in the ChemOx and EBR zones for the best-case scenario . Figure 3.11(c,d) depicts the model calculation of the cumulative BTX mass loss due to each individual process, and Figure 3.11(e,f) demonstrates the weighted contribution of each specific mass removal process with respect to the total removed mass over time. The sequential order of dominant mass removal processes in the ChemOx and EBR zones can be also inferred from Figure 3.11(e,f).

The model results indicated that during the plume generation phase, aerobic degradation was dominant in the ChemOx zone and then transitioned into sulfate reduction upon depletion of oxygen. The changes in flow rate and source concentration during the plume generation phase caused the observed shift between aerobic and sulfate reducing conditions prior to persulfate injection on Day 170 and Day 180. A similar trend was also captured by the molecular biology data (see Chapter 2 for details). As seen in Figure 3.11(e), immediately after persulfate injection, sulfate reduction was inhibited and persulfate oxidation dominated the BTX mass removal. Upon depletion of persulfate at Row 2 (~Day 221), microbial sulfate reduction was re-established and became the dominant mass removal process at this location (simulated profiles of oxygen, sulfate and persulfate and the temporal evolution of the aerobic and sulfate reducing bacteria are presented in Appendix C). Figure 3.11(a) shows enhancement in the rate of microbial sulfate reduction following persulfate injection and indicates the transient inhibitory impact of persulfate presence on the microbial sulfate reduction. Overall, persulfate oxidation was responsible for most (1.1 kg of the total 1.4 kg, 78%) of the mass loss that occurred in the ChemOx zone between Day 156 to Day 221. This was followed by sulfate reduction (21%) and aerobic biodegradation (~1%) (Figure 3.11 (c)).

Aerobic degradation and then sulfate reduction act as the dominant mass removal process in the EBR zone during the plume generation phase. Following the persulfate injections, the model prediction of the sequence and contribution of various mass removal processes in the EBR zone was also affected by the model overestimation of the role of persulfate oxidation at Row 3 (enclosed in the EBR zone). Nevertheless, microbial sulfate reduction was demonstrated to play a major, long-term

mass removal role in the EBR zone. As demonstrated in Figure 3.11(b,d), the contribution of microbial sulfate reduction to BTX mass removal in the EBR zone, although established prior to persulfate application, was substantially increased after the persulfate injections and upon persulfate depletion and the arrival of high sulfate concentrations. However, following the flow shutdown on Day 221, sulfate reduction was inhibited in the EBR zone (Figure 3.11(b,d)). This decreased role of microbial sulfate reduction in the EBR zone at later simulation times (~Day 293) was also illustrated by the field data suggesting the hindered activity of the SRB community and establishment of methanogenic biodegradation in the EBR zone at later stages of the experiment (see Chapter 2). The methanogenic biodegradation as a mass removal process was not included in this modelling effort.

3.5.3.2 Impact of Key Design Parameters on Remedial Performance

To explore the design options to optimize the efficiency of the persulfate/EBR treatment train, the role of various key design parameters (e.g., injected persulfate concentration, injection rate, duration and interval) was evaluated through simulating a series of exploratory scenarios. The flow shutdown on Day 221 (due to unfavorable winter conditions) was an experimental artifact of this pilot-scale trial. For a more generic exploration of the effect of design parameters on remedial performance, the flow dynamics of the best fit scenario was modified. The "non-stop flow scenario" included all the same characteristics of the best fit scenario except that the groundwater flow was not stopped on Day 221. To represent the elimination of the BTX source corresponding to the source shut down in the best fit scenario, the BTX source was removed in the non-stop flow scenario on Day 221. As seen in Figure 3.12, the continual groundwater flow in the non-stop flow scenario transported the by-product sulfate up to Row 5 and caused an increased BTX mass removal at this row, as opposed to the best fit scenario in which the flow was stopped on Day 221 and the sulfate plume did not reach beyond Row 4.

To evaluate the impact of the key design parameters on the performance of the combined persulfate/EBR remedy, new scenarios were built on the basis of this "non-stop flow" scenario. These scenarios investigate the optimization of the persulfate/EBR treatment train for dissolved BTX removal within about 24 m in a Borden-like aquifer. The impact of increasing persulfate concentration (by ten (10) fold), doubling the duration and rate of persulfate injection/extraction, and doubling the injection interval, one at a time, was investigated. The results are described in more detail in the following and the corresponding figures are presented in Appendix C.

The “high dosage scenario” involved a ten (10) fold increase in the concentration of the injected persulfate. The modelling results for this scenario show a significant increase (~80%) in the rate of BTX mass removal at Row 2 and Row 3 compared to the “non-stop flow” scenario (i.e., base case scenario). However, the longer persistence of persulfate in this scenario inhibited microbial sulfate reduction at Row 4 and Row 5, which in turn reduced BTX mass removal at these further downgradient rows. The low persulfate concentration at Row 4 and Row 5 could not maintain the mass removal at these locations. Therefore, despite the improved mass removal at locations in the vicinity of the persulfate injection, the “high dosage scenario” was found to have an adverse impact on the overall performance of the persulfate/EBR treatment train within the 24 m simulated domain. Nevertheless, it can be anticipated that the EBR zone would form and microbial sulfate reduction would occur further downgradient (beyond the model domain) in this scenario. This observation highlights the importance of implementing a proportionate amount of persulfate treatment for an improved overall efficiency of the treatment train.

Doubling the rate and duration of persulfate injection/extraction caused a slight increase (~25%) in the overall mass removal efficiency at locations close to the injection zone (i.e., Row 2 and Row 3) due to higher persulfate and sulfate concentrations at these locations (almost double). Due to lower persulfate concentrations in this scenario compared to the “high dosage scenario”, the increased persulfate levels persisted for a shorter duration in this scenario and thus, no adverse impact on the subsequent microbial processes was observed at locations further downgradient from the injection zone (i.e., at Row 4 and Row 5). The overall enhanced BTX mass removal in these scenarios compared to the base case scenario was due to the increased sulfate generation within the model domain. It can also be predicted that at locations further downgradient within the model domain, the microbial sulfate reduction would maintain mass removal for a longer period of time due to higher sulfate production in this scenario compared to the base case scenario.

Increasing the interval between the two injection episodes (from 10 to 20 days) caused no significant impact on the BTX mass removal rate at Row 2 and Row 3. Although the increased duration of the persulfate treatment and the increased length of the ChemOx zone in this scenario could have adversely affect BTX mass removal, the establishment of microbial sulfate reduction between the two injection episodes (with increased interval) maintained the mass removal. Compared to the base case scenario, the “increased interval” scenario caused a slight increase in BTX mass

removal in the ChemOx zone (~10%) whereas it caused a slight decrease in mass removal (~5 %) in the EBR zone. Increased persulfate presence in the system is believed to have caused the inhibition of microbial sulfate reduction in the EBR zone for a longer period of time. The overall adverse impact on the BTX mass removal in this scenario was attributed to the increased duration of persulfate presence within the model domain and the inhibitory effect on subsequent microbial processes.

In accordance with the literature (Sutton et al. 2010; Cassidy et al. 2009), this exploratory modelling effort demonstrated that a less aggressive persulfate oxidation step (i.e., low dosage and/or short duration), which minimizes the duration and extent of the direct contact between indigenous microorganisms and high oxidant concentration, would improve the overall performance of the persulfate/EBR treatment train. An aggressive and disproportionate persulfate treatment can cause long-term inhibition of microbial processes, secondary sulfate pollution and reduction of overall treatment efficiency.

3.5.3.3 Persulfate/EBR Treatment Train vs EBR Treatment

The next investigative modelling effort was aimed to compare the long-term performances of persulfate/EBR treatment train and the EBR treatment alone. The "EBR-only" scenario was built on the basis of the "non-stop flow" scenario except that persulfate was replaced with sulfate. In this scenario, the stoichiometric equivalent of the sulfate produced in the ChemOx zone (from the "non-stop flow" scenario) was injected at the same CIS nodes and with the same injection/extraction scheme used to inject the persulfate.

There exists another key difference between these two scenarios. The application of the chemical oxidation step in a treatment train has been demonstrated to enhance the subsequent microbial sulfate reduction rates through increasing the bioavailability of the remaining contaminant pool, producing sulfate, and increasing nutrient concentrations through oxidizing soil organic matter (see Chapter 2). In the "EBR-only" case, however, such enhanced microbial sulfate reduction rates are not expected. Therefore, for a justified comparison between the two scenarios, this advantage of the combined remedy was taken into account. For this, the maximum utilization rate used in the "EBR-only" scenario was arbitrarily decreased by half compared to that used in the non-stop flow scenario.

Figure 3.13 shows the higher BTX mass removal in the "non-stop flow" scenario (which represents the treatment train approach) compared to the "EBR only" scenario in both the ChemOx and EBR

zones (i.e., Row 2 and Row 3). Moreover, the BTX breakthrough curves at Row 4 and Row 5 (data not shown) demonstrate the extended persistence of the BTX mass in the experimental gate, had the persulfate/EBR treatment train been replaced by EBR treatment only. In general, a larger treatment area and shorter treatment time were found the primary advantages of the combined persulfate/EBR remedy over the EBR treatment alone. However, it should be noted that this comparison was approximate due to uncertainty regarding the actual change in sulfate reduction rates following persulfate treatment. For example, performing a complementary simulation illustrated that if the stimulatory impact of persulfate on the rate of subsequent microbial sulfate reduction is neglected, that would lead to a relatively similar performance between the persulfate/EBR treatment train and EBR treatment alone. Therefore, to select the proper treatment technique at a given site, it is required to improve our understanding of the persulfate impact on the rate of subsequent microbial processes indigenous to that intended site.

3.6 SUMMARY AND CONCLUSION

The main objective of this study was to develop and evaluate a modelling tool to simulate the processes involved in a persulfate/EBR treatment train. The BIONAPL/3D model was enhanced (BIONAPL/PS) with the capabilities of simulating most of processes involved in a persulfate/EBR treatment train including: density-dependent advective-dispersive transport, persulfate decomposition, sulfate production, chemical oxidation, and biodegradation of PHC compounds under various redox conditions. BIONAPL/PS was used to simulate a series of laboratory column experiments to validate the model formulation. The enhanced BIONAPL/PS model was then applied to simulate a pilot-scale investigation of a sequential persulfate/EBR treatment train. This latter effort was aimed to evaluate the model capability to simulate a complex system with multiple components within a dynamic flow system. The model was also used to evaluate options for performance optimization, identify the role of the intertwined mass removal processes and investigate the performance of a persulfate/EBR treatment train with EBR treatment only.

During the field experiment, a quasi steady-state plume of BTX compounds was first developed, which was then treated using two (2) persulfate injection episodes. The mixing between persulfate and BTX formed a chemical oxidation zone (ChemOx zone) in the portion of the plume confined between the two persulfate slugs. The production and transport of the sulfate plume (the by-product of persulfate decomposition) formed an enhanced bioremediation (EBR) zone downgradient of the

ChemOx zone. The BIONAPL/PS model could successfully simulate the generation of the dissolved BTX plume and the persulfate injection episodes. Degradation of the BTX plumes following persulfate injection, formation of the ChemOx and EBR zones, depletion of persulfate and generation/consumption of sulfate were all reproduced within an acceptable range of the observed field data. Temporary inhibition of microbial sulfate reduction in the ChemOx zone due to persulfate presence was also simulated using the inhibition term in the BIONAPL/PS model. The BIONAPL/PS mass loss estimates were utilized to quantify the role of competing mass removal processes in the ChemOx and EBR zones. Persulfate oxidation was responsible for the majority (78%) of the mass loss that occurred in the vicinity of the persulfate injections, followed by sulfate reduction (21%) and aerobic biodegradation (1%). Alternatively, it was estimated that microbial sulfate reduction was responsible for most of the mass removal in the EBR zone, with an increased rate that corresponded to the arrival of high sulfate concentrations.

Comparing the simulations of various investigative scenarios illustrated that reaction kinetics, groundwater flow and the design parameters such as persulfate dosage and injection period/interval and rate are the key factors influencing the long-term performance of a persulfate/EBR treatment train. The overall mass removal efficiency of a persulfate/EBR treatment train was found to be inversely proportional to the persulfate dosage and duration of persulfate treatment (i.e., persulfate persistence in the system). A less aggressive persulfate treatment step (i.e., lower dosage, duration and extent) was found to improve the overall treatment efficiency by minimizing the inhibitory effect of persulfate on the subsequent microbial processes. The combined application of persulfate and sulfate reduction was also found to increase the length of the treatment zone and decrease the required treatment period compared to the individual use of EBR treatment.

The general conclusion that can be drawn based on this study is that the enhanced BIONAPL/PS model provides a suitable platform in which the complex processes involved in a persulfate/EBR treatment train are captured. The model could successfully reproduce the general evolutionary trend of the observed laboratory and field data. It is believed that the BIONAPL/PS modelling tool, if implemented properly, can be used by remediation engineers and scientists to assess the feasibility of employing a persulfate/EBR treatment train as a remediation solution at other PHC-contaminated sites under various hydrogeological and biogeochemical conditions, and also to examine proper design parameters for optimized treatment efficiency. Modelling can also be used as a tool for

decision makers to choose between a combined remedy versus individual application of chemical oxidation or bioremediation treatment, and/or to examine the need for using additional bio-enhancement practices to improve the overall treatment efficiency. However, since mostof the model parameters, including the kinetic rates and transport parameters, are site-specific, to use the BIONAPL/PS model for simulating a different site under different conditions, such model parameters should be adjusted by performing benchmarking studies specific to the intended site.

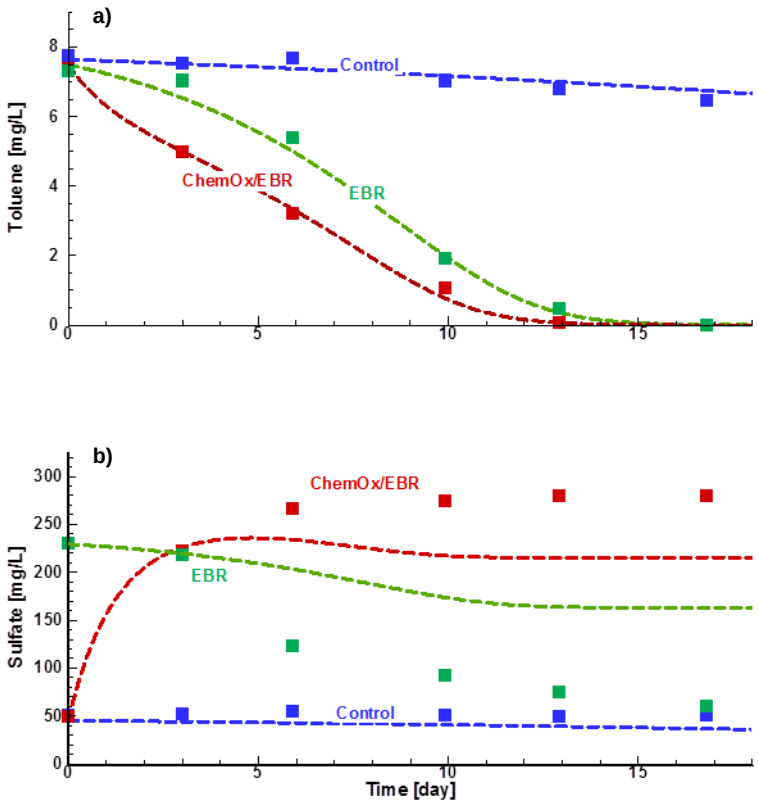

Figure 3.1 (a) Toluene and (b) sulfate breakthrough curves from the three experimental systems: observed (symbols) vs simulated (dashed line).

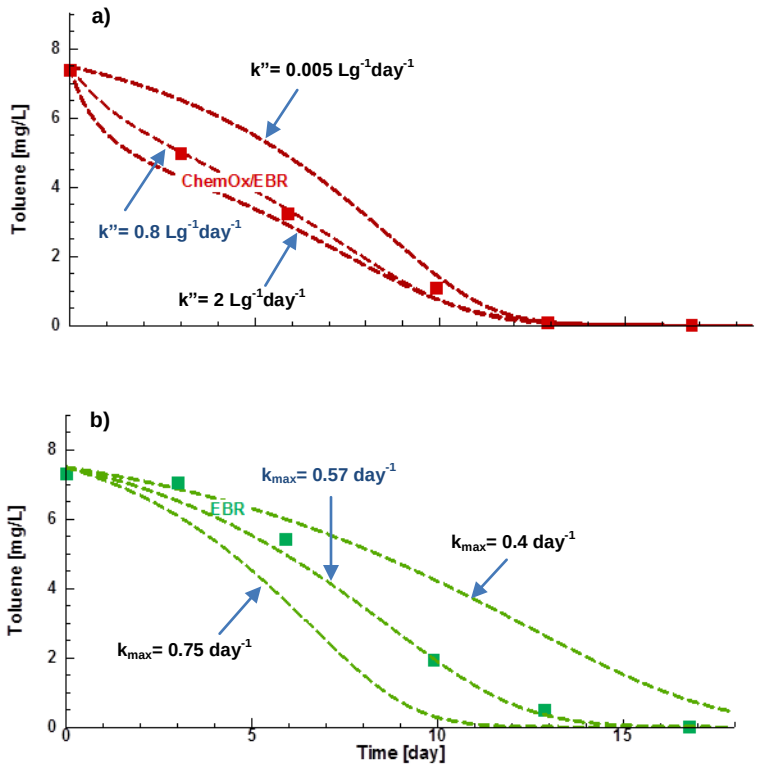

Figure 3.2 Effect of (a) second-order chemical oxidation rate coefficient on the toluene breakthrough curve in the ChemOx/EBR system, and (b) the maximum utilization rate on the toluene breakthrough curve for the EBR system.

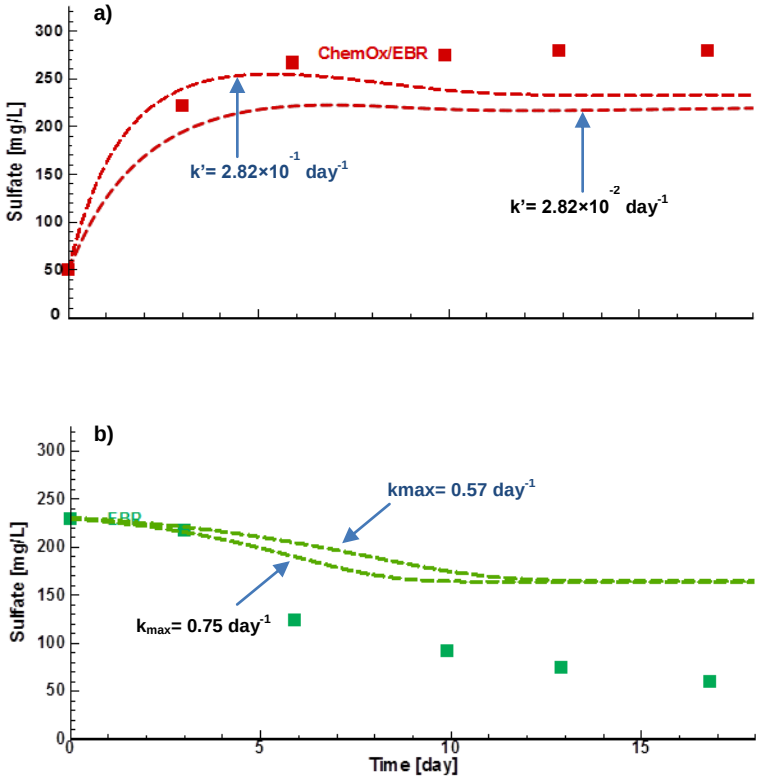

Figure 3.3 Effect of (a) first-order persulfate decomposition rate on the sulfate breakthrough curve in the ChemOx/EBR system and (b) the maximum utilization rate on sulfate breakthrough curve in the EBR system.

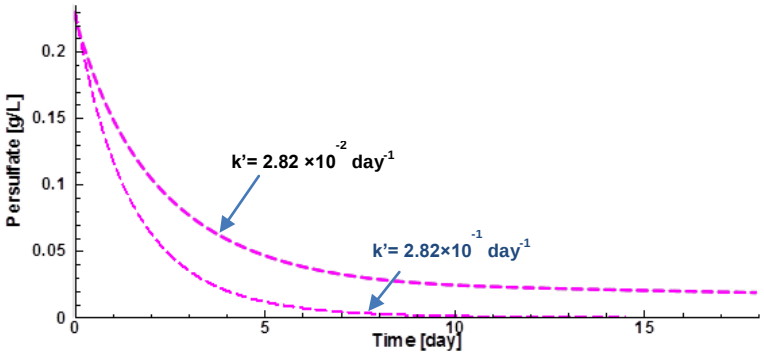

Figure 3.4 Simulated persulfate concentration in the ChemOx/EBR experimental system

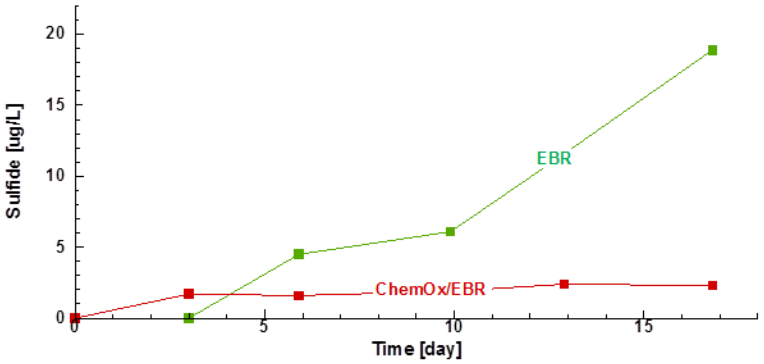

Figure 3.5 Observed sulfide concentration in the ChemOx/EBR and EBR experimental systems

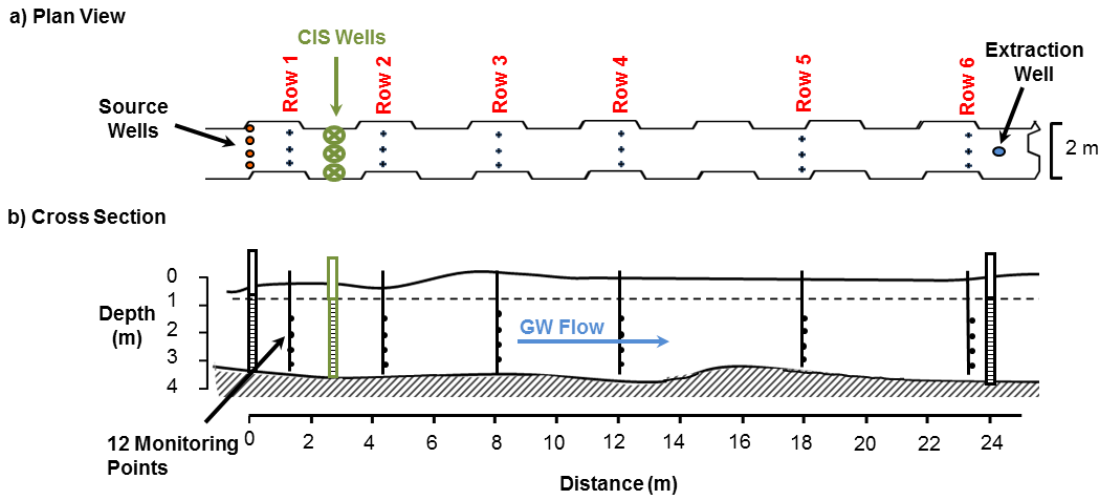

Figure 3.6 (a) Plan view and (b) cross sectional view of the experimental gate

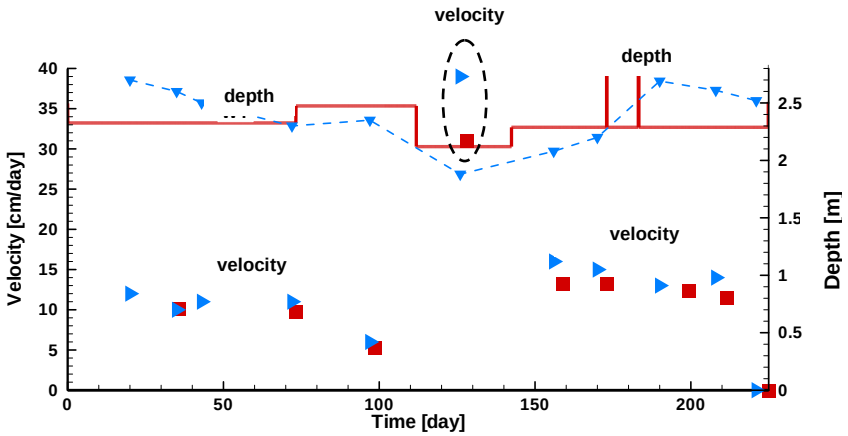

Figure 3.7 Temporal evolution of groundwater depth and velocity in the experimental gate: field data (blue) vs model prediction (red).

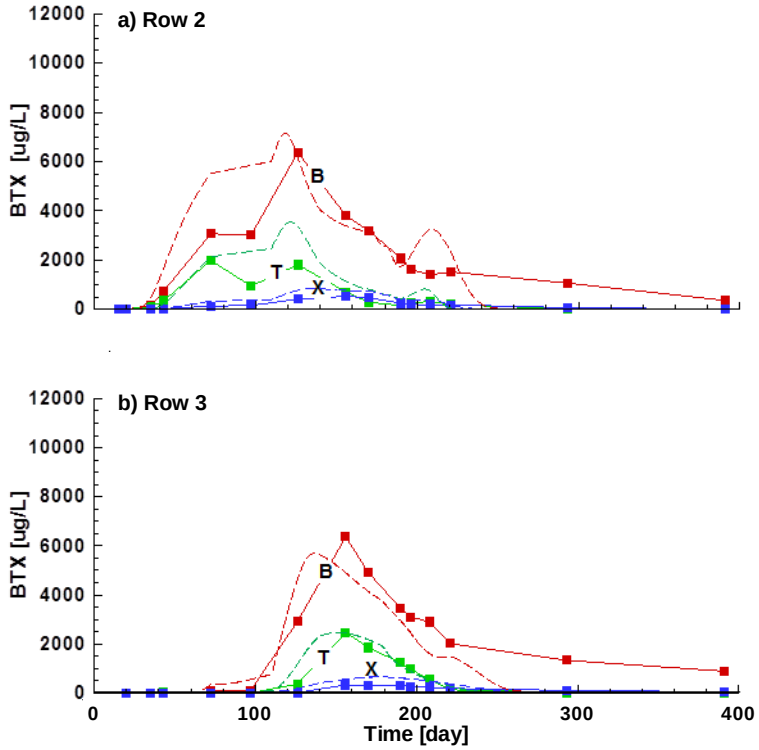

Figure 3.8 BTX breakthrough curves: observed (solid line) vs simulated (dashed line).

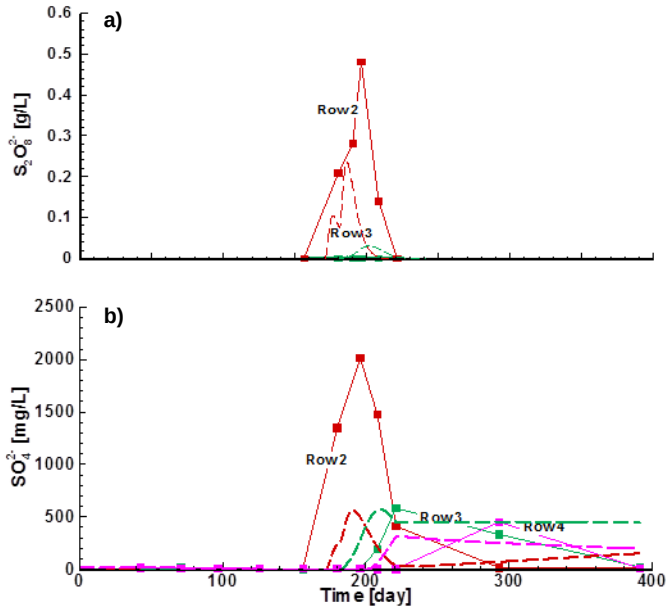

Figure 3.9 (a) Persulfate and (b) sulfate breakthrough curves: observed (solid line) vs. simulated (dashed line).

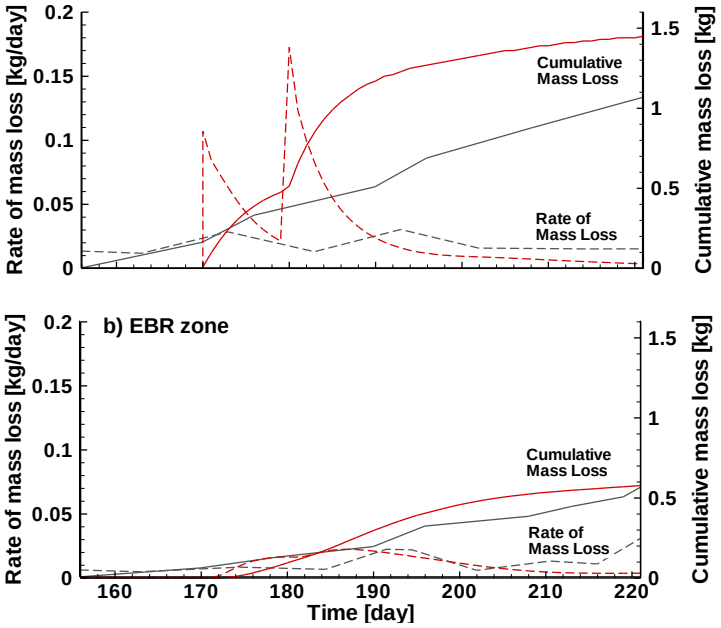

Figure 3.10 Cumulative BTX mass loss and the mass loss rates determined by BIONAPL/PS (red), vs the estimates based on the observed BTX concentrations and corresponding Darcy flux (gray) in the (a) ChemOx zone and (b) the EBR zone.

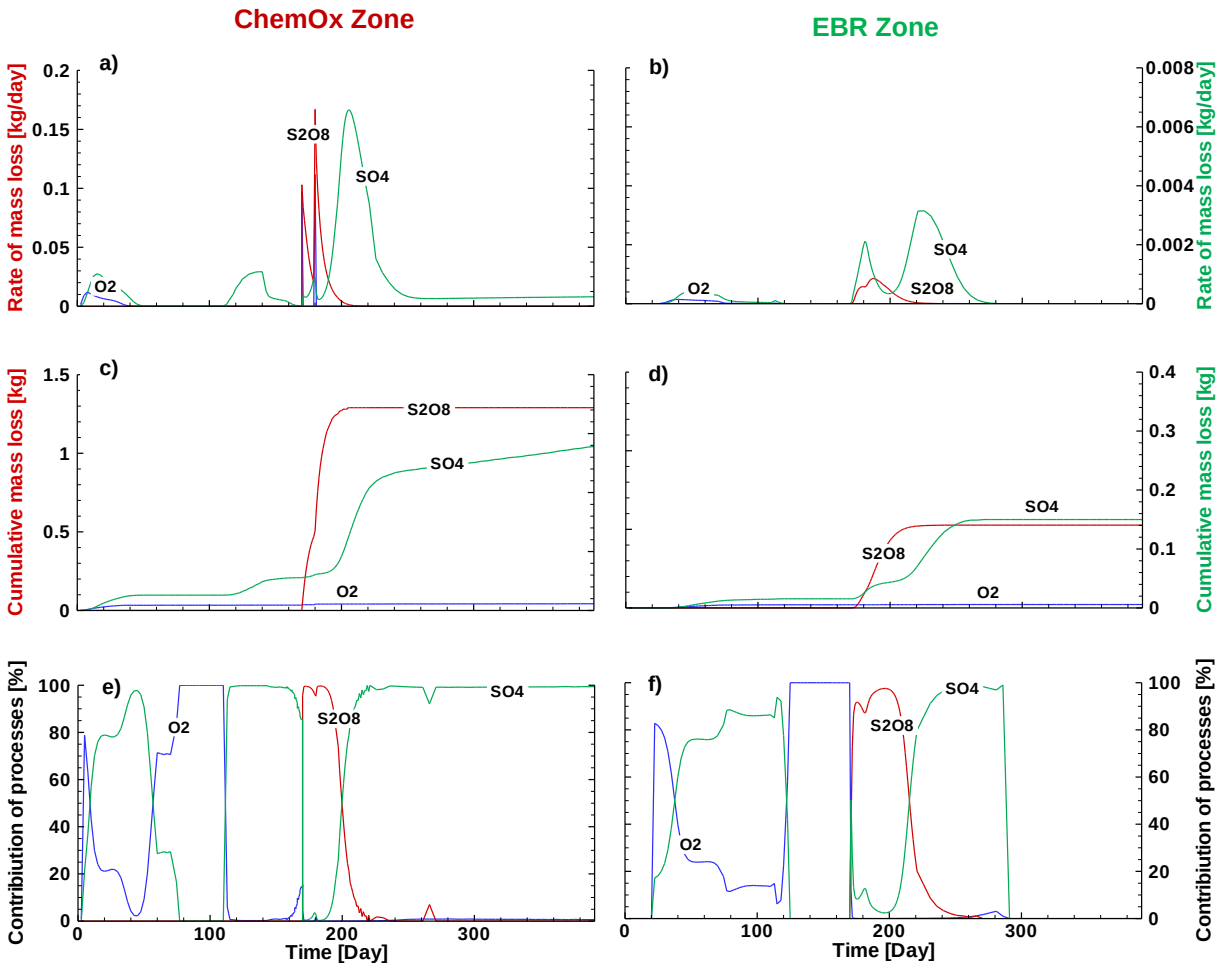

Figure 3.11 Temporal evolution of (a,b) rate of mass loss, (c,d) cumulative mass loss and (e,f) weighted contribution of individual mass removal processes with respect to the total removed mass in the ChemOx zone (left) and EBR zone (right). The blue line represents mass loss associated with aerobic biodegradation, green line represents sulfate reduction and persulfate oxidation is signified with the red line (Note: different labeling scale of the left axis and right axis highlights in figures a-d represent the higher kinetics of persulfate oxidation compared to aerobic and anaerobic biodegradation).

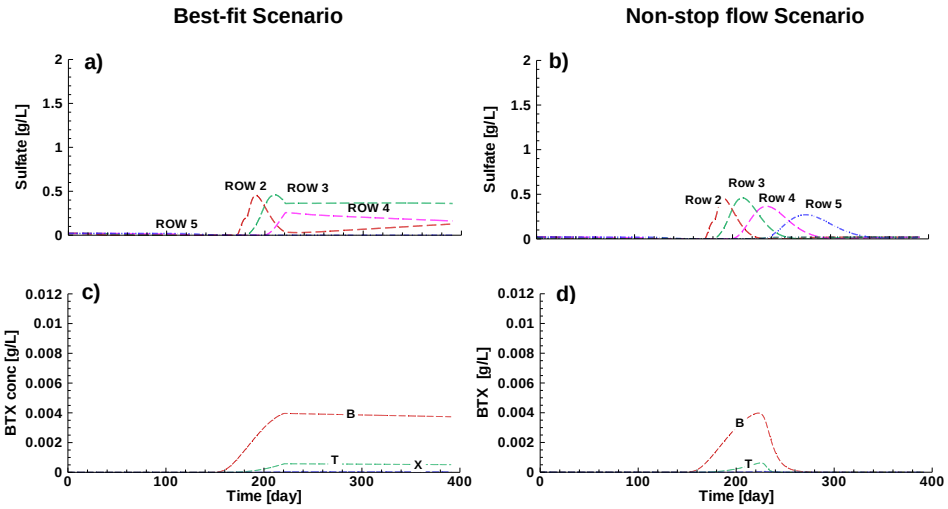

Figure 3.12 (a,b) Sulfate and (c,d) BTX breakthrough curves at Row 5 in the best fit scenario (left) and the Non-stop flow scenario (right).

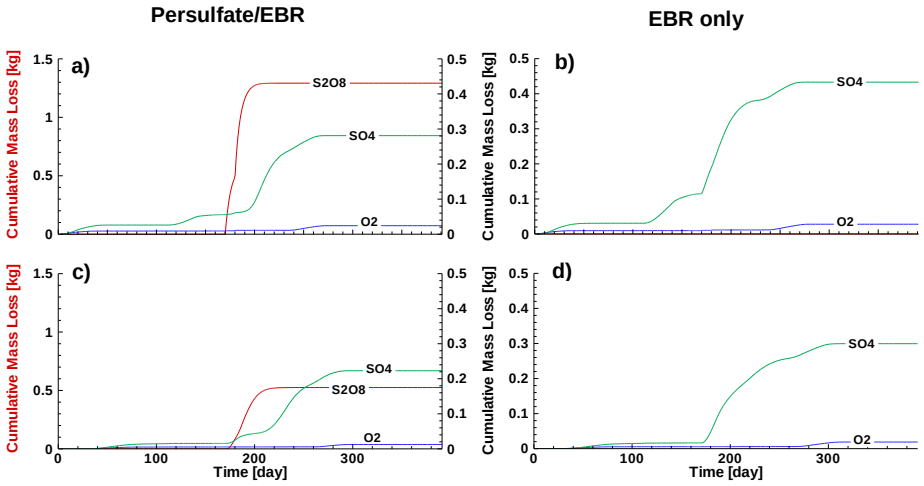

Figure 3.13 BTX mass loss in the (a,b) ChemOx zone and (c,d) EBR zone in the persulfate/EBR (left) and EBR-only (right) scenarios.

Table 3.1 Initial conditions and adjusted model parameters used to simulate the experimental systems

Parameter	**Value**		
Model Domain	0.5 m × 0.038 m		
Domain Discretization	100 × 1		
Time Step	0.05 day		
Porosity, θ	0.33		
Toluene			
Background concentration	0.0074 g/L		
Retardation factor, R*	1.8		
Diffusion coefficient, D*	5.7×10^{-5} m^2/day		
Maximum utilization rate, k_{max}	0.57 day^{-1}		
Half utilization constant, K_s^*	0.002 g/L		
Sulfate			
Initial concentration	***Control*** 0.05 g/L	***ChemOx/EBR*** 0.050 g/L	***EBR*** 0.230 g/L
Retardation factor, R	1.00		
Half utilization constant, K_A^*	0.01 g/L		
Mass ratio, X	4.7		
Microbial Population			
Background concentration*	0.001 g/L		
Maximum concentration*	0.014 g/L		
Yield coefficient (Y)*	0.5		
Decay coefficient (b)*	$10^{-12}$$day^{-1}$		
Persulfate			
Initial concentration	***Control*** 0.00 g/L	***ChemOx/EBR*** 0.230 g/L	***EBR*** 0.00 g/L
Retardation factor	1.00		
Mass ratio, X	37.6		
2^{nd} order oxidation rate (adjusted)	0.8 $Lg^{-1}day^{-1}$		
1^{st} order decomposition rate (adjusted)	2.82×10^{-1} day^{-1}		

*values based on Schirmer et al. (2000), Sra et al. (2013a,b), López-Pérez et al. (2013), Kalyuzhnyi et al. (1998), and Molson et al. (2014)

Table 3.2 Initial conditions and adjusted model parameters (corresponding to best fit scenario) used to simulate the controlled field experiment

Parameter	**value**		
Model Domain	26 m × 2 m × 2.5 m		
Domain Discretization	260 × 20 × 1		
Time Step	0.01-0.05 day		
Hydraulic conductivity*	0.8 m/day		
Porosity*	0.28		
Dispersivity*	α_L=0.5 m α_{TH}=0.05 m α_{TV}=0.005 m		
Retardation factor*	R_1=1.4 R_2=R_3= 2		
Diffusion coefficient**	D^*_1=6.7×10^{-5} m^2/day D^*_2=5.7×10^{-5} m^2/day D^*_3=4.8×10^{-5} m^2/day		
Aerobic biodegradation Monod kinetic rate coefficients**	$k_{max(1)}$=1.56 day^{-1} $k_{max(2)}$=5 day^{-1} $k_{max(3)}$=4 day^{-1}	$K_{C(1)}$= 0.002 g/L $K_{C(2)}$= 0.002 g/L $K_{C(3)}$= 0.002 g/L	K_{O2}=0.002 g/L Y_{O2}=0.05 M_{O2}=0.003 g/L b_{O2}=10^{-12} day^{-1}
Sulfate reduction Monod kinetic rate coefficients **	$k_{max(1)}$=0.15 day^{-1} $k_{max(2)}$=0.6 day^{-1} $k_{max(3)}$=0.2 day^{-1}	$K_{C(1)}$= 0.002 g/L $K_{C(2)}$= 0.002 g/L $K_{C(3)}$= 0.002 g/L	K_{SO4}=0.002 g/L Y_{SO4}=0.05 M_{SO4}=0.003 g/L b_{SO4}=10^{-12} day^{-1}
2nd order chemical oxidation rate coefficients ***	k"$_{(1)}$=0.2 day^{-1}g^{-1}L k"$_{(2)}$=0.25 day^{-1}g^{-1}L k"$_{(3)}$=0.12 day^{-1}g^{-1}L		
1st order persulfate decomposition rate coefficients ***	k'= 5.6×10^{-2} day^{-1}		
inhibition coefficients	$K_{I(oxygen)}$=1 $K_{I(persulfate)}$=0.001 $K_{I(Sulfate)}$=1		

(1) Benzene, (2) Toluene, (3) Xylene

* Based on: Schirmer et al. (2000); Devlin et al. (2002)

** Based on: MacQuarrie et al. (1990); Schirmer et al. (2000); Wiedemeier et al. (1999); Rifai & Newell (1998); Kalyuzhnyi et al. (1998); Fedorovich et al. (2003) and Wageningen et al. (2006)

*** Based on: Sra et al. (2013(a,b)); Huang et al. (2005)

Chapter 4
Closure

4.1 CONCLUSION AND CONTRIBUTIONS

The primary goal of this research was to provide a detailed understanding of a coupled persulfate/EBR treatment train as an *in situ* remediation system for BTX-contaminated sites. A controlled pilot-scale field experiment was conducted and a suite of novel and conventional diagnostic tools were used to assess the performance of the combined persulfate/EBR treatment, distinguish the dominant mass removal processes, and investigate the impact of persulfate on indigenous microbial processes. Also, a modelling tool was developed to capture the key physical, chemical and biological processes involved in the treatment train and to quantify the impact of various parameters on the performance of the persulfate/EBR treatment system.

The significant contributions of this research are:

- The pilot-scale experiment described in Chapter 2 is the first comprehensive and systematic investigation to assess the viability and effectiveness of treating a dissolved BTX plume using a persulfate/EBR treatment train. To the authors' knowledge, this is also the first field trial in which stable isotope analyses and molecular biology techniques have been applied in combination with conventional field measurements to identify and track the evolution of various mass removal processes, and to investigate the effect of persulfate oxidation on the population and activity of indigenous BTX-degrading microbial communities.
- The modelling study described in Chapter 3 is the first effort to develop and utilize a modelling tool to simulate the processes involved in a coupled ISCO/EBR treatment train. The BIONAPL/PS model provides a suitable platform in which the complex processes involved in a persulfate/EBR treatment train are captured. The model was used to identify the effect of ambient conditions and the key design parameters (i.e., persulfate concentration, and injection period/interval and rate) on the performance of the combined treatment system.

- The combination of experimental and modelling efforts provided key insights into an effective and balanced design of a combined persulfate/EBR remedy. The lessons learned are useful for remediation engineers and scientists who intend to implement this combined remedy at PHC-contaminated sites under various conditions.

The major conclusions emerging from this pilot-scale field trial and modelling study are:

- Persulfate oxidation coupled with enhanced bioremediation can be an effective *in situ* approach to remediate BTX-contaminated sites. It was found that to optimize treatment efficiency, a limited persulfate treatment should be implemented. The modelling study illustrated that an aggressive persulfate treatment step (i.e., high persulfate dosage, long exposure time or large contact area) can adversely affect the subsequent bioremediation step by causing inhibition of indigenous microbial communities, leading to secondary sulfate pollution and reducing the overall efficiency of the persulfate/EBR treatment train.
- Due to the limitations of the individual monitoring tools, the combined application of emerging and conventional tools was essential for the characterization of the intertwined mass removal processes and to understand the performance of the persulfate/EBR treatment train. Stable isotope analysis of BTX and sulfate, and monitoring of process-specific functional genes and intermediate metabolites proved useful in evaluating system performance and identifying the temporal changes of the dominant degradation pathways.
- Multiple lines of evidence from both the field and modelling results demonstrated that while chemical oxidation is the dominant mass removal process in the vicinity of the persulfate injection (i.e., ChemOx zone), enhanced bioremediation (including enhanced microbial sulfate reduction and methanogenesis) dominated BTX degradation in the downgradient portions of the plume (i.e., EBR zone).
- The ChemOx zone was observed to transform into an EBR zone as the groundwater migrated along the experimental gate, and persulfate was depleted. The population and activity of SRB communities, which were temporarily inhibited in the ChemOx zone immediately after persulfate injection, rebounded and multiplied after persulfate depletion.
- Factors such as incomplete inhibition of microbial processes due to the low dosage and short duration of the persulfate treatment, existence of subsurface heterogeneities and

persistence/growth of indigenous microbes in the dead-end pores, re-inoculation of microbial communities by groundwater flow, increased sulfate and nutrients concentration and enhanced biodegradability of the remaining contaminant pool were believed to cause the observed enhancement of the microbial sulfate reduction following persulfate treatment.

- It was also demonstrated that the flow and transport processes have a significant impact on the long-term performance of the combined persulfate/EBR remedy. When the groundwater flow in the experimental gate stopped, the activity and population of the SRB community decreased as a result of the cessation of the upgradient delivery of sulfate, and perhaps the limited mixing between the reactants.
- The molecular biology data and the increased methane concentration demonstrated the dominance of methanogenic condition (over sulfate reducing) following the system shut-down. Methanogenesis biodegradation maintained BTX degradation at late time.

The results of this research were used to provide insights/guidelines to optimize the efficiency of the persulfate/EBR treatment train as follows:

- It was demonstrated that the persulfate treatment impacts subsurface geochemistry, the population/activity of indigenous microbial communities and thus, the efficiency of the subsequent bioremediation. Therefore, providing ideal conditions for the enhancement of indigenous microbial processes should be a key consideration in the design of the chemical oxidation step. For example, disproportionate/aggressive ISCO treatment should be avoided to prevent permanent inhibition of subsequent microbial activity and to improve the overall treatment efficiency.
- Transport processes control the distribution and mixing of oxidants, PHCs, and electron acceptors (i.e., sulfate) and influence the long-term mass removal efficiency, particularly at locations further downgradient of the oxidant injection zone. Therefore, to design an effective ISCO/EBR treatment train, the groundwater transport processes (advection, dispersion, retardation) need to be known with a reasonable certainty level. Using simulation tools is recommended to assess the flow and transport processes during design and operation of a persulfate/EBR treatment train.

- Prior to the implementation of the coupled ISCO/EBR treatment system at sites with various hydrogeological and biogeochemical conditions, it is crucial to find proper design parameters (e.g., oxidant dose, delivery method and injection frequency) for optimum treatment efficiency. The BIONAPL/PS model can be used as an effective design tool. Modelling can also be used as a supporting tool for decision makers to choose between a combined remedy versus individual application of chemical oxidation or bioremediation, and/or to examine the need for using additional bio-enhancement practices to improve the overall treatment efficiency.

4.2 RECOMMENDATIONS FOR FUTURE WORK

While important conclusions were drawn and significant contributions were made at the end of this study, some questions remained unanswered and some interesting research topics raised during the course of this endeavor. The opportunities for further research are summarized as follow:

- To better assess the performance of persulfate/EBR treatment train, it is recommended to investigate the implementation of this technique under less-controlled conditions at a real contaminated site. Investigating the viability and effectiveness of persulfate/EBR combined remedy for source zone treatment, rather than only the dissolved portion of the plume, could be another topic for future consideration.

- While in the present pilot-scale experiment unactivated persulfate was injected into the subsurface, in many field applications of persulfate, various activation methods (e.g., heat, iron chelates, hydrogen peroxide or alkaline activation) are incorporated. Therefore, further research is recommended to investigate the impact of using such activation methods on the indigenous microbial processes and on the overall effectiveness of the persulfate treatment train.

- It is also recommended to explore the impact of *in situ* geochemical processes on the treatment train footprint (i.e., by-products such as sulfate, sulfide and the dissolved inorganic carbon) and also on the performance of the combined persulfate/EBR remedy. Simulating the geochemical processes is beyond the capabilities of the current version of BIONAPL/PS. Thus, as a step forward, it is also recommended to couple BIONAPL/PS with a full geochemistry code such as MINTEQ (Allison et al. 1991) or PHREEQC (Parkhurst et al.,

1999) to simulate the geochemical reactions which may potentially impact the observed biogeochemical footprints (e.g., mineral dissolution/precipitation, cation exchange reactions and CO_2/CH_4 gas dissolution/exsolution).

- The versatility of the BIONAPL/PS model formulation makes it well suited for future extensions and enhancements. It is recommended to focus the future enhancements of the code on capturing the irregular geometry domains, more complex flow regimes, aquifer heterogeneity, and additional biotic/abiotic reactions (e.g., methanogenesis biodegradation, sulfide generation/precipitation). Moreover, the model capability to simulate various kinetic models (e.g., first-order, second-order and Monod) can be potentially utilized to simulate the treatment trains with a variety of chemical oxidants other than persulfate (e.g., peroxide, permanganate, etc.).

- In the current state, there is a significant gap between the input requirement of the modelling tools used to simulate microbial processes (e.g., background populations and the growth/decay properties of microbial communities) and the extent of the biological data which can be captured from contaminated sites. Hence, another topic for future consideration could be conducting further laboratory and field experiments to determine a more reliable/accurate range for the dual Monod kinetic parameters associated with BTEX biodegradation under various redox conditions including sulfate reduction.

- Development/application of additional molecular biology techniques is also required for a better analysis of the impact of oxidants such as persulfate on the type, diversity and specially the abundance of the active microbial communities at contaminated sites. For example, analyzing and quantification of the bacteria attached to soil particles (in addition to those that appear in the liquid samples) can lead to a more comprehensive understanding of the microbial activity prior to and following chemical oxidation. Moreover, knowing the type and population of indigenous microbial communities and the specific substrate utilization rates (i.e., degradation rate per cell for each specific compound) can be used to estimate more accurate compound/site-specific biodegradation rates (H. R. Beller, personal communication, March 17, 2013). However, much more research (i.e., laboratory studies with pure/mixed bacterial cultures) is still needed not only to determine the specific utilization rates but also to

develop further qPCR techniques for detection of further functional genes capable of biodegrading BTX compounds under various redox conditions including sulfate reduction.

- It is also recommended to conduct further controlled field/lab experiments to obtain precise second-order rate coefficients for degradation of BTEX compounds with persulfate oxidation under natural conditions. The existing studies have reported first-order rate coefficients obtained via batch-scale experiments under no-flow conditions, low soil/water ratios or inadequate mixing conditions. The proposed future studies may minimize the gap between the chemical oxidation rates estimated based on the previous laboratory batch experiments and those obtained through benchmarking the BIONAPL/PS model results with observed field/lab data in the present study.
- The CSIA data in this study was only used to qualitatively demonstrate the occurrence and relative importance of the competing mass removal processes (chemical oxidation vs biodegradation). More research is required to apply such CSIA data for quantitative estimation of the rate constants of chemical oxidation and microbial sulfate-reduction processes.
- Many of the model parameters, including flow, transport and kinetic parameters are highly dependent on specific site conditions. Thus as a future task, the impact of such uncertain model parameters on the performance of the persulfate/EBR treatment train can be studied using a series of model sensitivity analyses.

References

Chapter 1

Alleman, B. C., Leeson, A. (Eds), 1999. In situ bioremediation of petroleum hydrocarbon and other organic compounds, Battle Press, Columbus, OH, 227-232.

Bou-Nasr, J., Cassidy, D., Hampton, D., 2006. Comparative study of the effect of four ISCO oxidants on PCE oxidation and aerobic microbial activity. In: *Proceedings of the Fifth International Conference on Remediation of Chlorinated and Recalcitrant Compounds.* Monterey, CA. Columbus, Ohio: Battelle Press.

Cassidy, D., 2008. The effect of klozur CR on sulfate-reducing bacteria (SRB) in sediments from the Kalamazoo river, Western Michigan University, report to FMC.

Cassidy, D., Northup, A., Hampton, D., 2009. The effect of three chemical oxidants on subsequent biodegradation of 2, 4−dinitrotoluene (DNT) in batch slurry reactors. *Journal of Chemical Technology & Biotechnology*, 84(6), 820-826.

Cozzarelli, I. M., Baehr, A. L., 2003. Volatile fuel hydrocarbons and MTBE in the environment, *Treatise on Geochemistry*, 9, 433-74.

Devlin, J.F., Katic, D. & Barker, J.F., 2004. In situ sequenced bioremediation of mixed contaminants in groundwater. *Journal of Contaminant Hydrology*, 69(3-4), pp.233–61.

Droste, E. X., Marley, M. C., Parikh, J. M., Lee, A. M., Dinardo, P. M., Woody, B. A., Hoag, G. E., and Chedda, P., 2002. Observed enhanced reductive dechlorination after in situ chemical oxidation pilot test. In: *Proceedings of the Third International Conference on Remediation of Chlorinated and Recalcitrant Compounds*. Monterey, CA. Columbus, Ohio: Battelle Press.

Gallagher, L., Crimi, M., 2007. Coupling Persulfate ISCO with Bioprocesses: A Review. In: *Proceedings of the Fifth International Conference on Oxidation and Reduction Technologies for the In Situ Treatment of Soil and Groundwater*. Niagara Falls, NY.

Huling, S. G., Pivetz, B. E., 2006. Engineering Issue: In-Situ Chemical Oxidation. EPA/600/R-06/072.U.S.Environmental Protection Agency, Office of Research and Development, National Risk Management Research Laboratory, Cincinnati, OH.

Krembs, F. J., Siegrist, R. L., Crimi, M. L., Furrer, R. F., Petri, B. G., 2010. ISCO for Groundwater Remediation : Analysis of Field Applications and Performance. *Ground Water Monitoring & Remediation*, 30, 42-53.

Marley, M. C., Parikh, J. M., Droste, E. X., Lee, A. M., 2006. A case study on enhanced reductive dechlorination resulting from a chemical oxidation pilot test. In *Proceeding of the First International Conference on DNAPL Characterization and Remediation*, Pittsburgh, PA.

Morkin, M., Devlin J. F., Barker J. F., Butler, B. J., 2000. In situ sequential treatment of a mixed contaminant plume. *Journal of Contaminant Hydrology*, 45(3-4), pp.283–302..

Munakata-Marr, J., Sorenson, K., Petri, B., Cummings, J., 2011. Principles of Combining ISCO with Other In Situ Remedial Approaches. In R. L. Siegrist, M. Crimi, & T. J. Simpkin (Eds.), *In Situ Chemical Oxidation for Groundwater Remediation* (Vol. 3, 285–317). New York, NY: Springer New York.

Richardson, S., 2010. Effects of In Situ Bioremediation Strategies on the Biodegradation and Bioavailability of Polycyclic Aromatic Hydrocarbons in Weathered Manufactured Gas Plant Soil. PhD Thesis, University of North Carolina at Chapel Hill, USA.

Richardson, S. D., Lebron, B. L., Miller, C. T., Aitken, M. D., 2011. Recovery of phenanthrene-degrading bacteria after simulated in situ persulfate oxidation in contaminated soil. *Environmental Science & Technology*, 45, 719–25.

Sahl, J. W., Munakata-Marr, J., 2006. The effects of in situ chemical oxidation on microbiological processes: A review. *Remediation Journal*, 16, 57–70.

Sahl, J. W., Munakata-Marr, J., Crimi, M. L., Siegrist, R. L., 2007. Coupling permanganate oxidation with microbial dechlorination of tetrachloroethene. *Water Environment Research : A Research Publication of the Water Environment Federation*, 79, 5–12.

Sessa, F., Paré, J., Studer, J. E., 2008 . Coupled ISCO-Bio via Activated Persulfate and Timed Oxygen Release using a Sodium Persulfate/Calcium Peroxide matrix. In *Proceeding of the Remediation Technologies Symposium 2008 (RemTech 2008)*. Banff, Canada.

Studer, J., Davis, G., Baldwin, B., Cronk, G., 2009. Impact of *In Situ* Chemical Oxidation on Native Biological Populations: Review of Case Studies. In *Proceeding of the Tenth International In Situ and On-Site Bioremediation Symposium*. Battelle, Baltimore

Sutton, N. B., Grotenhuis, J. T. C., Langenhoff, A. A. M., Rijnaarts, H. H. M., 2010. Efforts to improve coupled in situ chemical oxidation with bioremediation: a review of optimization strategies. *Journal of Soils and Sediments*, 11, 129–140.

Tsitonaki, A., 2008. *Treatment Trains for the Remediation of Aquifers Polluted with MTBE and other Xenobiotic Compounds*. PhD Thesis, Technical University of Denmark, Denmark.

Tsitonaki, A., Smets, B. F., Bjerg, P. L., 2008. Effects of heat-activated persulfate oxidation on soil microorganisms. *Water Research*, 42, 1013–1022.

Tsitonaki, A., Petri, B., Crimi, M., Mosbaek, H., Siegrist, R. L., Bjerg, P. L., 2010. In Situ Chemical Oxidation of Contaminated Soil and Groundwater Using Persulfate: A Review. *Critical Reviews in Environmental Science and Technology*, 40, 55–91.

Chapter 2

Abu Laban, N., 2009. Anaerobic benzene degradation by iron and sulfate-reducing enrichment cultures. PhD Thesis, Technische Universität München, Germany.

Aelion, C. M., Höhener, P., Hunkeler, D., Aravena, R., (Eds). 2010. Environmental Isotopes in Biodegradation and Bioremediation, Taylor and Francis, Boca Raton, FL.

Agrawal, A., Gieg, L. M., 2013. In situ detection of anaerobic alkane metabolites in subsurface environments. *Frontiers in Microbiology*, 4, 140.

Al-zuhair, S., El-naas, M. H., Al-hassani, H., 2008. Sulfate inhibition effect on sulfate reducing bacteria. *Journal of Biochemical Technology*, 1, 39–44.

Anderson, R. T., Lovley, D. R., 2000. Anaerobic Bioremediation of Benzene under Sulfate-Reducing Conditions in a Petroleum-Contaminated Aquifer. *Environmental Science & Technology*, 34, 2261–6.

Arildskov, N. P., Devlin, J. F., 2000. Field and Laboratory Evaluation of Diffusive Emitter for Semipassive Release of PCE to an Aquifer. *Ground Water*, 38, 129–138.

Aronson, D., Citra, M., Shuler, K., Printup, H., Howard, P. H., 1999. Aeorobic Biodegradation of Organic Chemicals in Environmental Media: A Summary of Field and Laboratory Studies. A report prepared for U.S. Environmental Protection Agency, Office of Research and Development. Athens, GA 30605.

Aronson, D. & Howard, P., 1997. Anaerobic Biodegradation of Organic Chemicals in Groundwater : A Summary of Field and Laboratory Studies, A report prepared for American Petroleum Institute, Chemical Manufacturer's Association, National Council of the Paper, Industry for Air and Stream Improvement, Edison Electric Institute, American Forest and Paper Association.

Azadpour-Keeley, A., Wood, L. A., Lee, T. R., Mravik, S. C., 2004. Microbial responses to in situ chemical oxidation, six-phase heating, and steam injection remediation technologies in groundwater. *Remediation Journal*, 14, 5–17.

Barton, L. L., Hamilton, W. A., 2007. Sulphate Reducing Bacteria Environmental and Engineered Systems. Cambridge University Press (p. 535)

Beller, H. R., Kane, S., R., Legler, T., C., Alvarez, P. J., 2002. A real-time polymerase chain reaction method for monitoring anaerobic, hydrocarbon-degrading bacteria based on a catabolic gene. *Environmental Science & Technology*, 36, 3977–84.

Beller, H. R. Kane S. R., Legler, T. C., McKelvie, J. R., Lollar, B. S., Pearson, F., Balser, L., Mackay, D. M., 2008. Comparative assessments of benzene, toluene, and xylene natural attenuation by quantitative polymerase chain reaction analysis of a catabolic gene, signature metabolites, and compound-specific isotope analysis. *Environmental Science & Technology*, 42, 6065–72.

Beller, H. R., Spormann, A. M., Sharma, P. K., Cole, J. R., Reinhardet, M., 1996. Isolation and characterization of a novel toluene-degrading, sulfate-reducing bacterium. *Applied and Environmental Microbiology*, 62, 1188–96.

Beller, H. R., Grbic-Galic, D., Reinhard, M., 1992(a). Microbial degradation of toluene under sulfate-reducing conditions and the influence of iron on the process. *Applied and Environmental Microbiology*, 58, 786–793.

Beller, H. R., Reinhard, M., Grbić-Galić, D., 1992(b). Metabolic by-products of anaerobic toluene degradation by sulfate-reducing enrichment cultures. *Applied and Environmental Microbiology*, 58, 3192–5.

Beller, H. R., Spormann, A M., 1999. Substrate range of benzylsuccinate synthase from Azoarcus sp. strain T. *FEMS Microbiology Letters*, 178, 147–53.

Benner, S., Blowes, D. W., Ptacek, C. J., Mayer, K. U., 2002. Rates of sulfate reduction and metal sulfide precipitation in a permeable reactive barrier. *Applied Geochemistry*, 17, 301–320.

Bolliger, C., Schönholzer, F., Schroth, M. H., Dittmar Hahn, D., Bernasconi, S. M., Zeyer, J., 2000. Characterizing Intrinsic Bioremediation in a Petroleum Hydrocarbon-Contaminated Aquifer by Combined Chemical, Isotopic, and Biological Analyses. *Bioremediation Journal*, 4, 359–71.

Bolliger, C., Höhener, P., Hunkeler, D., Häberli, K., Zeyer, J., 1999. Intrinsic bioremediation of a petroleum hydrocarbon-contaminated aquifer and assessment of mineralization based on stable carbon isotopes. *Biodegradation*, 10, 201–17.

Bolliger, C., Schroth, M. H., Bernasconi, S. M., Kleikemper, J., Zeyer, J., 2001. Sulfur isotope fractionation during microbial sulfate reduction by toluene-degrading bacteria. *Geochimica et Cosmochimica Acta*, 65, 3289–3298.

Borden, R. C., Hunt, M. J., Shafer, M. B., Barlaz, M. A., 1997. Anaerobic Biodegradation of BTEX in Aquifer Material, Environmental Research Brief, United States Environmental Protection Agency.

Bou-Nasr, J., Cassidy, D., Hampton, D., 2006. Comparative study of the effect of four ISCO oxidants on PCE oxidation and aerobic microbial activity. In: *Proceedings of the Fifth International Conference on Remediation of Chlorinated and Recalcitrant Compounds.* Monterey, CA. Columbus, Ohio: Battelle Press.

Buyuksonmez, F., Hess, T. F., Crawford, R. L., & Watts, R. J., 1998. Toxic Effects of Modified Fenton Reactions on Xanthobacter flavus FB71. *Applied Environmental Microbiology*, 64(10), 3759–3764.

Canfield, D. E., 2001. Isotope fractionation by natural populations of sulfate-reducing bacteria. *Geochimica et Cosmochimica Acta*, 65, 1117–24.

Cassidy, D., 2008. The Effect of Klozur® CR on Sulfate-Reducing Bacteria (SRB) in Sediments from

the Kalamazoo River. FMC Environmnetal Solutions, Peroxygen Talk

Cassidy, D., Northup, A., Hampton, D., 2009. The effect of three chemical oxidants on subsequent biodegradation of 2,4-dinitrotoluene (DNT) in batch slurry reactors. *Journal of Chemical Technology & Biotechnology*, 84, 820–826.

Chapelle, F. H., 2005. Bioremediation of Petroleum Hydrocarbon-Contaminated Ground Water: The Perspectives of History and Hydrology. *Ground water*, 37, 122–132.

Chapelle, F. H., Bradley, P. M., Casey, C. C., 2005. Behavior of a chlorinated ethene plume following source-area treatment with Fenton's reagent. *Ground Water Monitoring and Remediation*, 25, 131–141.

Cherry, J. A., Barker, J. F., Feenstra, S., Gillham, R. W., Mackay, D. M., Smyth, D. J. A., 1996. The Borden Site for Groundwater Contamination Experiments: 1978–1995. In H. Kobus, B. Barczewski, & H.-P. Koschitzky, eds. *Groundwater and Subsurface Remediation*. Berlin, Heidelberg: Springer Berlin Heidelberg, pp. 102-27.

Chin, K. J., Sharma M. L., Russell, L. A., O'Neill, K. R., Lovley, D. R., 2008. Quantifying expression of a dissimilatory (bi)sulfite reductase gene in petroleum-contaminated marine harbor sediments. *Microbial ecology*, 55, 489–99.

Critchley, C. E., 2010. Stimulating In Situ Denitrification in an Aerobic, Highly Conductive Municipal Drinking Water Aquifer, Master Thesis, University of Waterloo, Canada.

Cunningham, J. A., Hopkins G. D., Lebron, C. A., Reinhard, M., 2000. Enhanced anaerobic bioremediation of groundwater contaminated by fuel hydrocarbons at Seal Beach, California. *Biodegradation*, 11, 159–70.

Cunningham, J. A., Rahme, H., Hopkins, G. D., Lebron, C., Reinhard, M., 2001. Enhanced in situ bioremediation of BTEX-contaminated groundwater by combined injection of nitrate and sulfate. *Environmental science & technology*, 35, 1663–70.

Dance, J. T., Reardon, E. J.,1983. Migration of contaminants in groundwater at a landfill: A case study. *Journal of Hydrology*, 63(1-2), 109–130.

Davis, G. B., Barber, C., Power, T. R., Thierrin, J., Patterson, B. M., Rayner, J. L., Wu, Q., 1999. The variability and intrinsic remediation of a BTEX plume in anaerobic sulphate-rich groundwater. *Journal of Contaminant Hydrology*, 36, 265–290.

Detmers, J., Brüchert, V., Habicht, K. S., 2001. Diversity of Sulfur Isotope Fractionations by Sulfate-Reducing Prokaryotes. *Applied and Environmental Microbiology*, 67, 888–94.

Devlin, J. F., Barker, J. F., 1996. Field Investigation of Nutrient Pulse Mixing in an in Situ Biostimulation Experiment. *Water Resources Research*, 32, 2869–77.

Devlin, J. F., McMaster, M., & Barker, J. F., 2002. Hydrogeologic assessment of in situ natural attenuation in a controlled field experiment. *Water Resources Research*, 38(1), 3–1–3–11.

Devlin, J.F., Katic, D. & Barker, J.F., 2004. In situ sequenced bioremediation of mixed contaminants in groundwater. *Journal of contaminant hydrology*, 69(3-4), pp.233–61.

Drever, J. I., 1988. The Geochemistry of Natural Water, Pearson Education Canada.

Droste, E. X., Marley, M. C., Parikh, J. M., Lee, A. M., Dinardo, P. M., Woody, B. A., Hoag, G. E., and Chedda, P., 2002. Observed enhanced reductive dechlorination after in situ chemical oxidation pilot test. In: *Proceedings of the Third International Conference on Remediation of Chlorinated and Recalcitrant Compounds*. Monterey, CA. Columbus, Ohio: Battelle Press.

Edwards, E., Wills, L. E., Reinhard, M., Grbić-Galić, D., 1992. Anaerobic degradation of toluene and xylene by aquifer microorganisms under sulfate-reducing conditions. *Applied and Environmental Microbiology*, 58, 794–800.

Environment Canada, 2010. Acts & Regulations - Implementation Plan for Canada-Wide Standards on Petroleum Hydrocarbons in Soil. July 2011. http://www.ccme.ca/files/Resources/csm/phc_cws/phc_standard_1.0_e.pdf.

EPA, 2004. Chapter IX Monitored Natural Attenuation Contents. In *How to Evaluate Alternative Cleanup Technologies for Underground Storage Tank Sites: A Guide for Corrective Action Plan Reviewers*. U.S. EPA, Office of Underground Storage Tanks, EPA 510-R-04-002, p. 77. http://www.epa.gov/oust/pubs/tum_ch9.pdf

Evans, P. J., Ling, W., Goldschmidt, B., Ritter, E. R., Young, L. Y., 1992. Metabolites formed during anaerobic transformation of toluene and o-xylene and their proposed relationship to the initial steps of toluene mineralization. *Applied and Environmental Microbiology*, 58, 496–501.

Fowler, S. J., Dong, X., Sensen, C. W., Suflita, J. M., Gieg, L. M., 2012. Methanogenic toluene metabolism: community structure and intermediates. *Environmental Microbiology*, 14, 754–64.

Franzmann, P. D., Robertson, W. J., Zappia, L. R., Davis, G. B., 2002. The role of microbial populations in the containment of aromatic hydrocarbons in the subsurface. *Biodegradation*, 13, 65–78.

Fukui, M., Harms, G, Rabus, R., Schramm, A., Widdel, F., Zengler, K., Boreham, C., Wilkes, H., 1999. Anaerobic degradation of oil hydrocarbons by sulfate-reducing and nitrate-reducing bacteria. In *8th International Symposium on Microbial Ecology*.

Gallagher, L., Crimi, M., 2007. Coupling Persulfate ISCO with Bioprocesses: A Review. In: *Proceedings of the Fifth International Conference on Oxidation and Reduction Technologies for the In Situ Treatment of Soil and Groundwater*. Niagara Falls, NY.

Gierczak, R., Devlin, J. F., Rudolph, D. L., 2007. Field test of a cross-injection scheme for

stimulating in situ denitrification near a municipal water supply well. *Journal of Contaminant Hydrology*, 89, 48–70.

Glaze, W. H., Lin, C. C., 1983. Optimization of Liquid-Liquid Extraction Methods for Analysis of Organics in Water, *Project Report, United States Environmental Protection Agency* .

Grbić-Galić, D., Vogel, T. M., 1987. Transformation of toluene and benzene by mixed methanogenic cultures. *Applied and Environmental Microbiology*, 53, 254–60.

Griebler, C., Safinowski, M., Vieth, A., Richnow, H. H., Meckenstock, R. U., 2004. Combined Application of Stable Carbon Isotope Analysis and Specific Metabolites Determination for Assessing In Situ Degradation of Aromatic Hydrocarbons in a Tar Oil-Contaminated Aquifer. *Environmental Science & Technology*, 38, 617–31.

Gülensoy, N., Alvarez, P. J., 1999. Diversity and correlation of specific aromatic hydrocarbon biodegradation capabilities. *Biodegradation*, 10, 331–40.

Hao, O. J., Chen, J. M., Huang, L., Buglass, R. L., 1996. Sulfate reducing bacteria. *Critical Reviews in Environmental Science and Technology*, 26, 155–87.

Harms, G., Zengler, K., Rabus, R., Aeckersberg, F., Minz, D., Rosselló-Mora, R., Widdel, F., 1999. Anaerobic oxidation of o-xylene, m-xylene, and homologous alkylbenzenes by new types of sulfate-reducing bacteria. *Applied and Environmental Microbiology*, 65(3), 999–1004.

Henderson, J. E., Peyton, G. R., Glaze, W. H., 1976. A convenient liquid-liquid extraction method for the determination of halomethanes in water at the parts-per-billion level. IN: Identification and analysis of organic pollutants in water. L. H. Keith, ed., Ann Arbor Science Publishers Inc., Ann Arbor, MI.

Hess, A., 1988. Detection of Microbial Populations in Petroleum Hydrocarbon Contaminated Aquifers and Isolation of Denitrifying Hydrocarbon Degraders. PhD Thesis, Swiss Federal Institute of Technology, Zurich, Switzerland.

Hoelen, T. P., Cunningham, J. A., Hopkins, G. D., Lebrón, C. A., Reinhard, M., 2006. Bioremediation of cis-DCE at a Sulfidogenic Site by Amendment with Propionate. *Ground Water Monitoring & Remediation*, 26, 82–91.

Hosoda, A., Kasai, Y., Hamamura, N., Takahata, Y., Watanabe ,K., 2005. Development of a PCR method for the detection and quantification of benzoyl-CoA reductase genes and its application to monitored natural attenuation. *Biodegradation*, 16, 591–601.

Huang, K. C., Zhao, Z., Hoag, G. E., Dahmani, A., Block, P. A., 2005. Degradation of volatile organic compounds with thermally activated persulfate oxidation. *Chemosphere*, 61, 551–60.

Huang, K. C., Couttenye, R. A., Hoag, G. E., 2002. Kinetics of heat-assisted persulfate oxidation of methyl tert-butyl ether (MTBE). *Chemosphere*, 49, 413–20.

Huling, S. G., Pivetz, B. E., 2006. Engineering Issue:In-Situ Chemical Oxidation. EPA/600/R-06/072.U.S.Enviromnmental Protection Agency Office of Research and Developement,National Risk Management Research Laboratory,Cincinnati, OH.

Hunkeler, D., Meckenstock, R. U., Lollar, B., Schmidt, T. C., Wilson, J. T., 2008. A Guide for Assessing Biodegradation and Source Identification of Organic Ground Water Contaminants using Compound Specific Isotope Analysis (CSIA), *EPA Science Inventory*, Protection Agency, Washington, D.C., EPA/600/R-08/148.

Hunkeler, D., Aravena, R., Parker, B. L., Cherry, J. A., Diao, X., 2003. Monitoring oxidation of chlorinated ethenes by permanganate in groundwater using stable isotopes: laboratory and field studies. *Environmental Science & Technology*, 37, 798–804.

Hunkeler, D., Aravena, R., Butler, B. J., 1999. Monitoring Microbial Dechlorination of Tetrachloroethene (PCE) in Groundwater Using Compound-Specific Stable Carbon Isotope Ratios: Microcosm and Field Studies. *Environmental Science & Technology*, 33, 2733–8.

ITRC, 2011. *Environmental Molecular Diagnostics Fact Sheets*. Ed. 1. Prepared by The Interstate Technology & Regulatory Council Environmental Molecular Diagnostics Team.November 2011. http://www.itrcweb.org/GuidanceDocuments/EMD1.pdf

ITRC, 2005. Technical / Regulatory Guideline Technical and Regulatory Guidance for In Situ Chemical Oxidation of Contaminated Soil and Groundwater. Ed. 2. Prepared by The Interstate Technology & Regulatory Council In Situ Chemical Oxidation Team. January 2005. http://www.itrcweb.org/Guidance/GetDocument?documentID=45

Jin, Q., Bethke, C. M., 2009. Cellular energy conservation and the rate of microbial sulfate reduction. *Geology*, 37, 1027–30.

Junca, H., Pieper, D. H., 2005. Diagnosing the biodegradation potential of soils. In P. Lens, ed. *Soil and Sediment Remediation: Mechanisms, Technologies and Applications*. IWA Publishing, 523.

Kampbell, D. H., Vandegrift, S. A., 1998. Analysis of dissolved methane, ethane, and ethylene in ground water by a standard gas chromatographic technique. *Journal of Chromatographic Science*, 36, 253–6.

Kampbell, D. H., Wilson, J. T., Vandegrift, S. A., 1989. Dissolved Oxygen and Methane in Water by a GC Headspace Equilibration Technique. *International Journal of Environmental Analytical Chemistry*, 36, 249–57.

Kane, S. R., Beller H. R., Legler, T. C., Anderson, R. T., 2002. Biochemical and genetic evidence of benzylsuccinate synthase in toluene-degrading, ferric iron-reducing Geobacter metallireducens. *Biodegradation*, 13, 149–54.

Kastner, J. R., Domingo, J. S., Denham, M., Molina, M., Brigmon, R., 2000. Effect of Chemical Oxidation on Subsurface Microbiology and Trichloroethene (TCE) Biodegradation. *Bioremediation*

Journal, 4, 219–36.

Kazy, S. K., Monier, A. L., Alvarez, P. J. J., 2010. Assessing the correlation between anaerobic toluene degradation activity and bssA concentrations in hydrocarbon-contaminated aquifer material. *Biodegradation*, 21, 793–800.

King, M. W. G., Barker, J. F., 1999. Migration and natural fate of a coal tar creosote plume. *Journal of Contaminant Hydrology*, 39, 249–79.

Kleikemper, J., 2003. Activity and diversity of sulfate-reducing and methanogenic microorganisms in a petroleum-contaminated aquifer. PhD Thesis, Swiss Federal Institute of Technology, Zurich, Switzerland.

Kleikemper, J., Schroth, M. H., Sigler, W. V., Schmucki, M., Bernasconi, S. M., Josef Zeyer, J., 2002(a). Activity and Diversity of Sulfate-Reducing Bacteria in a Petroleum Hydrocarbon-Contaminated Aquifer. *Applied and Environmental Microbiology*, 68, 1516–23.

Kleikemper, J., Pelz, O., Schroth, M., H., Zeyer, J., 2002(b). Sulfate-reducing bacterial community response to carbon source amendments in contaminated aquifer microcosms. *FEMS Microbiology Ecology*, 42, 109–18.

Kleikemper, J., Schroth, M. H., Bernasconi, S. M., Brunner, B., Zeyer, J., 2004. Sulfur isotope fractionation during growth of sulfate-reducing bacteria on various carbon sources. *Geochimica et Cosmochimica Acta*, 68, 4891–904.

Knöller, K., Vogt, C., Richnow, H. H., Weise, S. M., 2006. Sulfur and oxygen isotope fractionation during benzene, toluene, ethyl benzene, and xylene degradation by sulfate-reducing bacteria. *Environmental Science & Technology*, 40, 3879–85.

Krembs, F. J., Siegrist, R. L., Crimi, M. L., Furrer, R. F., Petri, B. G., 2010. ISCO for Groundwater Remediation : Analysis of Field Applications and Performance. *Ground Water Monitoring & Remediation*, 30, 42-53.

Kulik, N., Goi, A., Trapido, M., Tuhkanen, T., 2006. Degradation of polycyclic aromatic hydrocarbons by combined chemical pre-oxidation and bioremediation in creosote contaminated soil. *Journal of Environmental Management*, 78(4), 382–391.

Lawrence, S., 2006. Description, Properties, and Degradation of Selected Volatile Organic Compounds Detected in Ground Water — A Review of Selected Literature, Open-File Report, 1338.

Lee, B. T., Kim, K. W., 2002. Ozonation of diesel fuel in unsaturated porous media. *Applied Geochemistry*, 17, 1165–70.

Lee, J., Jung, K., Choi, S. H. O., 1995. Combination of the tod and the tol pathways in redesigning a metabolic route of Pseudomonas putida for the mineralization of a benzene , toluene , and p-xylene mixture. *Applied and Environmental Microbiology*, 61, 2211-7.

Liang, C., Huang, C. F., Chen, Y. J., 2008. Potential for activated persulfate degradation of BTEX contamination. *Water Research*, 42, 4091–100.

Longbottom, J. E., Lichtenberg, J. J. (Eds.), 1982. Methods for Organic Chemical Analysis of Municipal and Industrial Wastewater", EPA-600/4-82-057, USEPA/EMSL: Cincinnati, OH, Appendix A – Definition and Procedure for the Determination of the Method Detection Limit.

Luhrs, R. C., Lewis, R. W., Huling, S. G., 2006. ISCO's Long-Term Impact on Aquifer Conditions and Microbial Activity. In *Remediation of Chlorinated and Recalcitrant Compounds—2006. Proceedings of the Fifth International Conference on Remediation of Chlorinated and Recalcitrant Compounds*. Monterey, CA: Battelle Press, Columbus, OH.

MacFarlane, D. S., Cherry, J. A., Gilham, R. W., Sudicky, E. A., 1983. Migration of Contaminants in Groundwater at a NDFILL: A Case-Groundwater Flow and Plume Delineation. *Journal of Hydrology*, 63, 1–29.

Mackay, D. M., Freyberg, D. L., Roberts, P. V., Cherry, J. A., 1986. A natural gradient experiment on solute transport in a sand aquifer: 1. Approach and overview of plume movement. *Water Resources Research*, 22, 2017–29.

Mackay, D. M., Wilson, R., Durrant, G., 2000. Field of Enhanced Intrinsic Remediation of an MTBE Plume, *ACS National Meeting*, 4.

MacQuarrie, K. T. B., Sudicky, E. A., Frind, E. O., 1990. Simulation of biodegradable organic contaminants in groundwater: 1. Numerical formulation in principal directions. *Water Resources Research*, 26, 207–22.

Mancini, S. A., Ulrich, A. C., Lacrampe-Couloume, G., Sleep, B., Edwards, Lollar, B. S., 2003. Carbon and Hydrogen Isotopic Fractionation during Anaerobic Biodegradation of Benzene. *Applied and Environmental Microbiology*, 69, 191–98.

Marchesi, M., Thomson, N. R., Aravena, R., Sra, K. S., Otero, N., Soler, A., 2013. Carbon isotope fractionation of 1,1,1-trichloroethane during base-catalyzed persulfate treatment. *Journal of Hazardous Materials*, 260, 61–6.

Marley, M. C., Parikh, J. M., Droste, E. X., Lee, A. M., 2006. A case study on enhanced reductive dechlorination resulting from a chemical oxidation pilot test. In *First International Conference on DNAPL Characterization and Remediation*, Pittsburgh, PA.

McCormick, D. W., 2005. An Investigation Into In Situ Biodegradation Under Sulphate-Reducing Conditions In A Petroleum Contaminated Shallow Aquifer. Master Thesis, University of Cape Town, South Africa.

McDonald, M., Harbaugh, A., 1988. A Modular Three-Dimensional Finite-Difference Ground-Water Flow Model, Geological Survey Techniques of Water-Resources Investigations, Book 6,1 Chapter A1. 586.

Meckenstock, R. U., Morasch, B., Warthmann, R., Schink, B., Annweiler, E., Michaelis, W., Richnow, H. H., 1999. 13C/12C isotope fractionation of aromatic hydrocarbons during microbial degradation. *Environmental Microbiology*, 1, 409–14.

Meckenstock, R. U., Morasch, B., Griebler, C., Richnow, H. H., 2004. Stable isotope fractionation analysis as a tool to monitor biodegradation in contaminated acquifers. *Journal of Contaminant Hydrology*, 75, 215–55.

Miao, Z., Brusseau, M. L., Carroll, K. C., Carreón-Diazconti, C., Johnsonet, B., 2012. Sulfate reduction in groundwater: characterization and applications for remediation. *Environmental Geochemistry and Health*, 34, 539–50.

Mikesell, M. D., Kukor, J. J., Olsen, R. H., 1993. Metabolic diversity of aromatic hydrocarbon-degrading bacteria from a petroleum-contaminated aquifer. *Biodegradation*, 4, 249–59.

Miller, C. M., Valentine, R. L., Roehl, M. E., Alvarez, P. J. J., 1996. Chemical and microbiological assessment of pendimethalin-contaminated soil after treatment with Fenton's reagent. *Water Research*, 30, 2579–86.

Millner, G. C., James, R. C., Nye, A. C., 1992. Human health-based soil cleanup guidelines for diesel fuel no. 2. *Soil and Sediment Contamination*, 1, 103–57.

Morasch, B., Richnow, H. H., Schink, B., Meckenstock, R. U., 2001. Stable hydrogen and carbon isotope fractionation during microbial toluene degradation: mechanistic and environmental aspects. *Applied and Environmental Microbiology*, 67, 4842–9.

Munakata-Marr, J., Sorenson, K., Petri, B., Cummings, J., 2011. Principles of Combining ISCO with Other In Situ Remedial Approaches. In R. L. Siegrist, M. Crimi, & T. J. Simpkin (Eds.), *In Situ Chemical Oxidation for Groundwater Remediation* (Vol. 3, 285–317). New York, NY: Springer New York.

Muyzer, G., Stams, A. J. M., 2008. The ecology and biotechnology of sulphate-reducing bacteria. *Nature Reviews. Microbiology*, 6, 441–54.

Nam, K., Rodriguez, W., & Kukor, J. J., 2001. Enhanced degradation of polycyclic aromatic hydrocarbons by biodegradation combined with a modified Fenton reaction. *Chemosphere*, 45(1), 11–20.

Neretin, L. N., Schippers, A., Pernthaler, A., Hamann, K., Amann, R., Jørgensen, B. B., 2003. Quantification of dissimilatory (bi)sulphite reductase gene expression in Desulfobacterium autotrophicum using real-time RT-PCR. *Environmental Microbiology*, 5, 660–71.

Nicholson, R. V., Cherry, J. A., Reardon, E. J., 1983. Migration of contaminants in groundwater at a landfill: A case study 6. Hydrogeochemistry. *Journal of Hydrology*, 63, 131–76.

National Research Council (NRC), 1994. Alternatives for Ground Water Cleanup, Washington, DC,

US: National Academic Press.

Oka, A. R., 2009. Anaerobic benzene degradation in culture and hydrocarbon degradation in the subsurface environment. PhD Thesis, State University of New Jersey, USA.

Oude Elferink, S. J. W. H., 1998. Sulfate-reducing Bacteria in Anaerobic Bioreactors, PhD Thesis, van de Landbouwuniversiteit Wageningen, Netherlands.

Pardieck, D. L., Bouwer, E. J., & Stone, A. T.,1992. Hydrogen peroxide use to increase oxidant capacity for in situ bioremediation of contaminated soils and aquifers: A review. *Journal of Contaminant Hydrology*, 9(3), 221–242.

Pawlak, Z., Rauckyte, T. & Oloyede, A., 2008. Oil, grease and used petroleum oil management and environmental economic issues. *Journal of Achievements in Materials and Manufacturing Engineering*, 26, 11–7.

Petri, B. G, Watts, R. J., Tsitonaki, A., Crimi, M., Thomson, R. T., Teel, A. L., 2011. Fundamentals of ISCO using persulfate. In R. L. Siegrist, M. Crimi, & T. J. Simpkin (Eds.), In Situ Chemical Oxidation for Groundwater Remediation (Vol. 3, 285–317). New York, NY: Springer New York.

Piskonen, R., Nyyssönen, M., Itävaara, M., 2008. Evaluating the biodegradation of aromatic hydrocarbons by monitoring of several functional genes. *Biodegradation*, 19, 883–95.

Plugge, C. M., Zhang, W., Scholten, J. C. M., Stams, A. J. M., 2011. Metabolic flexibility of sulfate-reducing bacteria. *Frontiers in Microbiology*, 2, 81.

Poulson, S. R., Naraoka, H., 2002. Carbon isotope fractionation during permanganate oxidation of chlorinated ethylenes (cDCE, TCE, PCE). *Environmental Science & Technology*, 36, 3270–4.

Rabus, R., Heider, J., 1998. Initial reactions of anaerobic metabolism of alkylbenzenes in denitrifying and sulfate-reducing bacteria. *Archives of Microbiology*, 170, 377–84.

Reinhard, M., Shang, S., Kitanidis, P. K., Orwin, E., Hopkins, G. D., Lebron, C. A., 1997. In Situ BTEX Biotransformation under Enhanced Nitrate- and Sulfate-Reducing Conditions. *Environmental Science & Technology*, 31, 28–36.

Richardson, S. D., Lebron, B. L., Miller, C. T., Aitken, M. D., 2011. Recovery of phenanthrene-degrading bacteria after simulated in situ persulfate oxidation in contaminated soil. *Environmental Science & Technology*, 45, 719–25.

Rifai, H. S., Newell, C. J., 1998. Estimating First-Order Decay Rates for BTEX Using Data from 115 Sites. In: *Proceedings of the 1998 NGWA Conference on Petroleum Hydrocarbons and Organic Chemicals in Ground Water: Prevention, Detection and Restoration*. Houston, Texas: National Ground Water Association, Westerville, OH, 31 – 41.

Roychoudhury, A. N., McCormick, D. W., 2006. Kinetics of Sulfate Reduction in a Coastal Aquifer

Contaminated with Petroleum Hydrocarbons. *Biogeochemistry*, 81, 17–31.

Roychoudhury, A. N., Merrett, G. L., 2006. Redox pathways in a petroleum contaminated shallow sandy aquifer: Iron and sulfate reductions. *The Science of the Total Environment*, 366, 262–74.

Sahl, J., Munakata-Marr, J., 2006. The effects of in situ chemical oxidation on microbiological processes: A review. *Remediation Journal*, 16, 57–70.

Sahl, J. W., Munakata-Marr, J., Crimi, M. L., Siegrist, R. L., 2007. Coupling permanganate oxidation with microbial dechlorination of tetrachloroethene. *Water environment research: a research publication of the Water Environment Federation*, 79, 5–12.

Schirmer, M., Schirmer, M., Molson, J. W., Frind, E. O., Barker, J. F., 2000. Biodegradation modelling of a dissolved gasoline plume applying independent laboratory and field parameters. *Journal of Contaminant Hydrology*, 46, 339–374.

Schirmer, M., Butler, B. J., 2004. Transport behaviour and natural attenuation of organic contaminants at spill sites. *Toxicology*, 205, 173–9.

Schmidt, T. C., Zwank, L., Elsner, M., Berg, M., Meckenstock, R. U., Haderlein, S. B., 2004. Compound-specific stable isotope analysis of organic contaminants in natural environments: a critical review of the state of the art, prospects, and future challenges. *Analytical and Bioanalytical Chemistry*, 378, 283–300.

Schnarr, M., Truax, C., Farquhar, G., Hood, E., Gonullu, T., Stickneycet, B., 1998. Laboratory and controlled field experiments using potassium permanganate to remediate trichloroethylene and perchloroethylene DNAPLs in porous media. *Journal of Contaminant Hydrology*, 29, 205–24.

Schroth, M. H., Kleikemper, J., Bolliger, C., Bernasconi, S. M., Zeyer, J., 2001. In situ assessment of microbial sulfate reduction in a petroleum-contaminated aquifer using push-pull tests and stable sulfur isotope analyses. *Journal of contaminant hydrology*, 51, 179–95.

Scott, J. P., Ollis, D. F., 1995. Integration of chemical and biological oxidation processes for water treatment: Review and recommendations. *Environmental Progress*, 14, 88–103.

Sessa, F., Paré, J., Studer, J. E., 2008 . Coupled ISCO-Bio via Activated Persulfate and Timed Oxygen Release using a Sodium Persulfate/Calcium Peroxide matrix. In *Proceeding of the Remediation Technologies Symposium 2008 (RemTech 2008)*. Banff, Canada.

Shen, Y. & Buick, R., 2004. The antiquity of microbial sulfate reduction. *Earth-Science Reviews*, 64, 243–72.

Shim, H., Hwang, B., Lee, S. S., Kong, S. H., 2005. Kinetics of BTEX biodegradation by a coculture of Pseudomonas putida and Pseudomonas fluorescens under hypoxic conditions. *Biodegradation*, 16, 319–27.

Siegrist R. L., Crimi, M., Simpkin, T. J., (eds). 2011. In Situ Chemical Oxidation for Groundwater Remediation. Springer Science+Business Media, LLC, New York, New York. A reference book in the SERDP/ESTCP Remediation Technology Monograph Series, C.H. Ward (Series ed).

Sirguey C., Silva P., Schwartz C., Simonnot M. O., 2008. Impact of chemical oxidation on soil quality. *Chemosphere,* 72:282–289.

Smith, M. R., 1990. The biodegradation of aromatic hydrocarbons by bacteria. *Biodegradation*, 1, 191–206.

Solano, F. M., 2014. Persulfate Treatment of Manufactured Gas Plant Residuals and Dual Compound-Specific Isotope Analysis to Assess the Performance of the Chemical Oxidation. Master Thesis, University of Waterloo, Canada.

Song, D. L., Conrad M. E., Sorenson K. S., Alvarez-Cohen L., 2002. Stable carbon isotope fractionation during enhanced in situ bioremediation of trichloroethene. *Environmental Science & Technology*, 36, 2262–8.

Spormann, A. M., Widdel, F., 2000. Metabolism of alkylbenzenes, alkanes, and other hydrocarbons in anaerobic bacteria. *Biodegradation*, 11, 85–105.

Sra, K. S., 2010. Persulfate Persistence and Treatability of Gasoline Compounds. PhD Thesis, University of Waterloo, Canada.

Sra, K. S., Thomson, N. R., & Barker, J. F., 2010. Persistence of persulfate in uncontaminated aquifer materials. *Environmental Science & Technology*, 44(8), 3098–104.

Sra, K. S., Thomson, N. R., Barker, J. F., 2013a. Persulfate injection into a gasoline source zone. *Journal of Contaminant Hydrology*, 150, 35–44.

Sra, K. S., Thomson, N. R., Barker, J. F., 2013b. Persulfate Treatment of Dissolved Gasoline Compounds. *Journal of Hazardous, Toxic, and Radioactive Waste*, 17, 9–15.

Strebel, O., Bottcher, J., Fritz, P., 1990. Use of isotope fractionation of sulfate-sulfur and sulfate-oxygen to assess bacterial desulfurication in a sandy aquifer. *Journal of Hydrology*, 121, 155–172.

Struchtemeyer, C. G., Elshahed, M. S., Duncan, K. E., McInerney, M.J., 2005. Evidence for Aceticlastic Methanogenesis in the Presence of Sulfate in a Gas Condensate-Contaminated Aquifer. *Applied Environmental Microbiology*, 1, 5348-53.

Studer, J., Davis, G., Baldwin, B., Cronk, G., 2009. Impact of *In Situ* Chemical Oxidation on Native Biological Populations: Review of Case Studies. In: *proceeding of the Tenth International In Situ and On-Site Bioremediation Symposium*. Battelle, Baltimore.

Stumm, W., Morgan, J. J., 1981. Aquatic Chemistry, An Introduction Emphasizing Chemical Equilibria in Natural Waters, 2nd ed. Wiley, New York.

Suflita, J. M., Davidova, I. A., Gieg, L. M., Nanny, M., Prince, R. C., 2004. Chapter 10: Anaerobic hydrocarbon biodegradation and the prospects for microbial enhanced energy production. Studies in Surface Science and Catalysis 151 R. Vazquez-Duhalt and R. Quintero-Ramirez (Eds), Elsevier, pp 283-306.

Sun, W., Sun, X., Cupples, A. M., 2014. Presence, diversity and enumeration of functional genes (bssA and bamA) relating to toluene degradation across a range of redox conditions and inoculum sources. *Biodegradation*, 25, 189–203.

Sutton, N. B., Grotenhuis, J. T. C., Langenhoff, A. A. M., Rijnaarts, H H. M., 2010. Efforts to improve coupled in situ chemical oxidation with bioremediation: a review of optimization strategies. *Journal of Soils and Sediments*, 11, 129–40.

Tsai, T. T., Kao, C. M., Surampalli, R. Y., Chien, H. Y., 2009. Enhanced Bioremediation of Fuel-Oil Contaminated Soils: Laboratory Feasibility Study. *Journal of Environmental Engineering*, 135, 845–53.

Tsitonaki, A., Petri, B., Crimi, M., Mosbaek, H., Siegrist, R. L., Bjerg, P. L., 2010. In Situ Chemical Oxidation of Contaminated Soil and Groundwater Using Persulfate: A Review. *Critical Reviews in Environmental Science and Technology*, 40, 55–91.

Tsitonaki, A., 2008. Treatment Trains for the Remediation of Aquifers Polluted with MTBE and other Xenobiotic Compounds. PhD Thesis, Technical University of Denmark, Denmark.

Tsitonaki, A., Smets, B. F., Bjerg, P. L., 2008. Effects of heat-activated persulfate oxidation on soil microorganisms. *Water Research*, 42, 1013–22.

Villanueva, L., Haveman, S. A., Summers, Z. M., Lovley, D. R., 2008. Quantification of Desulfovibrio vulgaris dissimilatory sulfite reductase gene expression during electron donor- and electron acceptor-limited growth. Applied and environmental microbiology, 74, 5850–3.

Vroblesky, D. A., Bradley, P. M., Chapelle, F. H., 1996. Influence of Electron Donor on the Minimum Sulfate Concentration Required for Sulfate Reduction in a Petroleum Hydrocarbon-Contaminated Aquifer. *Environmental Science & Technology*, 30, 1377–81.

Waddell, J. P., Mayer, G. C., 2003. Effects of Fenton's reagent and potassium permanganate applications of indigenous subsurface microbiota: a literature review. In *Proceedings of the 2003 Georgia Water Resources Conference, University of Georgia*. Georgia Institute of Technology Institute of Ecology.

Westersund J., Fernandes L., Jones S., Clought H., 2006. Stimulating anaerobic reductive dechlorination following chemical oxidation treatment. In *Proceedings of the fifth international conference on Remediation of Chlorinated and Recalcitrant Compounds*. Battelle, Monterey.

Watts, R. J., Teel, A. L., 2006. Treatment of Contaminated Soils and Groundwater Using ISCO. *Practice Periodical of Hazardous Toxic, and Radioactive Waste Management*, 10, 2–9.

Weelink, S. A., 2008. Degradation of benzene and other aromatic hydrocarbons by anaerobic bacteria. PhD Thesis, Wageningen University, Netherlands.

Weiner, J. M., Lauck, T. S., Lovley, D. R., 1998. Enhanced anaerobic benzene degradation with the addition of sulfate. *Bioremediation Journal*, 2, 159–73.

WHO, 2005. Petroleum Products in Drinking-water, World Health Organization, Geneva.

Wiedemeier, T. H., Rifai, H. S., Newell, C. J., Wilson, J. T., 1999. Natural Attenuation of Fuels and Chlorinated Solvents in the Subsurface.John Wiley &Sons, Inc., New York.

Wilhelm, E., Battino, R., Wilcock, R. J., 1977. Low-pressure solubility of gases in liquid water. *Chemical Reviews*, 77, 219–62.

Wilkes, H., Boreham, C., Harms, G., Zengler, K., Rabusc, R., 2000. Anaerobic degradation and carbon isotopic fractionation of alkylbenzenes in crude oil by sulphate-reducing bacteria. *Organic Geochemistry*, 31, 101–15.

Williams, P. A., Sayers, J. R., 1994. The evolution of pathways for aromatic hydrocarbon oxidation in Pseudomonas. *Biodegradation*, 5, 195–217.

Wilson, R. D., Mackay, D. M., 1995. A Method for Passive Release of Solutes from an Unpumped Well. *Ground water*, 33, 936–945.

Xu, X., Thomson, N. R., 2008. Estimation of the Maximum Consumption of Permanganate by Aquifer Solids Using a Modified Chemical Oxygen Demand Test. *Journal of Environmental Engineering*, 134, 353–61.

Yagi, J. M., Neuhauser, E. F., Ripp, J. A., Mauro, D. M., Madsen, E. L., 2010. Subsurface ecosystem resilience: long-term attenuation of subsurface contaminants supports a dynamic microbial community. *The ISME journal*, 4, 131–43.

Yang, G. C., Wu, L. C., Wu, C. S., Hsu, I. Y., 2005. Treatment train for site remediation at a petrochemicals-contaminated site within a petroleum refinery. *Bulletin of environmental contamination and toxicology*, 74, 904–12.

Yerushalmi, L., Lascourreges, J. F., Rhofir, C., Guiot, S. R., 2001. Detection of intermediate metabolites of benzene biodegradation under microaerophilic conditions. *Biodegradation*, 12, 379–91.

Zheng, C., Wang, P., 1998. MT3DMS: A modular three-dimensional multispeces transport model for simulation of advection, dispersion, and chemical reactions of contaminants in groundwater systems. Technical report, Waterways Experiment Station, US Army Corps of Engineers, Vicksburg, MS.

Zhou, J., He, Q., Hemme, C. L., Mukhopadhyay, A., Hillesland, K., Zhou, A., Arkin, A. P., 2011. How sulphate-reducing microorganisms cope with stress: lessons from systems biology. *Nature*

Reviews: Microbiology, 9(6), 452–66.

Zwolinski, M. D., Harris, R. F., Hickey, W. J., 2000. Microbial consortia involved in the anaerobic degradation of hydrocarbons. *Biodegradation*, 11, 141–58.

Chapter 3

Adriano, D., 1994. *Contamination of Groundwaters*, Boca Raton, FL. CRC Press.

Alvarez, P. J., Anid, P. J., Vogel, T. M., 1991. Kinetics of aerobic biodegradation of benzene and toluene in sandy aquifer material. *Biodegradation*, 2, 43–51.

Ahmad, M., Teel, A. L., Watts, R. J., 2013. Phenoxide activation of persulfate. *Environmental Science and Technology* ,47, no. 11: 5864–5871.

Anipsitakis, G. P., Dionysiou, D. D., 2004. Radical generation by the interaction of transition metals with common oxidants. *Environmental Science & Technology*, 38(13), pp.3705–12.

Ballarini, E., Beyer, C., Bauer, R. D., Griebler, C., Bauer, S., 2013. Model based evaluation of a contaminant plume development under aerobic and anaerobic conditions in 2D bench-scale tank experiments. *Biodegradation*, 25, 351–71.

Barry, D. A., Prommer, H., Miller, C. T., Engesgaard, P., Brun, A., Zheng, C., 2002. Modelling the fate of oxidisable organic contaminants in groundwater. *Advances in Water Resources*, 25, 945–83.

Borden, R. C., Cha, K. Y., Simpkin, T. J., Lieberman, M. T., 2009. Design Tool for Planning Permanganate Injection Systems, Draft Technical Report Project ER-0626. *Submitted to Environmental Security Technology Certification Program (ESTCP),*. Arlington, VA, USA.

Chen, Y. M., Abriola, L. M., Alvarez, P. J. J., Anid, P. J., Vogelet, T. M., 1992. Modeling transport and biodegradation of benzene and toluene in sandy aquifer material: Comparisons With experimental measurements. *Water Resources Research*, 28, 1833–47.

Clement, T. P., Sun, Y., Hooker, B. S., Petersen, J. N., 1998. Modeling Multispecies Reactive Transport in Ground Water. *Ground Water Monitoring & Remediation*, 18, 79–92.

Edwards, E., Wills, L. E., Reinhard, M., Grbić-Galić, D., 1992. Anaerobic degradation of toluene and xylene by aquifer microorganisms under sulfate-reducing conditions. *Applied and Environmental Microbiology*, 58, 794–800.

Elloy, F. C., Teel, A. L.,Watts, R. J., 2014. Activation of Persulfate by Surfactants. Submitted to *Groundwater Monitoring & Remediation*

Essaid, H. I., Bekins, B. A., Michael, E., Warren, G. E., Baedecker, M. J., Cozzarell, I. M., 1995. Simulation of aerobic and anaerobic biodegradation processes at a crude oil spill site. *Water Resources Research*, 31, 3309–27.

Fedorovich, V., Lens, P., Kalyuzhnyi, S., 2003. Extension of Anaerobic Digestion Model No. 1 with processes of sulfate reduction. *Applied Biochemistry and Biotechnology*, 109, 33–45.

Frind, E. O., Molson, J. W., Schirmer, M., Guiguer, N., 1999. Dissolution and mass transfer of

multiple organics under field conditions: The Borden emplaced source. *Water Resources Research*, 35, 683–94.

Fukui, M., Harms, G, Rabus, R., Schramm, A., Widdel, F., Zengler, K., Boreham, C., Wilkes, H., 1999. Anaerobic degradation of oil hydrocarbons by sulfate-reducing and nitrate-reducing bacteria. In *8th International Symposium on Microbial Ecology*.

Fukui, M., Takii, S., 1994. Kinetics of sulfate respiration by free-living and particle-associated sulfate-reducing bacteria. *FEMS Microbiology Ecology*, 13, 241–7.

Geng, X., Boufadel, M. C., Wrenn, B., 2013. Mathematical modeling of the biodegradation of residual hydrocarbon in a variably-saturated sand column. *Biodegradation*, 24, 153–63.

Greer, K. D., Molson, J. W., Barker, J. F., Thomson, N. R., Donaldson, C. R., 2010. High-pressure injection of dissolved oxygen for hydrocarbon remediation in a fractured dolostone aquifer. *Journal of Contaminant Hydrology*, 118, 13–26.

Heiderscheidt, J. L., Illangasekare, T. H., Borden, R. C., Thomson, N. R., 2011. Principles of ISCO Related Subsurface Transport and Modeling. Siegrist, M. Crimi, & T . Simpkin, eds. *In Situ Chemical Oxidation for Groundwater Remediation*. Springer New York, Vole 3, pp. 233–84.

Heiderscheidt, J. L., 2005. DNAPL Source Zone Depletion during In Situ Chemical Oxidation (ISCO): Experimental and Modeling Studies. PhD Thesis, Colorado School of Mines, USA.

Heiderscheidt, J. L., Crimi, M., Siegrist, R. L., Singletary, M. A., 2008. Optimization of Full-Scale Permanganate ISCO System Operation: Laboratory and Numerical Studies. *Ground Water Monitoring & Remediation*, 28, 72–84.

Henderson, T. H., Mayer, K. U., Parker, B. L., Al, T. A., 2009. Three-dimensional density-dependent flow and multicomponent reactive transport modeling of chlorinated solvent oxidation by potassium permanganate. *Journal of Contaminant Hydrology*, 106, 195–211.

Höhener, P., Duwig, C., Pasteris, G., Kaufmann, K, Dakhel, N., Harms, H., 2003. Biodegradation of petroleum hydrocarbon vapors: laboratory studies on rates and kinetics in unsaturated alluvial sand. *Journal of Contaminant Hydrology*, 66, 93–115.

Huang, K. C., Zhao, Z., Hoag, G. E., Dahmani, A., Block, P. A., 2005. Degradation of volatile organic compounds with thermally activated persulfate oxidation. *Chemosphere*, 61, 551–60.

Huling, S. G., Pivetz, B. E., 2006. Engineering Issue:In-Situ Chemical Oxidation. EPA/600/R-06/072.U.S.Enviromnmental Protection Agency Office of Research and Developement,National Risk Management Research Laboratory,Cincinnati, OH.

Ingvorsen, K., Zehnder, A. J., Jørgensen, B. B., 1984. Kinetics of Sulfate and Acetate Uptake by Desulfobacter postgatei. *Applied and Environmental Microbiology*, 47, 403–8.

Jin, Q., Bethke, C. M., 2009. Cellular energy conservation and the rate of microbial sulfate reduction. *Geology*, 37, 1027–30.

Kalyuzhnyi, S., Fedorovich, V., Lens, P., Pol, L. H., Lettinga, G., 1998. Mathematical modelling as a tool to study population dynamics between sulfate reducing and methanogenic bacteria. *Biodegradation*, 9, 187–99.

Kim, D. J., Choi, J. W., Choi, N. C., Mahendran, B., Lee, C. E., 2005. Modeling of growth kinetics for Pseudomonas spp. during benzene degradation. *Applied Microbiology and Biotechnology*, 69, 456–62.

Kissel, J. C., McCarty, P. L., Street, R. L., 1985. Numerical Simulation of Mixed-Culture Biofilm. *Journal of Environmental Engineering*, 110, 393–411.

Kulik, N., Goi, A., Trapido, M., Tuhkanen, T., 2006. Degradation of polycyclic aromatic hydrocarbons by combined chemical pre-oxidation and bioremediation in creosote contaminated soil. *Journal of Environmental Management*, 78(4), 382–391.

López-Pérez, P. A., Neria-González, M. I., Flores-Cotera, L. B., & Aguilar-López, R., 2013. A mathematical Model for Cadmium Removal using A sulfate Reducing Bacterium: Desulfovibrio alaskensis 6SR. *International Journal of Environmental Research*, 7(2), 501–512.

Lu, G., Clement, T. P., Zheng, C., Wiedemeier, T. H., 1999. Natural Attenuation of BTEX Compounds: Model Development and Field-Scale Application. *Ground water*, 37(5), pp.707–717.

MacFarlane, D. S., Cherry, J. A., Gilham, R. W., Sudicky, E. A., 1983. Migration of Contaminants In Groundwater at A-NDFILL: A Case Study 1-Groundwater Flow and Plume Delineation. *Journal of Hydrology*, 63, 1–29.

Mackay, D. M., Freyberg, D. L., Roberts, P. V., Cherry, J. A., 1986. A natural gradient experiment on solute transport in a sand aquifer: 1. Approach and overview of plume movement. *Water Resources Research*, 22, 2017–29.

MacQuarrie, K. T. B., Sudicky, E. A., Frind, E. O., 1990. Simulation of biodegradable organic contaminants in groundwater: 1. Numerical formulation in principal directions. *Water Resources Research*, 26, 207–22.

Mayer, K. U., Frind, E. O., Blowes, D. W., 2002. Multicomponent reactive transport modeling in variably saturated porous media using a generalized formulation for kinetically controlled reactions. *Water Resources Research*, 38, 13–21.

Miller, C. M., Valentine, R. L., Roehl, M. E., Alvarez, P. J. J., 1996. Chemical and microbiological assessment of pendimethalin-contaminated soil after treatment with Fenton's reagent. *Water Research*, 30, 2579–86.

Molson, J., Mocanu, M., Barker, J., 2008. Numerical analysis of buoyancy effects during the

dissolution and transport of oxygenated gasoline in groundwater. *Water Resources Research*, 44, 1–15.

Molson, J.W., 2014. BIONAPL/3D User's Guide, Department of Geology & Geological Engineering, Université Laval, Québec, QC

Molson, J. W., Barker, J. F., Frind, E. O., Schirmer, M., 2002. Modeling the impact of ethanol on the persistence of benzene in gasoline-contaminated groundwater. *Water Resources Research*, 38, 4–12.

Munakata-Marr, J., Sorenson, K., Petri, B., Cummings, J., 2011. Principles of Combining ISCO with Other In Situ Remedial Approaches. In R. L. Siegrist, M. Crimi, & T. J. Simpkin (Eds.), *In Situ Chemical Oxidation for Groundwater Remediation* (Vol. 3, 285–317). New York, NY: Springer New York.

Nam, K., Rodriguez, W., & Kukor, J. J., 2001. Enhanced degradation of polycyclic aromatic hydrocarbons by biodegradation combined with a modified Fenton reaction. *Chemosphere*, 45(1), 11–20.

Nicholson, R. V., Cherry, J. A., Reardon, E. J., 1983. Migration of contaminants in groundwater at a landfill: A case study 6. Hydrogeochemistry. *Journal of Hydrology*, 63, 131–76.

Nicol, J. P., Wise, W. R., Molz, F. J., Benefield, L. D., 1994. Modeling biodegradation of residual petroleum in a saturated porous column. *Water Resources Research*, 30, 3313–25.

Ocampo A. 2009. Persulfate activation by organic compounds. PhD Thesis, Washington State University, Pullman, Washington

Oude Elferink, S. J. W. H., 1998. Sulfate-reducing Bacteria in Anaerobic Bioreactors, PhD Thesis, van de Landbouw universiteit, Wageningen, Netherlands.

Poinapen, J., Ekama, G., 2010. Biological sulphate reduction with primary sewage sludge in an upflow anaerobic sludge bed reactor - Part 6: Development of a kinetic model for BSR. *Water SA*, 36, 203–14.

Richardson, S. D., Lebron, B. L., Miller, C. T., Aitken, M. D., 2011. Recovery of phenanthrene-degrading bacteria after simulated in situ persulfate oxidation in contaminated soil. *Environmental Science & Technology*, 45, 719–25.

Rifai, H. S., Newell, C. J., 1998. Estimating First-Order Decay Rates for BTEX Using Data from 115 Sites. In: *Proceedings of the 1998 NGWA Conference on Petroleum Hydrocarbons and Organic Chemicals in Ground Water: Prevention, Detection and Restoration*. Houston, Texas: National Ground Water Association, Westerville, OH, 31 – 41.

Rifai, H. S., Rittaler, T., 2005. Modeling natural attenuation of benzene with analytical and numerical models. *Biodegradation*, 16, 291–304.

Roychoudhury, A. N., Van Cappellen, P., Kostka, J. E., Viollier, E., 2003. Kinetics of microbially mediated reactions: dissimilatory sulfate reduction in saltmarsh sediments (Sapelo Island, Georgia, USA). *Estuarine, Coastal and Shelf Science*, 56, 1001–10.

Roychoudhury, A. N., McCormick, D. W., 2006. Kinetics of Sulfate Reduction in a Coastal Aquifer Contaminated with Petroleum Hydrocarbons. *Biogeochemistry*, 81, 17–31.

Schirmer, M., Butler, B. J., Roy, J. W., Frind, E. O., Barker, J. F., 1999. A relative-least-squares technique to determine unique Monod kinetic parameters of BTEX compounds using batch experiments. *Journal of Contaminant Hydrology*, 37, 69–86.

Schirmer, M., Molson, J. W., Frind, E. O., Barker, J. F., 2000. Biodegradation modelling of a dissolved gasoline plume applying independent laboratory and field parameters. *Journal of Contaminant Hydrology*, 46, 339–74.

Shayan, M., Thomson, N. R., Barker, J. F., Aravena, R., Hunkeler, D., Madsen, E. L., Buscheck T., 2015. Integrated Plume Treatment using Chemical Oxidation Coupled with Microbial Sulfate Reduction, in preparation

Sra, K. S., 2010. Persulfate Persistence and Treatability of Gasoline Compounds. PhD Thesis, University of Waterloo, Canada.

Sra, K. S., Thomson, N. R., Barker, J. F., 2013(a). Persulfate injection into a gasoline source zone. *Journal of Contaminant Hydrology*, 150, 35–44.

Sra, K. S., Thomson, N.R. & Barker, J.F., 2013(b). Persulfate Treatment of Dissolved Gasoline Compounds. *Journal of Hazardous, Toxic, and Radioactive Waste*, 17, 9–15.

Sutton, N. B., Grotenhuis, J. T. C., Langenhoff, A. A. M., Rijnaarts, H H. M., 2010. Efforts to improve coupled in situ chemical oxidation with bioremediation: a review of optimization strategies. *Journal of Soils and Sediments*, 11, 129–40.

Teel, A. L., Ahmad, M., Watts, R. J., 2011. Persulfate activation by naturally occurring trace minerals. *Journal of Hazardous Materials*, 196, pp.153–9.

Tsitonaki, A., 2008. Treatment Trains for the Remediation of Aquifers Polluted with MTBE and other Xenobiotic Compounds. PhD Thesis, Technical University of Denmark, Denmark.

USEPA, 2004. Chapter XIII. Chemical Oxidation. http://www.epa.gov/OUST/pubs/tum_ch13.pdf

Vaezihir, A., Zare, M., Raeisi, E., Molson, J., Barker, J., 2012. Field-Scale Modeling of Benzene, Toluene, Ethylbenzene, and Xylenes (BTEX) Released from Multiple Source Zones. *Bioremediation Journal*, 16, 156–76.

Van Wageningen, H. S., Sötemann, S. W., Ristow, N. E., Wentzel, M. C., Ekama, G. A., 2006. Development of a kinetic model for biological sulphate reduction with primary sewage sludge as

substrate. *Water SA*, 32, 619–26.

Wilson, J. T., Kampbell, D. H., Bledsoe, B. E., Armstrong, J. M., 1990. Biotransformation of monoaromatic and chlorinated hydrocarbons at an aviation gasoline spill site. *Geomicrobiology Journal*, 8, 225–40.

WHO, 2005. Petroleum Products in Drinking-water, World Health Organization, Geneva.

Yang, G. C., Wu, L. C., Wu, C. S., Hsu, I. Y., 2005. Treatment train for site remediation at a petrochemicals-contaminated site within a petroleum refinery. *Bulletin of Environmental Contamination and Toxicology*, 74, 904–12.

Zacatenco, S. P., Division, B.E. & Morelos, E. D., 2013. A mathematical Model for Cadmium Removal using A sulfate Reducing Bacterium : Desulfovibrio alaskensis 6SR, *International Journal of Environmental Research*, 7, 501–12.

Chapter 4

Allison, J., Brown, D., Novo-Gradac, K., 1991. MINTEQA2/PRODEFA2, A Geochmical Assessment Model for Environmental Systems: Version 3.0 User's Manual, EPA/600/3-91/021

Kim, D. J., Choi, J. W., Choi, N. C., Mahendran, B., Lee, C. E., 2005. Modeling of growth kinetics for Pseudomonas spp. during benzene degradation. *Applied Microbiology and Biotechnology*, 69, 456–62.

Maurer, M., Rittmann, B. E., 2004. Modeling intrinsic bioremediation for interpret observable biogeochemical footprints of BTEX biodegradation: the need for fermentation and abiotic chemical processes. *Biodegradation*, 15, 405–17.

Parkhurst, D. L., Appelo, C. A.J., 2014. User's Guide to PHREEQC (Version 2): A Computer Program for Speciation, Batch-Reaction, One-Dimensional Transport, and Inverse Geochemical Calculations. U.S. Geological Survey Water-Resources Investigations Report 80-96, 195 p.

Waldemer, R. H., Tratnyek, P. G., Johnson, R. L., & Nurmi, J. T.,2007. Oxidation of chlorinated ethenes by heat-activated persulfate: kinetics and products. *Environmental Science & Technology*, 41(3), 1010–5.

Appendix A

Supplementary Material for Chapter 2

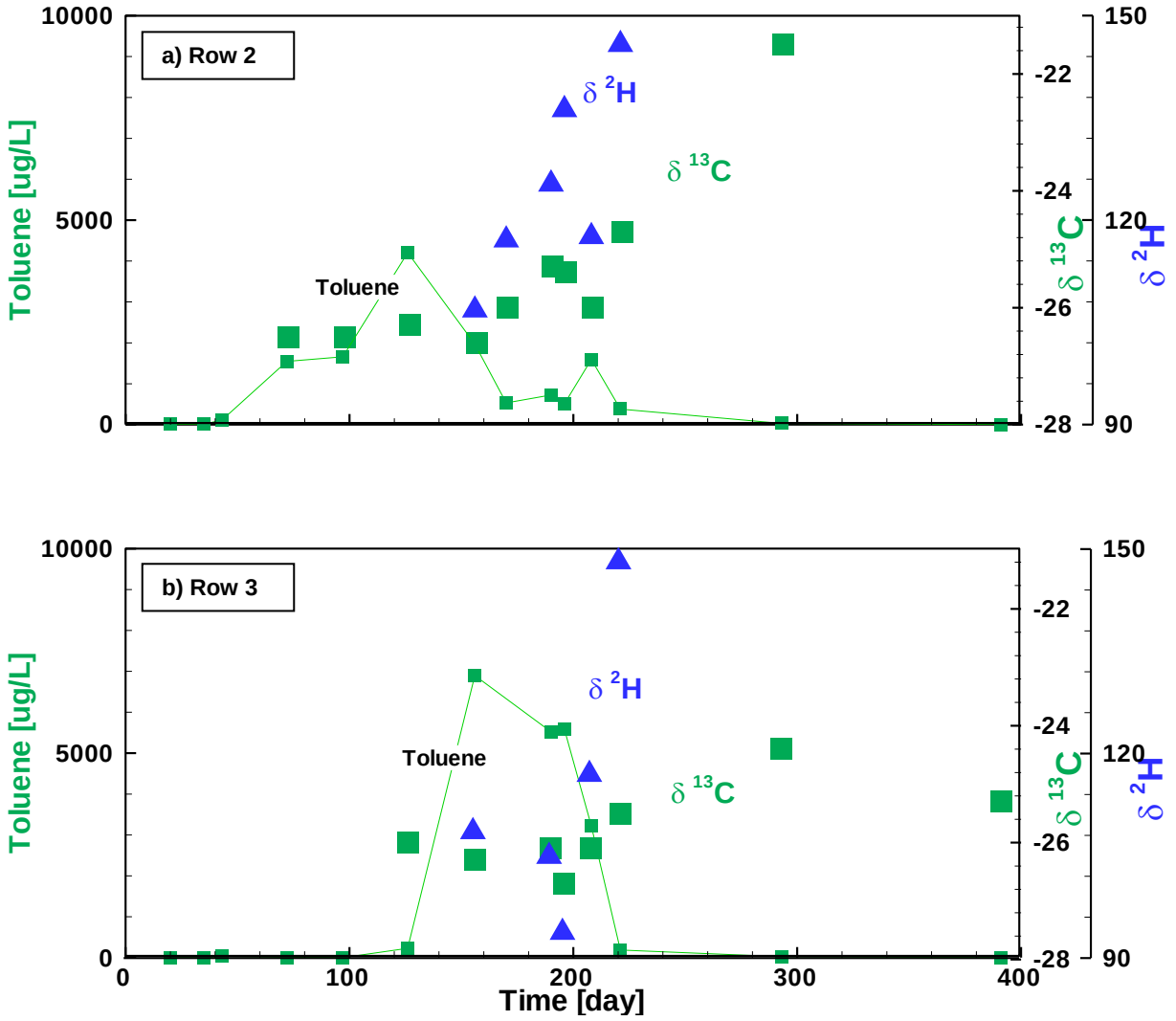

Figure A1. Carbon and hydrogen isotope data of toluene from two arbitrary sampling points at (a) Row 2 (ML2-L3) and (b) Row 3 (ML3-M3).

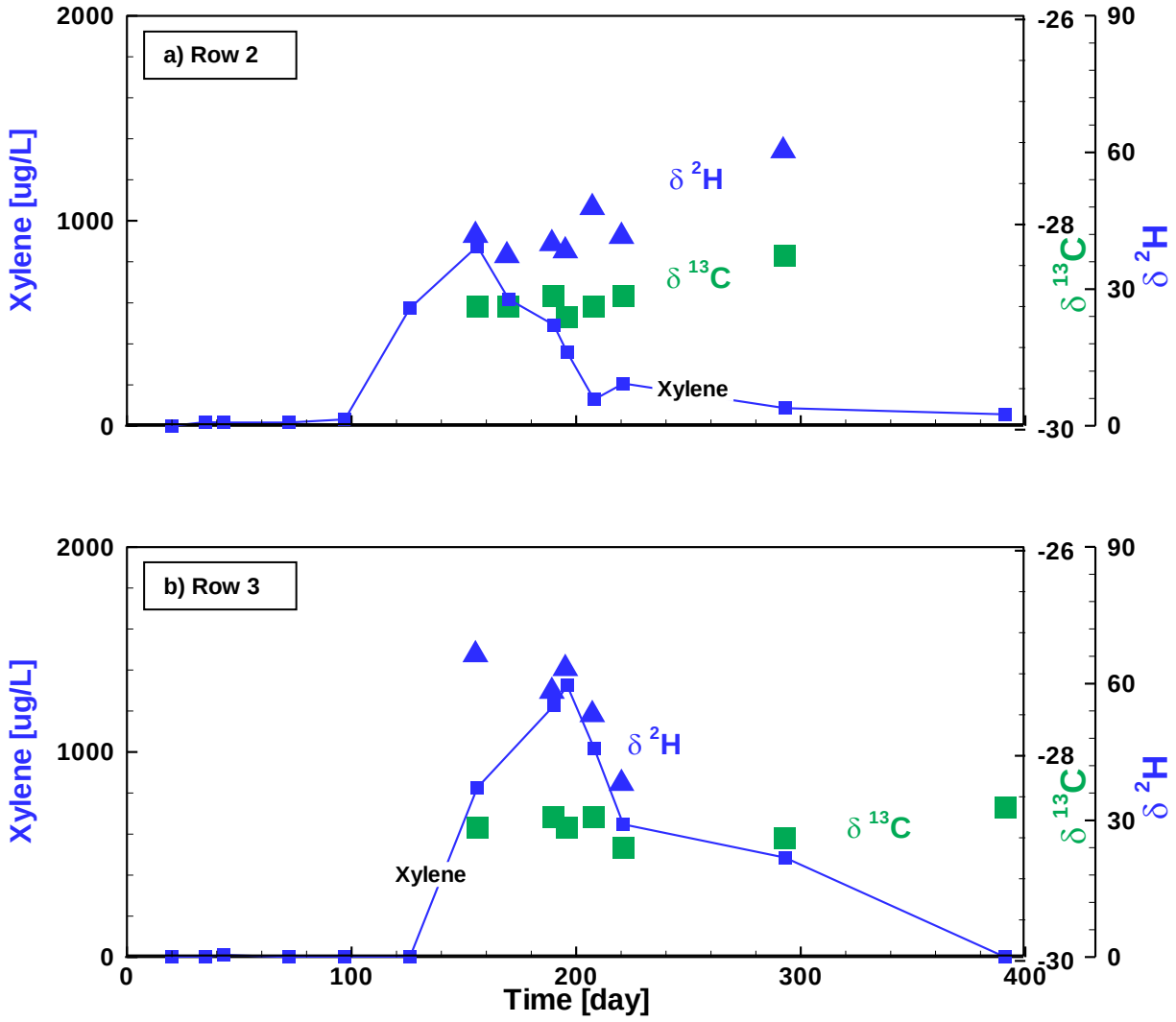

Figure A2. Carbon and hydrogen isotope data of xylene from two arbitrary sampling points at (a) Row 2 (ML2-L3) and (b) Row 3 (ML3-M3).

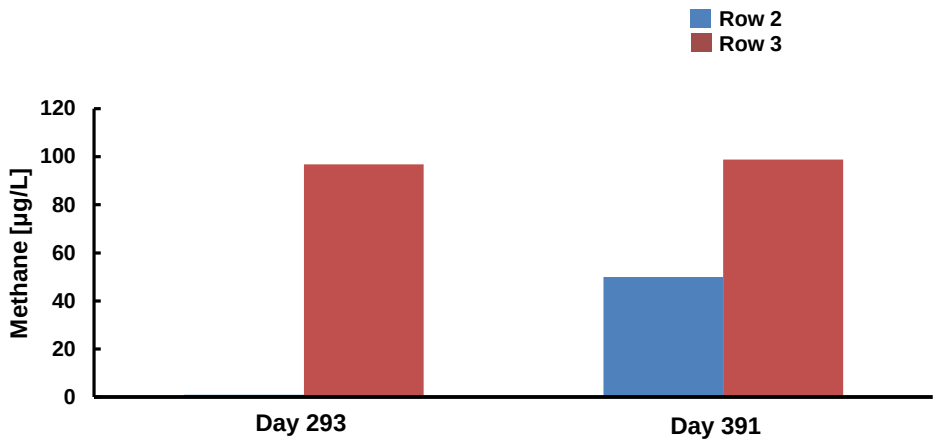

Figure A3. Increased methane concentration at Row 2 and Row 3 illustrates the enhancement of methanogenic biodegradation due to lower sulfate concentrations during the performance monitoring phase. Higher methane concentrations at Row 3 indicate the faster and more significant role of methanogenesis over sulfate reduction at this location compared to Row 2.

Table A1. PCR primers used in the present study

Target Gene	Primers	5'-3' sequence	Amplicon size (bp)	Reference
bssA	bssAf	ACG ACG GYG GCA TTT CTC	132	Beller 2002
	bssAr	GCA TGA TSG GYA CCG ACA		
bssA	SRBf	GTS CCC ATG ATG CGC AGC	97	Beller 2008
	SRBr	CGA CAT TGA ACT GCA CGT GRT CG		
todC	todf	ATC CTG CGA GGC CAC AAG	119	Liu 2012
	todr	TTC CTC GCT GTA GAC GTT GTT G		
nahAc	PAH-RHDa GNf	GAG ATG CAT ACC ACG TKG GTT GGA	306	Cebron 2008
	PAH-RHDa GNr	AGC TGT TGT TCG GGA AGA YWG TGC M		
abcA	1005f	GCCGACGGAAATGGTTATGC	287	DeRito (unpublished)
	1291r	ATGCCTTGCTCCAGGTTCTC		
dsrB	DSRp2060F	CAACATCGTYCAYACCCAGGG	350	Geets 2006
	DSR4R	GTGTAGCAGTTACCGCA		

Table A2. Evolution of (a) key functional genes and (b) key specific metabolites at Row 2 and Row 3

Time (day)	mRNA Transcripts (Copies/L)					
	Row 2			Row 3		
	$todC_{mRNA}$	bssA-SRB_{mRNA}	$dsrB_{mRNA}$	$todC_{mRNA}$	bssA-SRB_{mRNA}	$dsrB_{mRNA}$
97	0.00	124.97	0.00	0.00	0.00	0.00
156	0.00	369.06	928.53	0.00	87.02	0.00
170	0.00	246.02	64.27	0.00	N/A	0.00
190	0.00	39.86	10.94	0.00	1871.73	404.49
196	0.00	156.30	781.95	0.00	262.02	295.90
208	0.00	521.97	0.00	0.00	1004.87	478.71
221	0.00	214.96	667.39	0.00	171.23	207.66
293	0.00	1153.84	3851689.12	0.00	0.00	0.00
391	0.00	0.00	193541.31	0.00	0.00	0.00

b)

zone	Time (day)	Metabolite (µg/L)												
		Benzene-cDHD	Toluene-cDHD	Benzylsuccinate	2-MeBS	2,3-DMP	Phenol	Benzoate	Net Benzoate	Benzyl alcohol	o-Cresol	m-Cresol	p-Cresol	2-MBA
Row 2	97	0.00	0.04	18.76	1.13	0.00	38.57	2.94	1.78	0.25	1.22	0.09	0.14	0.15
	156	1.09	1.06	35.87	45.86	0.23	23.38	3.13	0.40	0.91	10.38	0.34	0.65	0.45
	170	0.52	0.22	20.74	37.65	0.16	38.93	2.15	0.00	1.70	4.89	0.43	0.72	0.67
	190	0.16	0.00	9.89	22.61	1.71	284.70	4.00	1.62	0.00	12.15	2.06	5.67	2.97
	196	0.07	0.00	5.36	25.16	4.14	418.77	1.13	0.34	0.00	26.71	5.23	11.95	4.51
	208	0.00	0.00	1.83	6.63	2.97	281.42	8.08	6.06	0.55	47.91	9.41	39.40	9.24
	293	0.00	0.00	0.00	19.61	3.61	152.26	3.06	2.88	0.27	123.62	7.17	2.53	N/A
	391	0.00	0.00	0.00	51.57	3.17	3.59	21.69	0.78	0.09	7.98	0.03	0.00	0.31
Row 3	97	0.00	0.00	3.90	0.14	0.00	12.93	2.19	1.03	0.14	0.69	0.00	0.02	0.15
	156	1.05	7.37	33.42	27.59	0.07	15.01	3.07	0.43	0.76	23.21	1.00	0.78	0.29
	170	0.36	1.00	8.30	20.78	0.09	61.09	4.25	1.87	0.16	9.15	0.36	0.35	0.40
	190	0.32	0.78	9.51	24.93	1.31	108.19	2.69	0.99	0.00	8.49	0.46	1.17	2.61
	196	0.24	0.54	6.06	20.75	0.05	11.85	4.27	1.89	0.00	4.44	0.11	0.07	0.33
	208	0.00	0.00	4.09	24.61	0.15	250.79	3.26	1.95	0.05	10.63	0.83	2.09	0.87
	293	0.00	0.00	0.00	15.37	0.97	88.12	3.18	3.18	0.05	5.58	0.33	1.05	0.86
	391	0.00	0.00	3.69	20.36	3.72	12.14	41.27	8.94	0.29	19.84	0.04	0.01	0.53

Appendix B

Verification of Model Formulation to Simulate Second-Order Reaction Term

Comparison with Analytical Solution

Analytical solution for the second-order chemical oxidation reaction:

$$\frac{dA}{dt} = k''[A][B]$$

is given by:

$$[A] = \frac{([B_0] - X[A_0])}{\frac{[B_0]}{[A_0]} e^{([B_0]-X[A_0])k''t} - X}$$

where $[A]$= Toluene concentration at time t, $[A_0]$ and $[B_0]$, respectively are toluene and persulfate concentrations at time t=0, X is the stoichiometry molar ratio between toluene and persulfate in the oxidation reaction, and k'' is the second-order rate coefficient.

In BIONAPL/PS, to represent the second order reaction term (Eq. 3.8) the parameters in the Monod kinetic term (Eq. 3.7) were manipulated, as given by

- $K_C >> [A_0]$
- $K_A >> [B_0]$
- $M_{initial}$ = 1.0 and M_{max}=1.0 (*i.e.*, M=const.=1.0)
- $k_{max} = k'' \times M \times K_C \times K_A \times R$

The following plots show the comparison between the BIONAPL/PS model result with the analytical solution for a series of hypothetical scenarios and with the data from the batch-scale laboratory experimental conducted by Sra et al. (2013b).

Hypothetical Scenarios:

- $[A_0] = 0.011$ g/L
- $[B_0] = 1.0$ g/L
- X = 18.0 (For toluene)
- k" = $0.005, 0.05, 0.5, 5\ Lg^{-1}day^{-1}$

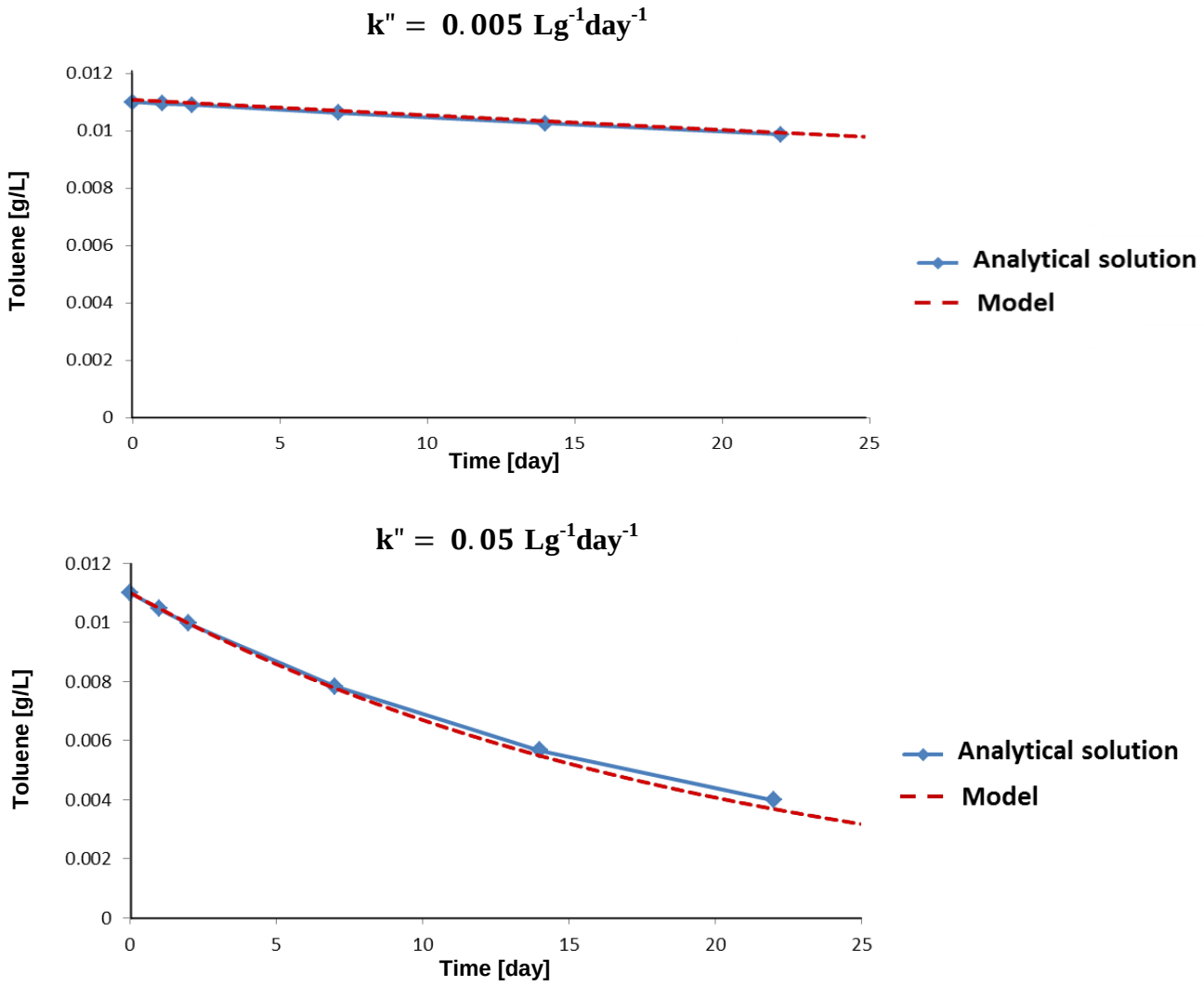

Figure B1 Comparison between BIONAPL/PS model output with the analytical solution for the second-order toluene degradation with persulfate.

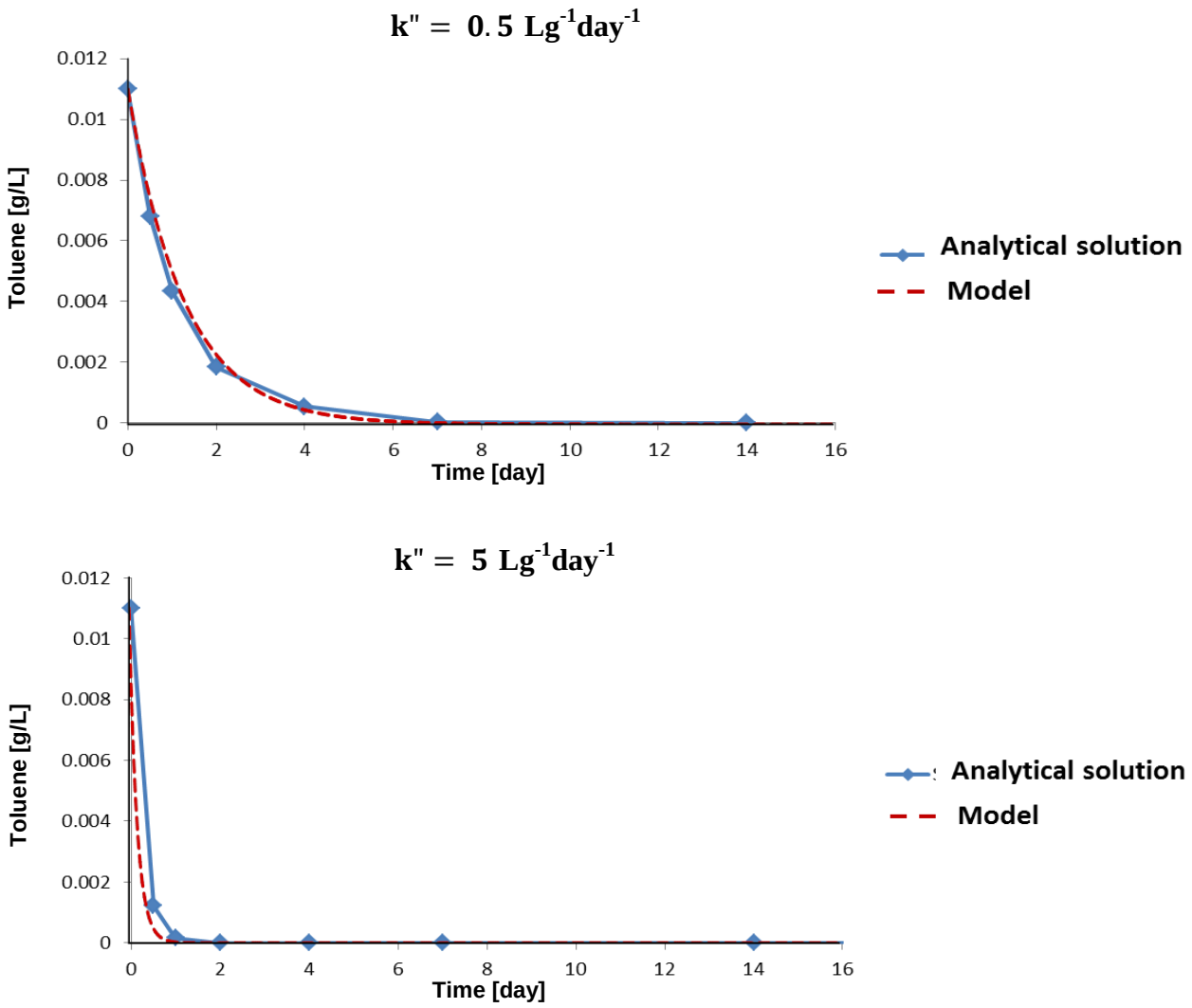

Figure B1 (cont'd) Comparison between BIONAPL/PS model output with the analytical solution for the second-order toluene degradation with persulfate.

Comparison with Observed Laboratory data

Simulation of BTX data from the batch experiment by Sra et al. 2013(b):

- $[A_0] = 0.008, 0.011, 0.0012$ g/L, respectively for benzene, toluene and xylene
- $[B_0] = 20.0$ g/L
- $X = 15.0, 18.0, 21.0$, respectively for benzene, toluene and xylene
- k" = $0.005, 0.0035, 0.0035$ $Lg^{-1}day^{-1}$, respectively for benzene, toluene and xylene

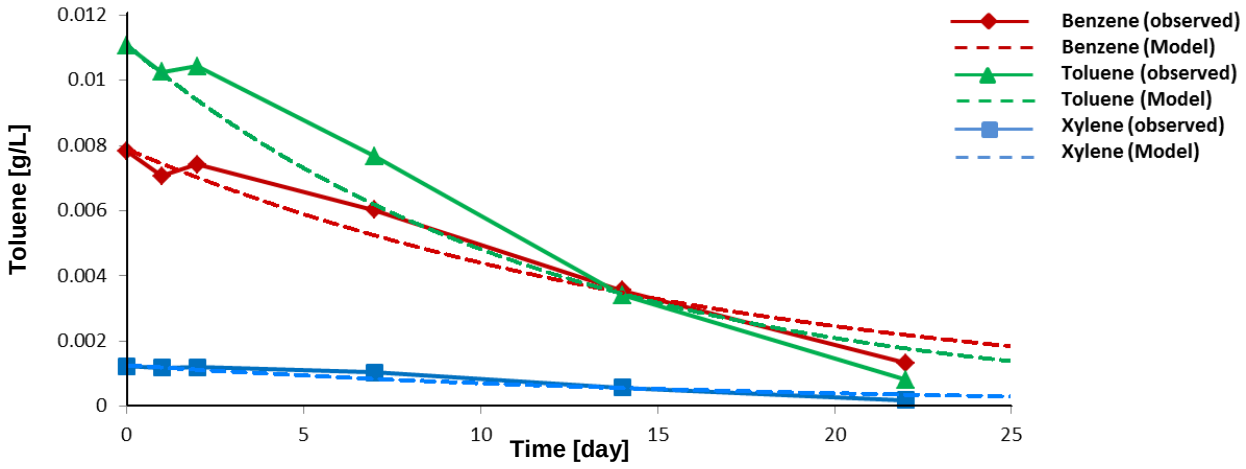

Figure B2 Comparison between BIONAPL/PS model output with the observed BTX data from the laboratory batch experiment by Sra et al. (2013b).

Appendix C

Supplementary Material for Chapter 3

Figure C1. Evolution of BTX plume in the pilot-scale field trial before the flow shutdown: observed (top) vs simulation results from the best-fit scenario (bottom).

Figure C2. Evolution of oxygen, sulfate and persulfate in the pilot-scale field trial before the flow shutdown: simulation results from the best-fit scenario.

Figure C3. Evolution of aerobes and sulfate reducing bacteria (SRB) in the pilot-scale field trial before the flow shutdown: simulation results from the best-fit scenario.

Figure C4. Effect of key design parameters on the rate of BTX mass loss in the ChemOx zone (left) and the EBR zone (right).

Figure C5. Effect of the key design parameters on the cumulative BTX mass loss in the (a) ChemOx zone and (b) the EBR zone.

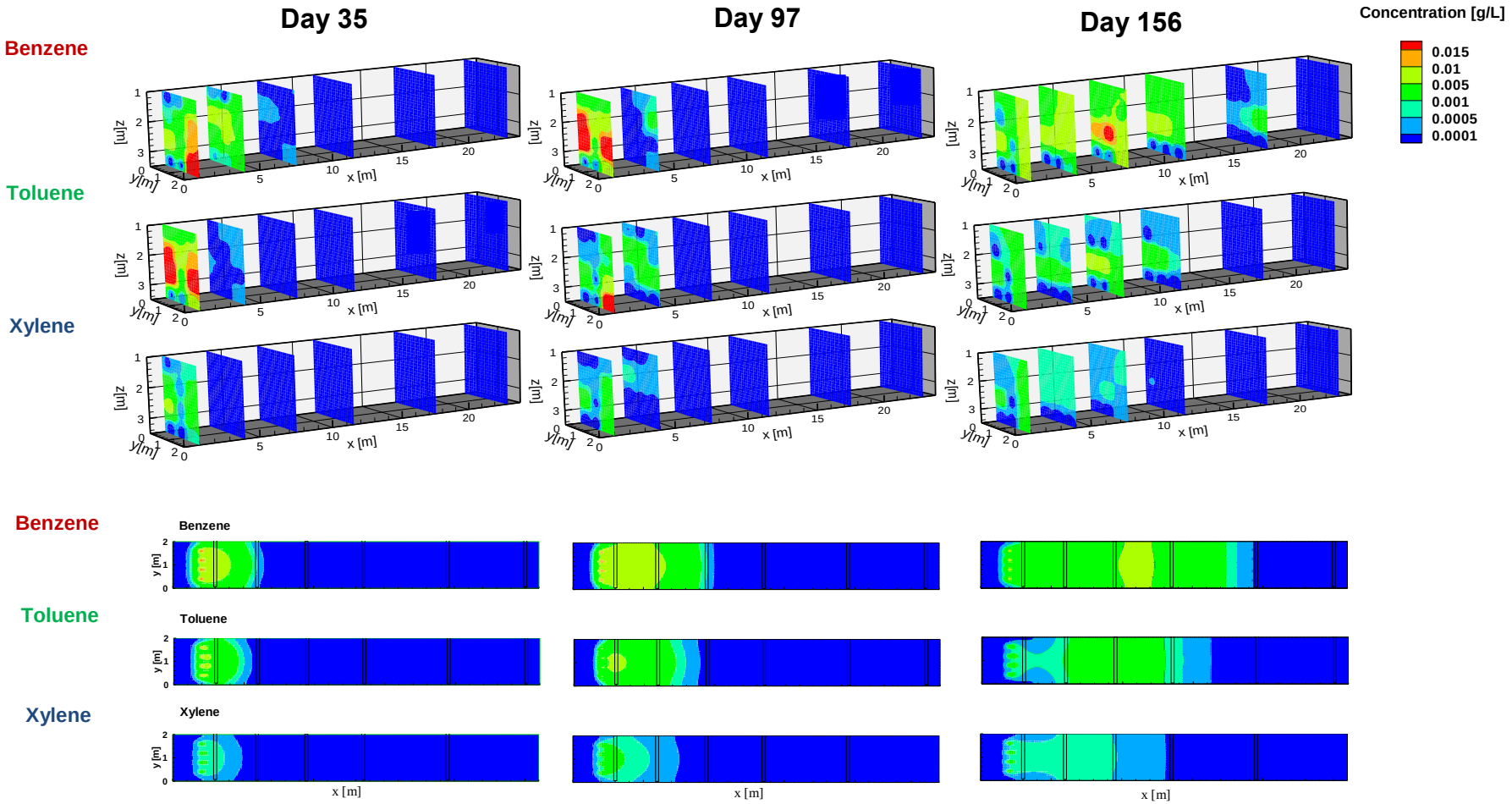

Figure C1 Evolution of BTX plume in the pilot-scale field trial before the flow shutdown: observed (top) vs simulation results from the best-fit scenario (bottom).

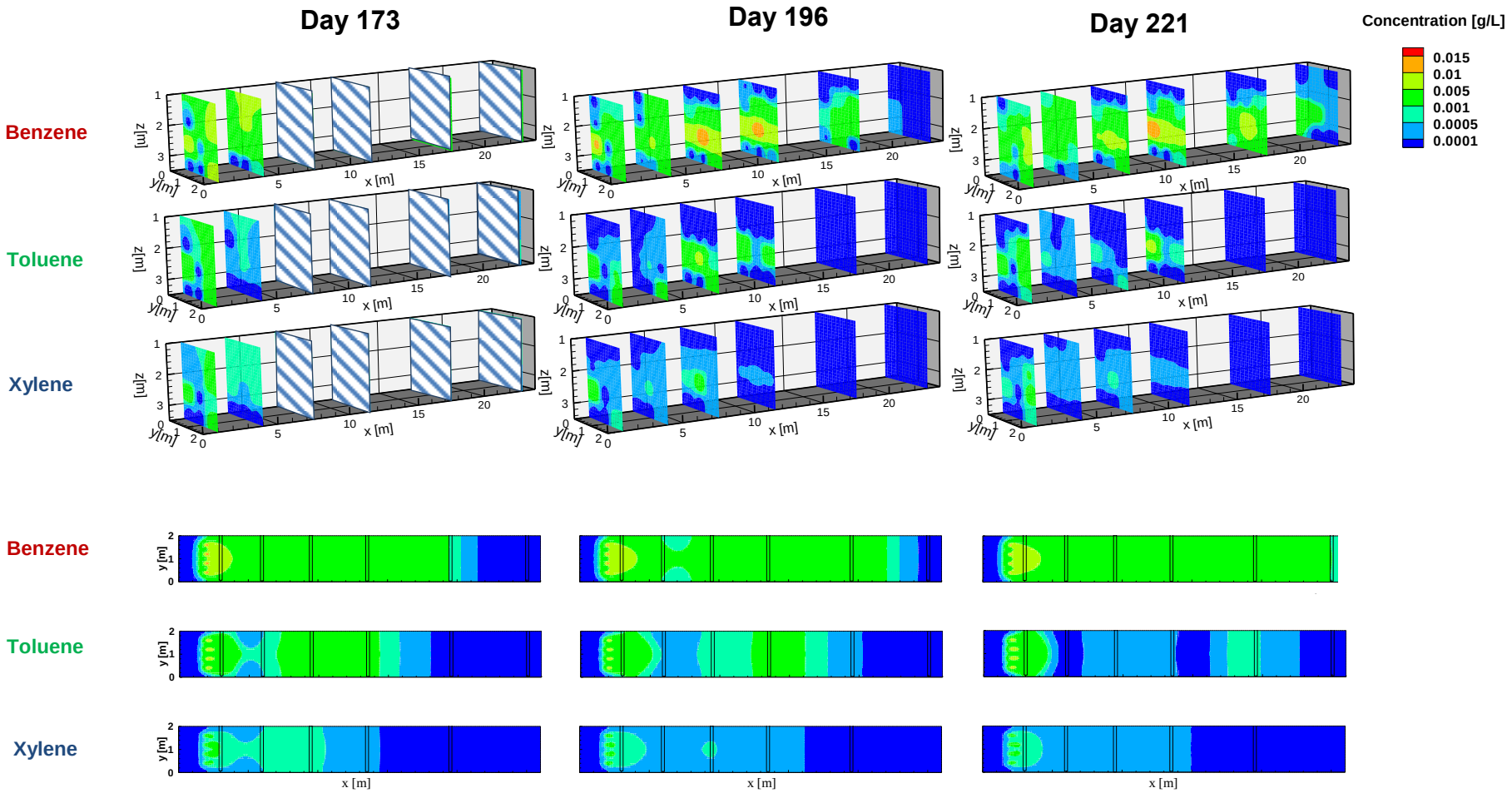

Figure C1 (Cont'd) Evolution of BTX plume in the pilot-scale field trial before the flow shutdown: observed (top) vs simulation results from the best-fit scenario (bottom)

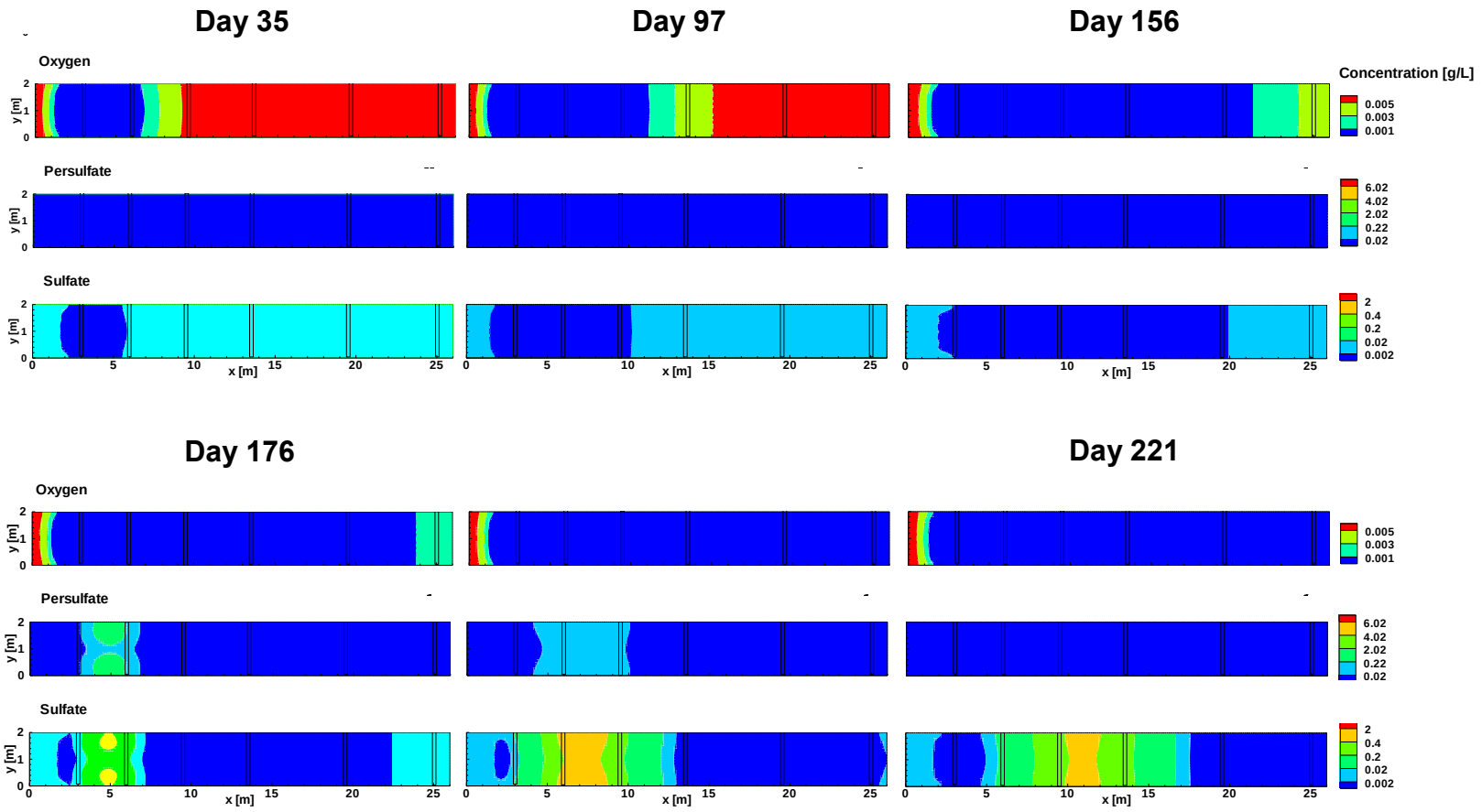

Figure C2 Evolution of oxygen, sulfate and persulfate in the pilot-scale field trial before the flow shutdown: simulation results from the best-fit scenario

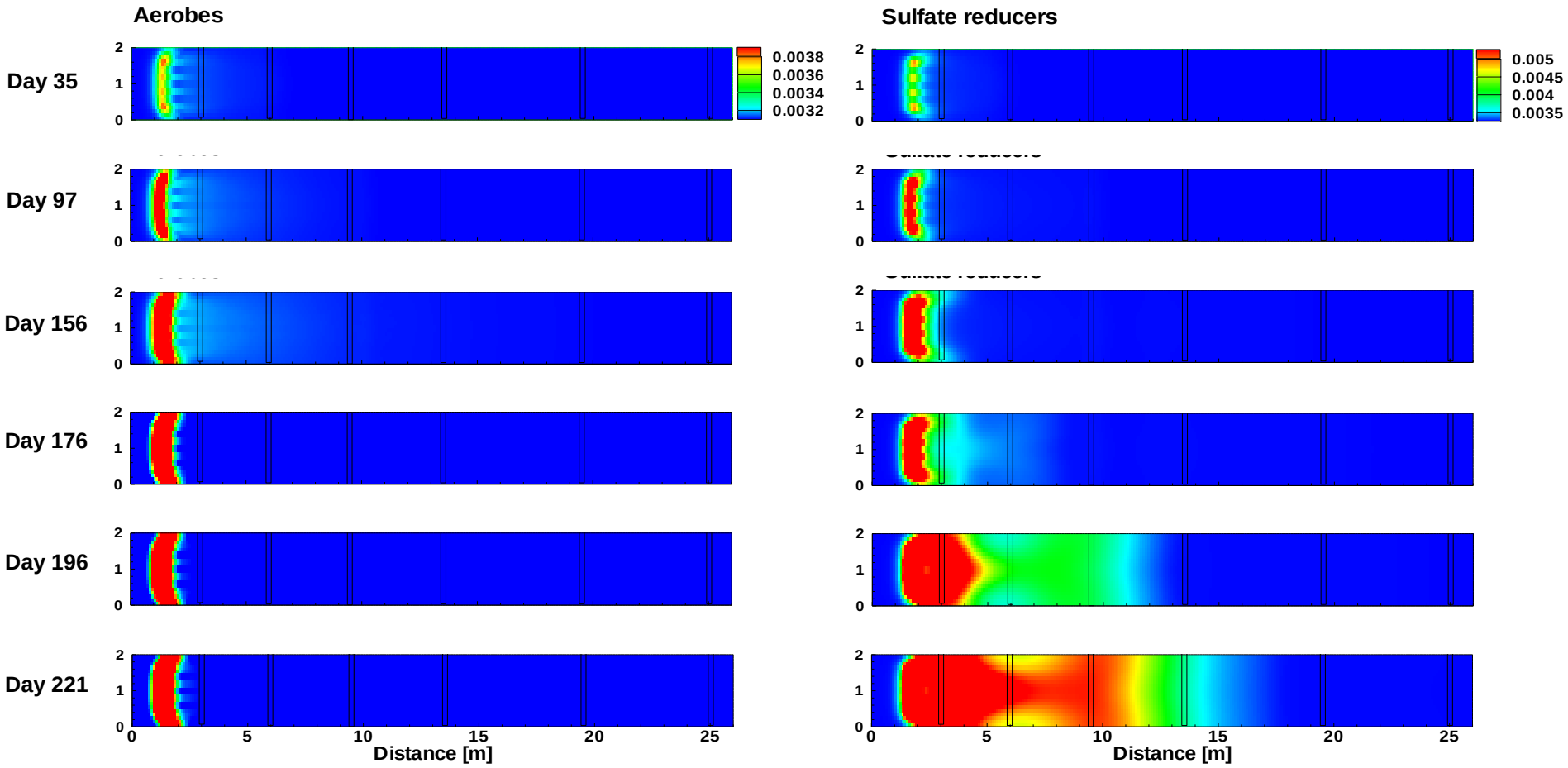

Figure C3 Evolution of aerobes and sulfate reducing bacteria (SRB) in the pilot-scale field trial before the flow shutdown: simulation results from the best-fit scenario

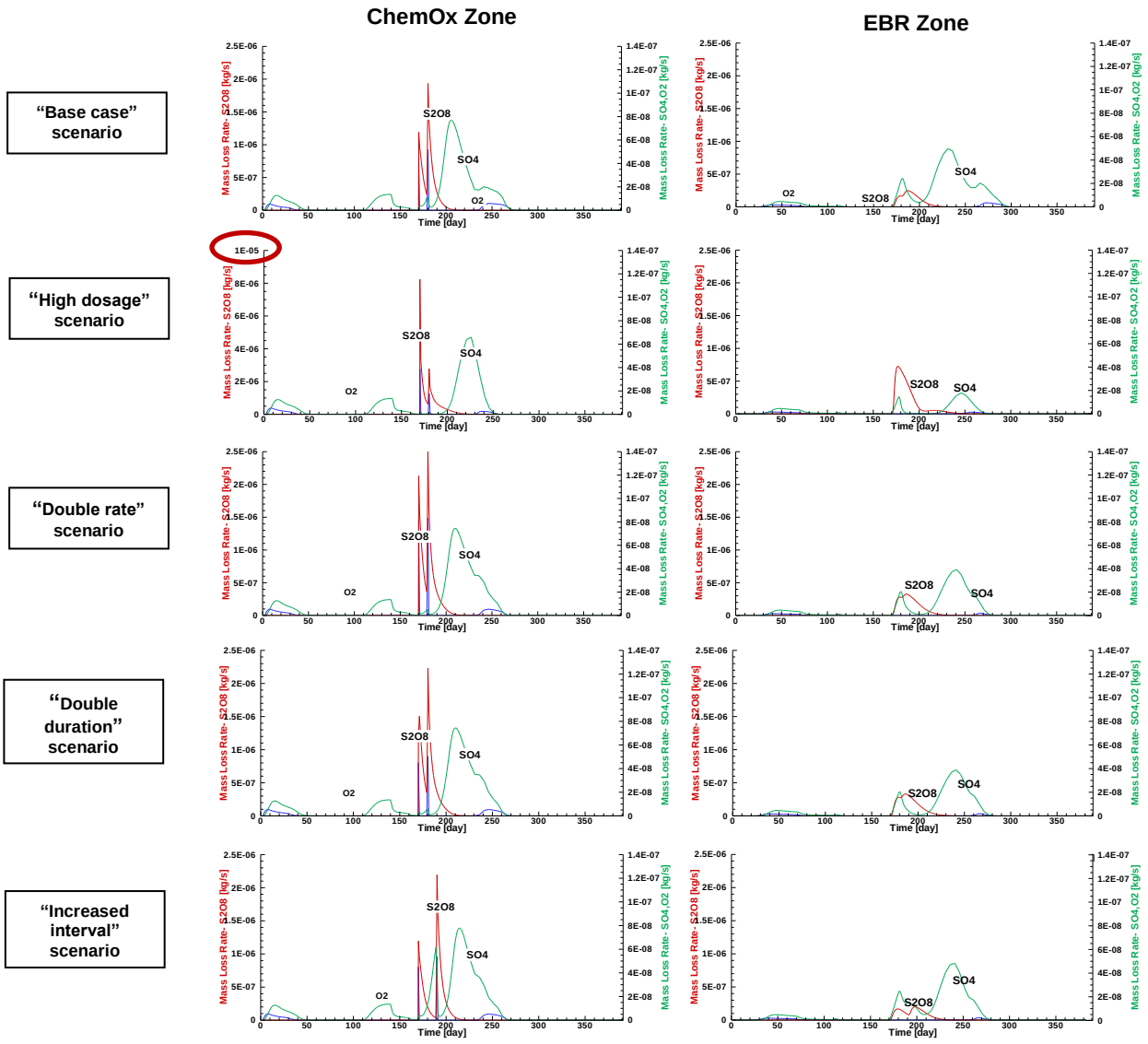

Figure C4 Effect of key design parameters on the rate of BTX mass loss in the ChemOx zone (left) and the EBR zone (right).

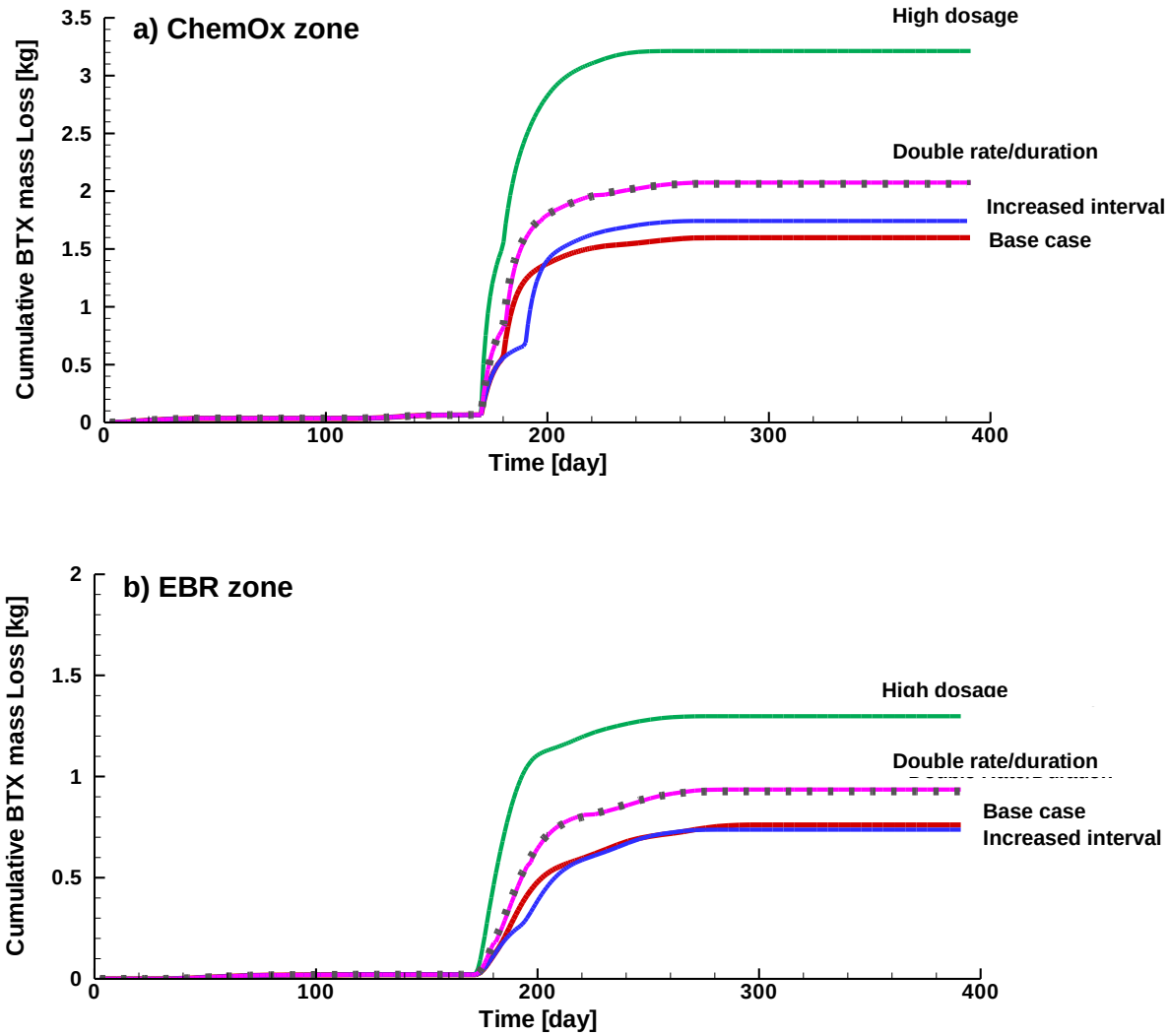

Figure C5 Effect of the key design parameters on the cumulative BTX mass loss in the (a) ChemOx zone and (b) the EBR zone.